Abstract

An Atlas of Neurotransmitter GPCR Cellular Expression Patterns in the *C. elegans* Egg-Laying Circuit

Robert W. Fernandez

2020

About seven neurotransmitters signal by activating a large set of G protein-coupled receptors (GPCRs) in the human brain. The nematode *C. elegans* has neurotransmitters and neural GPCRs conserved with those in the human brain, yet its simpler anatomy provides a system for studying how neural GPCR signaling is organized and utilized to help the nervous system carry out its functions. The ~5,000 synaptic connections between the 302 neurons of *C. elegans* have been completely mapped, and the individual neurons that express each have been catalogued. We are adding an additional layer to this nervous system signaling map by creating an Atlas of which cells express each of *C. elegans*' 26 GPCRs for small-molecule neurotransmitters. For each of the 26 neurotransmitter GPCRs, our GFP reporters include: 20 C-terminal::GFP reporters that express a GPCR with GFP fused at the C-terminus of the receptor protein, four reporters with an SL2 trans-splicing signal followed by GFP coding sequences inserted immediately downstream of the GPCR gene stop codon and

two reporters that were small promoter::GFP reporters that had been previously generated. We used a series of transgenes that label identified subsets of *C. elegans* neurons with red fluorescent proteins as markers to identify the GFP-expressing cells in our GPCR::GFP transgenic strains.

We tested the utility of this Atlas in the *C. elegans* egg-laying circuit, a simple circuit where the role of neurons and neurotransmitters involved in modulating this circuit have been well-studied. Some key results from our work: 1) A typical egg-laying neuron contains ~15 neurotransmitter GPCRs while the egg-laying muscles contain ~9 neurotransmitter GPCRs. 2) Several neurotransmitter GPCRs are expressed in non-neuronal cells. 3) There is a difference in GFP intensity of the chromosomally integrated GPCR::GFP transgene in specific cells of the egg-laying circuit, which could be functionally relevant. 4) There may be extensive extrasynaptic signaling that regulates egg laying as several neurotransmitter GPCRs are expressed in cells that do not receive direct synapses from their corresponding neurotransmitter-releasing neuron. We also conducted a functional screen on these neurotransmitter receptor knockouts and overexpressors to look for egg-laying defects. Completion of our Atlas, integrated with the synaptic wiring diagram and neurotransmitter maps, will provide a path to understand the functions of neurotransmitter signaling through GPCRs in each individual neural circuit and every behavior carried out in *C. elegans*, and should generate insights that generalize beyond *C. elegans* into how neural GPCR signaling is organized.

An Atlas of Neurotransmitter GPCR Cellular Expression Patterns in the *C. elegans* Egg-Laying Circuit

A Dissertation

Presented to the Faculty of the Graduate School

of

Yale University

In Candidacy for the Degree of

Doctor of Philosophy

By

Robert William Fernandez

Dissertation Director: Michael R. Koelle

May 2020

Table of Contents

Abstract **i**

Table of Contents **v**

List of Figures and Tables **ix**

Glossary of Terms **xiii**

Acknowledgements **xv**

Chapter 1: Introduction **1**

1.1 The complexity of understanding neurotransmitter signaling in neural circuits **1**

1.2 *C. elegans* as a model to study neural circuits **2**

1.3 Neurotransmitter GPCRs in *C. elegans* **3**

1.4 The *C. elegans* egg-laying circuit as a model to study neurotransmitter signaling **5**

Chapter 2: Pipeline to generate neurotransmitter GPCR::GFP transgenic strains **8**

2.1 Introduction **9**

2.2 GFP reporter transgenes for neurotransmitter GPCRs **10**

2.3 Generating GFP reporter transgenes **13**

2.4 Restriction digest of GPCR::GFP transgenes **17**

2.5 Generating neurotransmitter GPCR::GFP transgenic strains **33**

2.6 mCherry markers to identify cells of the *C. elegans* egg-laying system **35**

2.7 Strategy to identify GPCR::GFP expression in cells of the *C. elegans* egg-laying system **38**

2.8 Discussion and Conclusion **44**

Chapter 3: An atlas of neurotransmitter GPCRs expression in the *C. elegans* egg-laying circuit **45**

3.1 Introduction **45**

3.2 Serotonin GPCRs expressed in the *C. elegans* egg-laying circuit **46**

3.3 Dopamine GPCRs expressed in the *C. elegans* egg-laying circuit **50**

3.4 Octopamine GPCRs expressed in the *C. elegans* egg-laying circuit **53**

3.5 Tyramine GPCRs expressed in the *C. elegans* egg-laying circuit **55**

3.6 Acetylcholine GPCRs expressed in the *C. elegans* egg-laying circuit **57**

3.7 GABA GPCRs expressed in the *C. elegans* egg-laying circuit **59**

3.8 Glutamate GPCRs expressed in the *C. elegans* egg-laying circuit **61**

3.9 Orphan GPCRs expressed in the *C. elegans* egg-laying circuit **63**

3.10 Analysis of neurotransmitter GPCRs cellular expression patterns the *C. elegans* egg-laying circuit **65**

3.11 Synaptic vs. extrasynaptic signaling in the *C. elegans* egg-laying circuit **73**

3.12 Discussion and Conclusion **81**

Chapter 4: Functional role of Neurotransmitter GPCRs in the *C. elegans* egg-laying circuit **82**

4.1 Introduction **82**

4.2 Single knockouts of neurotransmitter GPCR genes does not reveal strong egg-laying defects **83**

4.3 $G\alpha_o$-coupled neurotransmitter GPCR knockouts does not reveal strong egg-laying defects **89**

4.4 Overcoming the absence of egg-laying phenotypes in neurotransmitter receptor knockout(s) through overexpression of the serotonin GPCR SER-1 **94**

4.5 Overexpression of neurotransmitter GPCRs expressed in the *C. elegans* egg-laying system reveals strong egg-laying defects **98**

4.6 Overexpression of octopamine GPCR SER-6 reveals strong egg-laying defects **104**

4.7 Overexpression of the tyramine GPCR SER-2 reveals modest egg-laying defects **109**

4.8 Overexpression of the acetylcholine GPCR GAR-1 reveals strong egg-laying defects **112**

4.9 Overexpression of glutamate GPCRs, MGL-1 and MGL-3, reveals strong egg-laying defects **114**

4.10 Discussion and Conclusion **120**

Chapter 5: Materials and Methods **122**

Chapter 5.1 General methods **122**

5.1.1 *C. elegans strains* **122**

Chapter 5.2 Methods for Chapter 2 **123**

5.2.1 Isolating and sequencing recombineered GPCR::GFP transgenes **123**

5.2.2 Microinjections of GPCR::GFP transgenes **124**

5.2.3 Chromosomal integrations **124**

5.2.4 mCherry marker strains **125**

5.2.5 GPCR::GFP transgenic strains **126**

5.2.6 Confocal imaging of GPCR::GFP transgenic strains **128**

5.2.7 Cell identification process **129**

Chapter 5.3 Methods for Chapter 3 **130**

5.3.1 Strong and weak GPCR::GFP expression **130**

5.3.2 Annotating cases where receptors are positioned to receive synaptic vs. extrasynaptic signals in the *C. elegans* egg-laying system **130**

Chapter 5.4 Methods for Chapter 4 **132**

5.4.1 Egg-laying assays **132**

5.4.2 Statistical analysis **132**

References **134**

Appendix **144**

Chapter 2 Appendix **144**

GFP reporter transgenes for 26 Neurotransmitter GPCRs **144**

Primers for Neurotransmitter GPCR::GFP Transgenes **148**

Chapter 4 Appendix **150**

Primers for Neurotransmitter GPCR Knockouts **150**

Chapter 5 Appendix **151**

Strains used in this thesis **151**

Alleles used in this thesis **159**

List of Figures and Tables

Table 1.1 Small-molecule neurotransmitter GPCRs in *C. elegans* **7**

Figure 2.1 GFP reporter transgenes for neurotransmitter GPCRs **12**

Figure 2.2 Isolation of GPCR::GFP transgenes from EPI300 *E. coli* cells **15**

Figure 2.3. Pipeline to generate...atlas of the *C. elegans* egg-laying circuit **16**

Figure 2.4 Restriction digest of the 45.442kb *dop-3::gfp* transgene **22**

Figure 2.5 Confirming the gel purified *dop-3::gfp*...expected size **23**

Figure 2.6 Restriction digest of the 53.802kb *tyra-2::gfp* transgene **24**

Figure 2.7 Confirming the gel purified *tyra-2::gfp*...expected size **25**

Figure 2.8 Restriction digest of the 49.065kb *tyra-3::gfp* transgene **26**

Figure 2.9 Confirming the gel purified *tyra-3::gfp*...expected size **27**

Figure 2.10 Restriction digest of the 44.894kb *mgl-3::gfp* transgene **28**

Figure 2.11 Confirming the gel purified *mgl-3::gfp*...expected size **29**

Figure 2.12 Restriction digest of the 44.624kb *dop-5::gfp* transgene **30**

Figure 2.13 Confirming the gel purified *dop-5::gfp*...expected size **31**

Figure 2.14 Confirming the ends...*mgl-3::gfp* and *dop-5::gfp* transgene **32**

Figure 2.15 mCherry markers...*C. elegans* egg-laying system **37**

Figure 2.16 Identification...*C. elegans* egg-laying system...OCTR-1 **40**

Figure 2.17 Consistent strong GFP expression...*octr-1::gfp* transgene **41**

Figure 2.18 Animal to animal variation in GFP...HSN...*octr-1::gfp* transgene **42**

Figure 2.19 Animal to animal variation in GFP...VC4...*octr-1::gfp* transgene **43**

Table 2.1 Restriction digest...GPCR::GFP transgenic strains **21**

Table 2.2 Neurotransmitter GPCR::GFP transgenic strains **34**

Figure 3.1 Serotonin GPCRs...in the *C. elegans* egg-laying circuit **49**

Figure 3.2 Dopamine GPCRs...in the *C. elegans* egg-laying circuit **52**

Figure 3.3 Octopamine GPCRs...in the *C. elegans* egg-laying circuit **54**

Figure 3.4 Tyramine GPCRs...in the *C. elegans* egg-laying circuit **56**

Figure 3.5 Acetylcholine GPCRs...in the *C. elegans* egg-laying circuit **58**

Figure 3.6 GABA GPCRs...in the *C. elegans* egg-laying circuit **60**

Figure 3.7 Glutamate GPCRs...in the *C. elegans* egg-laying circuit **62**

Figure 3.8 Orphan GPCRs...in the *C. elegans* egg-laying circuit **64**

Figure 3.9 Raw data...*C. elegans* egg-laying system **69**

Figure 3.10 Summary of neurotransmitter GPCR...egg-laying system **70**

Figure 3.11 Summary of neurotransmitters GPCRs...egg-laying circuit **71**

Figure 3.12 Comparison of the neurotransmitter GPCRs...publications **72**

Table 3.1 Application of neurotransmitter signaling maps...HSN **75**

Table 3.2 Application of neurotransmitter signaling maps...VC4 **76**

Table 3.3 Application of neurotransmitter signaling maps...VC5 **77**

Table 3.4 Application of neurotransmitter signaling maps...vm1 **78**

Table 3.5 Application of neurotransmitter signaling maps...vm2 **79**

Table 3.6 Synaptic vs. extrasynaptic...*C. elegans* egg-laying system **80**

Figure 4.1 Only one neurotransmitter GPCR...single knockout...worm **86**

Figure 4.2 The egg-laying defective...DOP-4 knockout...construct **87**

Figure 4.3 Neurotransmitter GPCR...single knockout...early-staged eggs laid **88**

Figure 4.4 Combination knockouts of Gαo-coupled...early-staged eggs laid **92**

Figure 4.5 Combination knockouts of Gαo-coupled... unlaid eggs...uterus **93**

Figure 4.6 Overexpression...serotonin GPCR...egg-laying defects...SER-1 **96**

Figure 4.7 Overexpression...serotonin GPCR...egg-laying defects...TPH-1 **97**

Figure 4.8 Overexpression of neurotransmitter GPCR...*ser-1* and *gbb-1* **100**

Figure 4.9 Overexpression of the GABA GPCR...GBB-1 **101**

Figure 4.10 Overexpression of four...GBB-1 does not reveal...egg-laying defects **102**

Figure 4.11 Overexpression of neurotransmitter...unlaid eggs...worm **103**

Figure 4.12 Overexpression of the Octopamine GPCR...SER-6 **106**

Figure 4.13 Overexpression of the Octopamine GPCR...SER-6...TBH-1 **107**

Figure 4.14 Overexpression of the extrachromosomal strain...SER-3 **108**

Figure 4.15 Overexpression of the tyramine GPCR...SER-2 **110**

Figure 4.16 Overexpression of the tyramine GPCR...SER-2...TDC-1 **111**

Figure 4.17 Overexpression of the acetylcholine GPCR...GAR-1 **113**

Figure 4.18 Overexpression of the glutamate GPCR...MGL-1 **116**

Figure 4.19 Overexpression of the glutamate receptor...MGL-1...EAT-4 **117**

Figure 4.20 Overexpression of the glutamate GPCR...MGL-3 **118**

Figure 4.21 Overexpression of the glutamate receptor...MGL-3...EAT-4 **119**

Table 4.1 $G\alpha_o$-coupled neurotransmitter GPCRs...egg-laying system **91**

Table 4.2 Neurotransmitter GPCRs...egg-laying defects...egg-laying system **121**

Figure A1. GFP reporter transgenes for Neurotransmitter GPCRs **144**

Table A5.1 mCherry marker strains **151**

Table A5.2 Neurotransmitter GPCR single knockout strains **151**

Table A5.3 Neurotransmitter GPCR combination knockouts strains **152**

Table A5.4 Neurotransmitter GPR::GFP transgenic strains **153**

Table A5.5 Neurotransmitter GPCR::GFP double-labeled strains **155**

Table A5.6 Other strains used in this study **158**

Table A5.7 Allele information for mCherry markers **159**

Table A5.8 Allele information for Neurotransmitter GPCR mutants **160**

Table A5.9 Allele information for Neurotransmitter GPCR::GFP transgene **161**

Glossary of Terms

ADOR	Adenosine Receptor homolog
AJM	Apical Junction Molecule
BWM	Body Wall Muscle
CGC	Caenorhabditis Genetics Center
DOP	Dopamine receptor
E. coli	Escherichia coli
EAT	Eating: abnormal pharyngeal pumping
EGL	Egg Laying Defective
EX	Extrachromosomal
Gα_o	G protein o alpha subunit
Gα_q	G protein q alpha subunit
Gα_s	G protein s alpha subunit
GAR	G-protein-linked Acetylcholine Receptor
GBB	GABA B receptor subunit
GFP	Green Fluorescent Protein
GPCR	G-protein coupled receptor
HSN	Hermaphrodite-specific neuron
IDA	Islet Cell Diabetes Autoantigen
KO	Knockout
L4	Larval stage 4
MGL	Metabotropic Glutamate Receptor family

NBRP	National BioResource Project
NGM	Nematode Growth Medium
NLS	Nuclear Localization Sequence
OCTR	Octopamine Receptor
OX	Overexpression
SER	Serotonin/octopamine receptor family
SL2	Spliced Leader 2
SP	Spermatheca
SP-UT	Spermatheca-uterine
TBH	Tyramine Beta Hydroxylase
TDC	Tyrosine Decarboxylase
TMP	Trimethylpsoralen
TPH	Tryptophan Hydroxylase
TYRA	Tyramine receptor
UM	Uterine Muscle
UNC	Uncoordinated
UT	Uterine Toroid Cell
UTSE	Uterine Seam
UV	Uterine Ventral Cell
VC	Ventral Cord Type C Neuron
VM	Vulval Muscle
VNC	Ventral Nerve Cord
WT	Wild Type

Acknowledgements

I would like to thank my advisor Michael R. Koelle for believing in me and giving me the chance to become the scientist I am today. I am forever grateful that he took a chance on me when I was at my lowest academically and because of his mentorship and training, I was able to grow as a scientist beyond my expectations. I am thankful that Michael gave me the independence to pursue a novel project in his lab, from the idea stage all the way to fruition. I am especially thankful for the two amazing MB&B undergraduates Kimberly Wei and Erin Wang whom I was privileged to mentor and have seen grown into amazing individuals and scientists. This thesis would have taken much longer if it not was for their unwavering drive to push the project forward, especially during the troubleshooting phase where Erin and I spend a lot of time trying to get every step of the pipeline to work and Kim's hard work and dedication to continuing the project after Erin graduated. Kim started off as a 1st year college student and she was invaluable in wrapping up the project beyond what I ever expected. I am also thankful for the rest of the lab members who helped with various steps of the pipeline to bring this project into fruition: Andrew Olson, Seongseop Kim, Judy Pepper, Deimante Mikalauskaite. I thank Andrew for being a supportive labmate and several microinjections of the GPCR::GFP transgenes. I also want to thank Nakeirah Christie who designed amazing figures of the *C. elegans* egg-laying circuit for our first paper. What I am the most grateful for is that I often felt the experience of leading my own lab as Michael gave me the independence to

develop my own research projects in which the undergraduates and rotation students I mentored took the lead in making great strides towards these projects. I am thankful for Nilusha Navodiya, a former Biomed SURF student, who reminded me of the impact of mentorship. I also want to thank former lab member Dipon Ghosh for his snarky mentorship who provided me valuable advice when I needed it the most. I also want to thank Santosh Kumar who provided the idea of using restriction enzymes to digest the recombineered transgenes, which really helped push my thesis project forward. I want to thank Judy Pepper for being the mom of the lab. I also want to thank Luba Copela for all of the NGM plates that she poured, going the extra mile when we needed an abundance of NGM plates for chromosomal integrations. I also want to thank my thesis committee members (Mark Solomon, Marc Hammarlund) for pushing to see beyond mapping receptors for my project and helping me come up with functional studies based on our Atlas. I also am grateful for the Yale Worm Community and the MB&B Hall Seminar community who helped me see my thesis project from different angles and pushed me to think outside the box.

I want to thank the entire MB&B Department for being a welcoming and supportive community. Initially, I felt like I did not belong in higher education as I was one of the few Latinx graduate students at the time, being the first scientist in my family and coming from a small school. However, I was able to strive and rise, and the support from MB&B helped me achieve that. I learned from MB&B that graduate school is not a journey that you do alone, rather it is one with your colleagues, labmates, and professors. I want to thank Mark Solomon for giving

me a chance to continue graduate school after facing a rough first semester. I also really want to thank Tony Koleske as he was the reason I decided to go to Yale as his support during the recruitment weekend made all the difference in my decision to come to Yale. Throughout my time in graduate school, Tony has been an invaluable mentor since the day I met him. He guided me to apply for the Paul and Daisy Soros Fellowship, pushed me to become a better scientist by leading by example and his words of wisdom fueled my drive when I needed it the most, and has been a strong source of support whether it came to science or diversity initiatives at Yale. I also want to thank Enrique De La Cruz and Andrew Miranker for being supportive mentors and a source of support as they helped me push diversity initiatives forward; I'm grateful that they invested in me and I can go to them for valuable advice when I needed it the most. I also want to thank Stephen Chin-Bow from the Konigsberg lab, who has been a constant source of support whose cheerful presence has been helpful throughout the years. I am grateful for the support he gave me when I worked long hours, whether it was valuable advice, stories, or food. I also want to thank Susan Baserga as her support early on in my graduate school career was very helpful. The support from MB&B faculty and colleagues has been invaluable and I am forever grateful for it.

I want to thank the Yale BBS graduate community for I am extremely grateful that I met amazing scientists and friends (Cathy Amaya, Daisy Duan, Jaylissa Torres, Gabriela Bosque Ortiz, Gabriela Casanova, Nicolle Rosa Mercado, Paola Figueroa-Delgado, Termara Parker, Rocío Saavedra, Sebastian Diaz, Titilayo Omotade; Adrian Mehrtash, Ben Oni, Gadareth Higgs, Ian

Gonzalez) who made the entire graduate school journey easier. I hope that they all continue to be amazing scientists and professionals, continuing to push the BBS community forward with diversity initiatives, and go on to be future leaders in their field. I also want to thank former BBS graduate students: Yagmur Muftuoglu, Parwiz Abrahimi, and Mitch Omar who were a strong source of support and guided me when I felt lost when I was starting graduate school.

I also want to thank the STARS students. These amazing undergraduates will go on to be great doctors, scientists, lawyers, and professionals. No matter how rough things got in graduate school, being able to help these students, learn from them, and listen to their dreams, fueled me at my lowest and pushed me to become a better person. If it wasn't for these students, I don't think I would have kept my sanity or humanity from non-stop research in the lab. I am forever grateful for all of them and wish them nothing but the best.

Lastly, I want to thank my family. My mom taught me the definition of hard work and to never give up and it has guided me to where I am today. Her constant source of support and of my family got me through graduate school and I am forever thankful for them. I also want to thank my friends who were there for me at different steps of my journey (Omar Feliciano [aka The Phoenix Within], Andre Machado, Olivia Goldman, Adesanya Akinleye) and made time for me even when I would disappear for months due to science. I want to thank my undergraduate PI, Dr. Simon, who saw the potential in me and led me to this path. I will continue to pass on the torch to as many future generations of minority

scientists I meet, guide them along their journey and I look forward to the day we make an everlasting change.

Chapter 1: Introduction

The majority of the text in Chapter 1 was written by Robert W. Fernandez with revisions from Michael R. Koelle as adapted from:

Fernandez, R.W., Wei, K., Wang, E.Y., Mikalauskaite, D., Olson, A., Pepper, J., Kim, S., Christie, N., Hasse, S., Sarov, M., and Koelle, M.R. Cellular expression and functional roles of 26 neurotransmitter GPCRs in the *C. elegans* egg-laying circuit. (2020)

In this chapter, I discuss the complexity of studying neurotransmitter signaling within large neural circuits such as those found in humans. I explain the advantages of using *C. elegans* as a model to study neurotransmitter signaling and how the Neurotransmitter GPCR Atlas of the *C. elegans* egg-laying system can help us better understand the function of neurotransmitter GPCRs in *the C. elegans* egg-laying circuit.

1.1 The complexity of understanding neurotransmitter signaling in neural circuits

Neurotransmitters signal through G protein-coupled receptors (GPCRs) to modulate neural circuits, but how this type of signaling acts within neural circuits to regulate specific behaviors remains poorly understood. Currently, a major challenge in understanding how neurotransmitters control neural circuit function is dissecting their roles as neuromodulators acting through G protein coupled receptors (GPCRs) (Marder 2012). There are many challenges to understanding neural GPCR signaling: 1) Each neurotransmitter has multiple GPCRs (Hobert,

2013) and different GPCRs can couple to different G proteins to have different effects. Serotonin, for example, has 12 different GPCRs expressed in the human brain (McCorvy & Roth, 2015). 2) Neurotransmitters bind GPCRs with high affinity, allowing these receptors to respond to neurotransmitters released at a distance, an effect known as extrasynaptic or volume transmission (Chase et al., 2004; Fuxe et al., 2005; Agnati et al., 2006; Fuxe et al., 2012). Thus, mapping the synaptic connections between a set of neurons that form a circuit is insufficient to define the GPCR signaling that may occur between them. 3) GPCRs can sometimes signal as part of heteromeric complexes as in the cases of the GABA receptor heterodimer (Bamber et al., 1999; Dittman and Kaplan, 2008). 4) A single GPCR can often bind (albeit with different affinities) several different neurotransmitters (Suo et al., 2003).

One approach to understanding the brain is the detailed analysis of small neural circuits, such as those of genetically-tractable model organisms, with the aim of uncovering principles that generalize to circuits of more complex nervous systems (Bargmann and Marder, 2013). Deeply understanding a neural circuit might involve mapping the synaptic and gap junction connections between all cells in the circuit, identifying the neurotransmitters released by each neuron in the circuit, identifying the neurotransmitter receptors present on each cell of the circuit, and defining how signaling through each receptor affects the function of the circuit. This depth of understanding has not yet been achieved for any neural circuit.

1.2 *C. elegans* as a model to study neural circuits

C. elegans is an excellent model organism for studies of neurotransmitter GPCR signaling because: 1) The neural connectome has been completed, detailing ~7,000 synaptic connection between all 302 neurons in this organism (Albertson & Thomas, 1976; White et al., 1986; Xu et al., 2013). 2) A neurotransmitter map has been completed, showing which of the seven small-molecule neurotransmitters (serotonin, dopamine, octopamine, tyramine, acetylcholine, GABA, and glutamate) found in *C. elegans* is released by each of its 302 neurons (Serrano-Saiz et al., 2013; Pereira et al., 2016; Gendrel et al., 2016). 3) *C. elegans* has ~26 close homologs of human neurotransmitter GPCRs, 21 of which have been assigned as receptors for one of the seven neurotransmitters, while the remainder five are "orphan" receptors without assigned ligands. 4) Knockout mutants for all of these neurotransmitter GPCR genes are available (Koelle 2018).

1.3 Neurotransmitter GPCRs in *C. elegans*

Almost all of the 26 GPCRs for small-molecule neurotransmitters in *C. elegans* have been knocked out, but so far few defects have been detected in these mutants (Chase et al., 2004; Dittman and Kaplan, 2008). This is in large part because we still do not know what specific cells express the 26 neurotransmitter GPCRs, and this makes it difficult to determine which behaviors to examine for defects in any GPCR knockout. Since the connectome tells us what circuits each neuron is a part of, knowing what neurons express each GPCR would allow us to make specific testable hypotheses for what circuits, and thus what behaviors a

specific GPCR controls. Previous attempts to identify the cells that GPCRs are present in (Koelle, 2018) have yielded incomplete and inconsistent results because they relied on tools that did not label all the cells that actually express each receptor, and also because poor methods were used to identify the labeled cells. Furthermore, past studies of *C. elegans* GPCRs have focused on analysis of one receptor at time, or on how small subsets of the receptors affect a single circuit or behavior.

To tackle these issues, our long-term goal is to generate the first Neurotransmitter GPCR Atlas in any model organism, in which every cell in the entire *C. elegans* nervous system that expresses each of the 26 neurotransmitter GPCRs found in *C. elegans* will be catalogued. This atlas will help provide a better understanding of how neurotransmitter signaling through GPCRs are involved in modulating neural circuits to regulate different behaviors. For example, if we want to determine the function of a neurotransmitter GPCR, we can use the identity of the cells that the GPCR is expressed in as our starting point. As the role of neurons in regulating different behaviors are well known, the expression patterns of a neurotransmitter GPCR in a specific neuron within a neural circuit can help us narrow down the type of behaviors that this receptor might be involved in. We can generate testable hypotheses on the function of these receptors based on the identity of the neurons it is expressed in. For example, if we were interested in determining the function of octopamine GPCRs, the neurotransmitter GPCR Atlas can tell us the neural circuits and individual cells of the circuit these receptors are expressed in. If we found

octopamine GPCR expression in the *C. elegans* egg-laying circuit, the identity of these receptors in specific egg-laying cells such as cells that are known to promote or inhibit egg-laying events, can give us a solid starting point as to determine how the octopamine GPCRs modulate egg laying events. Furthermore, we can test single octopamine GPCR knockouts to look for egg-laying defects and in the absence of an egg-laying defect in the single octopamine receptor knockout, the atlas tells us if there are other octopamine GPCRs expressed in the same egg-laying cells. With this information, we will know what combination of octopamine receptor knockouts to generate to overcome functional redundancy and find egg-laying defects. With the Neurotransmitter GPCR Atlas, these are the type of approaches that can be used to help determine the function of a neurotransmitter GPCR in any neural circuit.

1.4 The *C. elegans* egg-laying circuit as a model to study neurotransmitter signaling

The *C. elegans* egg-laying circuit is a simple and well-studied circuit, as we know the identity of the cells and the neurotransmitters involved in regulating this circuit. The command neuron of the circuit, the HSN neurons promote egg-laying events by releasing serotonin and neuropeptides (Waggoner et al., 1998; Shyn et al., 2003; Hapiak et al., 2009; Emtage et al., 2012; Brewer et al., 2019). The uv1 neuroendocrine cells release tyramine and neuropeptides to inhibit egg-laying (Collins et al., 2016; Banerjee et al., 2017). The VC4 and VC5 neurons release acetylcholine via synapses onto the vm2 egg-laying muscles (Collins et al., 2016). We know that eggs are laid when vm1 and vm2 muscle cells open up the vulva

and the um1 and um2 muscles squeeze eggs out the uterus through the vulva to the outside of the animal (Kim et al., 2001; Waggoner et al., 2001; Bany et al., 2003; Ringstad et al., 2008; Collins et al., 2016). However, we still do not know the cellular expression patterns of every single neurotransmitter GPCR in this circuit and thus which neurotransmitter GPCRs modulate the activity of this egg-laying circuit. Interestingly, the expression patterns for thirteen of these receptors have been previously analyzed (Cho et al., 2000; Lee et al., 2000; Tsalik et al., 2003; Chase et al., 2004; Rex et al., 2004; Carnell et a., 2005; Dempsey et al., 2005; Carre-Pierrat et al., 2006; Suo et al., 2006; Wragg et al., 2007; Hapiak et al., 2009; Plummer (2011); Gürel et al., 2012; Yemini et al., 2019) in different subsets of the *C. elegans* egg-laying system as described in Table 1.1. However, the only neurotransmitter GPCRs that are known to be involved in regulating egg laying are the serotonin GPCRs which are expressed in the vulval muscles (Desai et al., 1988, Shyn et al., 2003, Carnell et al., 2005; Hobson et at. 2006; Hapiak et al., 2009). We hope that by completely mapping all of the neurotransmitter GPCRs in the *C. elegans* egg-laying circuit, this will provide an insight as to the function of these receptors in this circuit.

While this thesis only covers using the Neurotransmitter GPCR Atlas of the *C. elegans* egg-laying system to better study the *C. elegans* egg-laying circuit, we hope that once the Neurotransmitter GPCR Atlas of the entire *C. elegans* nervous system is completed, the *C. elegans* neuroscience community can use this Atlas to better study function of their neurotransmitter GPCR in their neuronal circuit of interest.

Neurotransmitter GPCRs	G protein coupling	Previous expression patterns in the *C. elegans* egg-laying circuit
Serotonin receptors		
SER-1	$G\alpha_q$	Vulval muscles (Cho et al., 2000; Carnell et al., 2005; Dempsey et al., 2005), uterine cells (Carnell at al., 2005)
SER-4	$G\alpha_o$	vm2 (Gürel et al., 2012)
SER-5	$G\alpha_s$	Vulval muscle and body wall muscle (Hapiak et al., 2009; Carre-Pierrat et al., 2006)
SER-7	$G\alpha_s$	Vulval muscles (Carre-Pierrat et al., 2006)
Dopamine receptors		
DOP-1	$G\alpha_q$	
DOP-2	$G\alpha_o$	
DOP-3	$G\alpha_o$	Body wall muscles (Chase et al., 2004)
DOP-4	$G\alpha_s$	
Octopamine Receptors		
OCTR-1	$G\alpha_o$	Spermatheca and uterine toroid cell (Wragg et al., 2007)
SER-3	$G\alpha_q$	Spermatheca (Suo et al, 2006)
SER-6	$G\alpha_s$	
Tyramine Receptors		
SER-2	$G\alpha_o$	Body wall muscles (Tsalik et al., 2003) and uterine toroid cells 1 and 2 (Rex et al., 2004)
TYRA-2	$G\alpha_o$	
TYRA-3	$G\alpha_q$	Spermatheca (Carre-Pierrat et al., 2006) and vulval muscles (Wragg et al., 2007)
Acetylcholine Receptors		
GAR-1	$G\alpha_o$	
GAR-2	$G\alpha_o$	HSN (Lee et al., 2000)
GAR-3	$G\alpha_o$; $G\alpha_q$	
GABA Receptors		
GBB-1	$G\alpha_o$	HSN (Yemini et al., 2019)
GBB-2	$G\alpha_o$	
Glutamate Receptors		
MGL-1		
MGL-2	$G\alpha_q$	HSN (Yemini et al., 2019)
MGL-3		
Orphan Receptors		
ADOR-1		Vulval muscles (Plummer, 2011)
F35H10.10		
DOP-5		
DOP-6		

Table 1.1 Small-molecule neurotransmitter GPCRs in *C. elegans*. The 26 small-molecule neurotransmitter GPCRs are sorted into different families based on their ligand assignment. The G protein that each neurotransmitter GPCR couples to is shown. Previous expression patterns for neurotransmitter GPCRs in the *C. elegans* egg-laying circuit are shown.

Chapter 2: Pipeline to generate neurotransmitter GPCR::GFP transgenic strains

Some text, figures, and captions in Chapter 2 adapted from:

Fernandez, R.W., Wei, K., Wang, E.Y., Mikalauskaite, D., Olson, A., Pepper, J., Kim, S., Christie, N., Hasse, S., Sarov, M., and Koelle, M.R. Cellular expression and functional roles of 26 neurotransmitter GPCRs in the *C. elegans* egg-laying circuit. (2020)

This work was done in collaboration with undergraduate students Kimberly Wei and Erin Wang, former post-graduate student Deimante Mikalauskaite, postdoctoral researchers Andrew Olson and Seongseop Kim, former lab manager Judy Pepper, and our outside collaborators from Max Planck Institute of Molecular Cell Biology and Genetics in Dresden, Germany, Susanne Hasse and Mihail Sarov. Specifically, Robert W. Fernandez, Kimberly Wei and Erin Wang all contributed to screening extrachromosomal transgenic strains after microinjection, UV/TMP Chromosomal Integration of extrachromosomal transgenic strains, crossing integrated GPCR::GFP reporters to mCherry marker strains, and restriction digest of recombineered fosmids to get rid of unwanted genes or vector backbone. Deimante Mikalauskaite made recombineered GFP constructs for four neurotransmitter GPCRS. Andrew Olson and Seongseop Kim helped in the microinjection of GPCR::GFP transgenes. Robert W. Fernandez and Judy Pepper helped in the isolation of recombineered GPCR::GFP transgenes. Our outside collaborators Susanne Hasse and Mihail Sarov generated some recombineered GPCR::GFP transgenes.

2.1 Introduction

In this chapter, we describe how we made the Neurotransmitter GPCR Atlas of the *C. elegans* egg-laying system. We discuss the large fosmid-based GFP reporter transgenes for the 26 neurotransmitter GPCR genes, which includes: a) 20 C-terminal::GFP reporters that express a GPCR with GFP fused at the C-terminus of the receptor protein. b) Four reporters with an SL2 trans-splicing signal followed by GFP coding sequences inserted immediately downstream of the GPCR gene stop codon. c) Two reporters that were small promoter::GFP reporters that had been previously generated. Our pipeline to generate neurotransmitter GPCR::GFP transgenic strains includes: 1) Isolating the neurotransmitter GPCR::GFP transgenes from EPI300 *E. coli* cells. 2) Microinjection of GPCR::GFP transgenes to generate extrachromosomal GPCR::GFP transgenic strains. 3) UV/TMP chromosomal integration to generate several, integrated neurotransmitter GPCR::GFP lines. We also discuss using a restriction digest approach to get rid of other genes on the backbone of five GPCR::GFP transgenes, as microinjection of the entire GPCR::GFP transgene leads to lethality. We explain the three different mCherry markers we use that label the *C. elegans* egg-laying neurons, egg-laying muscles, and other non-neuronal and non-muscle cells near the egg-laying circuit. We discuss how we are identifying GPCR::GFP expression in different cells of the egg-laying circuit, taking into account variability and GFP intensity of the GPCR::GFP expressing cell. Lastly, we go over the type of analysis that can be done using the cellular

expression patterns of the neurotransmitter GPCRs expressed in the *C. elegans* egg-laying circuit.

2.2 GFP reporter transgenes for neurotransmitter GPCRs

Our goal is to create a map of all the 26 small-molecule neurotransmitter GPCRs in the *C. elegans* egg-laying system. This includes 21 neurotransmitter GPCRs for monoamines and classical neurotransmitters plus five additional "orphan" GPCRs (Table 1.1). Summarized in Table 1.1, the cellular expression patterns for thirteen of these receptors have been previously analyzed (Cho et al., 2000; Lee et al., 2000; Tsalik et al., 2003; Chase et al., 2004; Rex et al., 2004; Carnell et al., 2005; Dempsey et al., 2005; Carre-Pierrat et al., 2006; Suo et al., 2006; Wragg et al., 2007; Hapiak et al., 2009; Plummer, 2011; Gürel et al., 2012; Yemini et al., 2019) mostly based on green fluorescent protein (GFP) reporter transgenes in which GPCR gene promoter fragments of a few kilobases each were used to drive GFP expression with the exception of Yemini et al., 2019, which used a fosmid-based reporter for the GABA GPCR. Recent work has shown that obtaining accurate expression patterns often requires using much larger GFP reporter transgenes (Sarov et al., 2012; Serrano-Saiz et al., 2013; Pereira et al., 2016; Gendrel et al., 2016; Yemini et al., 2019). These are generated by inserting GFP coding sequences into a fosmid clones of *C. elegans* genomic DNA, including the full gene of interest and up to ~20 kb of flanking DNA on either side (Tursun et al., 2009).

Therefore, we sought to generate large GFP reporter transgenes for the 26 neurotransmitter GPCR genes (Figure 2.1 and Appendix Chapter 2). Thirteen

were already constructed as part of an effort to generate such transgenes for a large fraction of *C. elegans* genes (Sarov et al. 2012), and we constructed GFP reporters for seven more GPCR genes in a similar fashion. These "C-terminal::GFP" reporters express a GPCR with GFP fused at or very close to the C-terminus of the receptor protein (Figure 2.1 and Appendix Chapter 2). For a few receptors, such C-terminal::GFP fusion proteins were strongly localized to neural processes and excluded from the cell bodies, making it difficult to identify the GFP-expressing neurons. So, for four such receptors (the dopamine receptors DOP-1 and DOP-4, the acetylcholine receptor GAR-2, and the orphan receptor F35H10.10) we generated reporters with an SL2 trans-splicing signal followed by GFP coding sequences inserted immediately downstream of the GPCR gene stop codon (Tursun et al., 2009). Such "SL2::GFP" reporters (Figure 2.1 and Appendix Chapter 2) produce a single primary RNA transcript that is trans-spliced to produce separate GPCR and GFP mRNAs, so that the GFP produced fully fills out the cells that express the GPCR gene. For the remaining two receptors (the glutamate receptor MGL-2 and the serotonin receptor SER-4), technical issues precluded use of fosmid-based reporters, so we analyzed expression of smaller promoter::GFP reporters that had been previously generated (Tsalik et al., 2003; Gürel et al., 2012; Yemini et al., 2019).

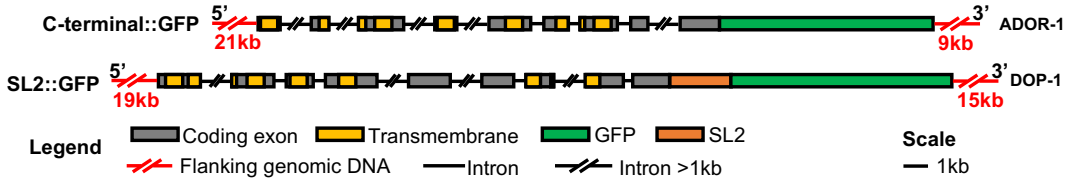

Figure 2.1 GFP reporter transgenes for neurotransmitter GPCRs. Schematics of two types of GFP reporters used in this study. C-terminal::GFP constructs are illustrated by the reporter for the orphan receptor ADOR-1. The fosmid clone used provides 21 kilobase (kb) of promoter region DNA 5' to the coding exons, and 9 kb of 3' DNA. GFP coding sequences were inserted into the last ADOR-1 coding exon so that the transgene expresses the receptor with GFP fused to its C terminus. SL2::GFP constructs are illustrated by the reporter for the dopamine receptor DOP-1. This reporter has 19 kb 5' and 15 kb 3' regions of *C. elegans* genomic DNA flanking the coding region. An SL2 trans-splicing signal followed by GFP coding sequences were inserted immediately downstream of the DOP-1 stop codon so that this reporter co-expresses DOP-1 and GFP as separate proteins. Analogous schematics of all 26 receptor::GFP reporter transgenes are found in the Appendix Chapter 2 and described in Table 2.1.

2.3 Generating GFP reporter transgenes

The GFP reporters for all 26 neurotransmitter GPCRs consist of 20 C-terminal GFP reporters, four SL2::GFP reporters, and two promoter::GFP reporters (Table 2.1 and Appendix Chapter 2).

Due to the recombination method used in Sarov et al., 2012, the C-terminal GPCR::GFP transgenes were stored in EPI300 *E.coli* non-clonal cells, where in the publication it states that 83% of the clones contain the correct recombineered GPCR::GFP construct, 7% of the clones contained the recombineered GPCR::GFP construct with mismatches, 4% of the clones were intermediate products of the recombineering process to generate the GPCR::GFP transgene, and 5% of the clones were cross-contaminants. Non-clonal EPI300 cells containing our C-terminal GPCR::GFP transgene with selection markers in the backbone were streaked onto a triple antibiotic plate (as described in the Methods Chapter 5.2.1) to ensure the colonies that grew contained our construct of interest. From the triple antibiotic plates containing EPI300 cells that express our GPCR::GFP transgene, we picked an individual colony to isolate our C-terminal GPCR::GFP transgene using a modified protocol from the Qiagen Plasmid Mini Kit. To ensure that our C-terminal GPCR::GFP transgene was at the correct size and not sheared, we ran it on a 0.4% Agarose Gel (Figure 2.2). Due to a population of the non-clonal EPI300 cells containing intermediate products, we wanted to make sure that the C-terminal GPCR::GFP transgene that was isolated actually contained GFP at the C-terminal. Therefore, we used two sets of sequencing primers to verify that GFP was inserted at the C-

terminal (Figure 2.3 and Appendix Chapter 2). This process was repeated for all 20 C-terminal GPCR::GFP transgenes. The SL2::GFP transgenes were recombineered by a former post-graduate researcher in the lab, Deimante Mikalauskaite, who followed the protocol provided by Tursun et al., 2009 where she recombineered SL2::GFP into the fosmid for each of the four neurotransmitter GPCRs (Appendix Chapter 2). These recombineered SL2::GFP fosmid constructs were run on a 0.4% agarose gel to determine the construct was at the correct size. For the remaining two promoter::GFP reporters, we received a plasmid for the glutamate GPCR MGL-2 (Yemini et al., 2019) and for the serotonin GPCR SER-4, a chromosomally integrated line was previously made (Gürel et al., 2012).

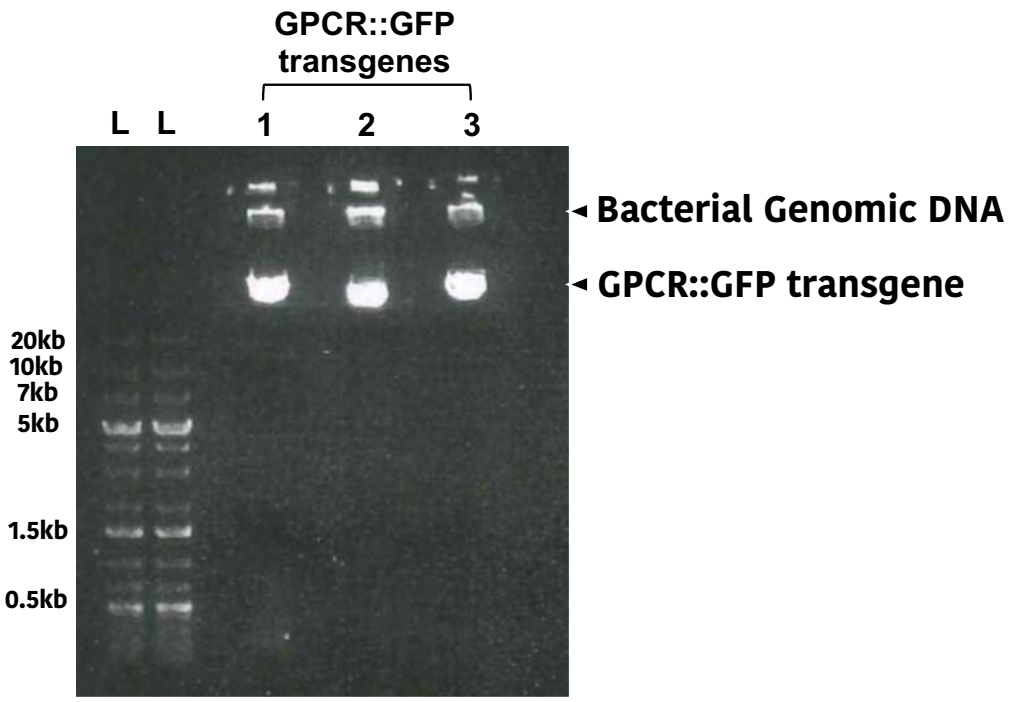

Figure 2.2. Isolation of GPCR::GFP transgenes from EPI300 *E. coli* cells. Three independent GPCR::GFP transgenes were isolated from EPI300 *E. coli* cells using a Qiagen Plasmid Mini Kit and run on a 0.4% agarose gel to determine the GPCR::GFP transgene was at the expected size and separated from the bacterial genomic DNA. L: GeneRuler 1kb Plus DNA Ladder.

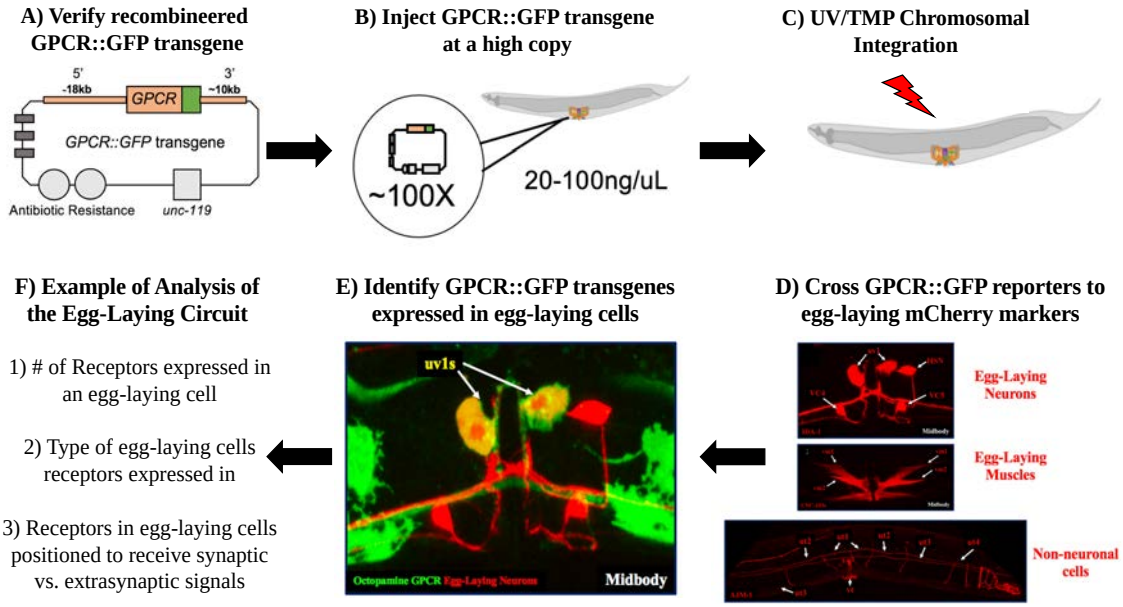

Figure 2.3 Pipeline to generate a Neurotransmitter GPCR Atlas of the *C. elegans* egg-laying circuit. A) Recombineered transgenes isolated from non-clonal bacterial culture were send out for sequencing to determine GFP was tagged at the C-terminal of the neurotransmitter receptor gene of interest. **B)** Recombineered neurotransmitter receptor transgene were microinjected at a high concentration to generate extrachromosomal GPCR::GFP transgenic strains. **C)** UV/TMP Chromosomal integration of extrachromosomal transgenic strains to generated integrated GPCR::GFP transgenic strains. **D)** GPCR::GFP transgenic strains crossed to mCherry marker strains that label subsets (egg-laying neurons, egg-laying muscles, or other cells near the egg-laying circuit) of the egg-laying system. **E)** Confocal microscopy of double-labeled animals to accurately identify neurotransmitter GPCRS in the all of the cells of the *C. elegans* egg-laying system. **F)** Type of analysis that can be done on the Neurotransmitter GPCR Atlas of the *C. elegans* egg-laying system.

2.4 Restriction digest of GPCR::GFP transgenes

After isolating the recombineered C-terminal GFP transgenes for 20 neurotransmitter GPCRs, the next step in the pipeline is the microinjection of the transgenes to generate extrachromosomal GPCR::GFP transgenic strains (Figure 2.3). Initially, we attempted microinjection of five recombineered transgenes (*dop-3::gfp*; *tyra-2::gfp*; *tyra-3::gfp*; *mgl-3::gfp*; *dop-5::gfp*) along with their *lin-15* rescue marker into *lin-15(765ts)* animals. As *lin-15(765ts)* animals have a multi-vulva phenotype at 20°C, a successful transformation is indicated by the absence of the multi-vulva phenotype and bright GFP+ animals in independent lines. However, microinjection of the five recombineered transgenes resulted in lines that were rescued for the multi-vulva phenotype but there was no visible GFP expression.

We rationalized that other genes on the fosmid of the C-terminal GFP reporter transgenes may have been responsible for silencing GFP in the extrachromosomal lines. Our approach was to use restriction enzymes to cut out other genes on the fosmid for each of our five recombineered transgenes (Table 2.1 and Appendix Chapter 2), isolate our smaller GPCR::GFP transgene and microinject the smaller GPCR::GFP transgene to get stable, extrachromosomal lines expressing GFP for each of our five transgenes. To ensure that we had enough product (shorter GPCR::GFP transgene) for microinjection after the restriction digest, our starting product contained three to ten replicates using 1-3 µg of our recombineered transgene.

We piloted our strategy of restriction digest of GPCR::GFP transgenes with the *dop-3::gfp* transgene, where the entire construct was 45.4kb. Three replicates of 2 µg of the *dop-3::gfp* transgene was digested with 10 U NotI-HF and 10 U AfeI incubated at 37°C for 2 hours and ran the entire restriction digest on a 0.4% agarose gel at 26 V for 10 hours to ensure proper separation. As seen in Figure 2.4, our shorter *dop-3::gfp* transgene was 26.8kb in size. Using a modified protocol of the QIAEX II Gel Extraction Kit, we isolated our 26.8kb *dop-3::gfp* transgene. We ran the 26.8kb *dop-3::gfp* transgene on a 0.4% agarose gel to verify it is at the correct size (Figure 2.5) followed by a successful microinjection as we had stable DOP-3::GFP transgenic strains brightly expressing GFP.

After success of this restriction digest approach to use short GPCR::GFP transgenes to generate stable extrachromosomal lines expressing GFP, we proceeded to repeat this process for the rest of the four remaining transgenes (Table 2.1). Ten replicates of 2 µg of the 53.8kb *tyra-2::gfp* transgene was digested with 10 U SacII and 10 U StuI incubated at 37°C for 2 hours, the restriction digest was run on a 0.4% agarose gel at 57 V for 10hrs, and we had a shorter 39.7kb *tyra-2::gfp* transgene (Figure 2.6). We ran the 39.7kb *tyra-2::gfp* transgene on a 0.4% agarose gel to verify it is at the correct size (Figure 2.7). Microinjection of this transgene resulted in a TYRA-2::GFP transgenic strain.

Ten replicates of 1 µg of the 49.1kb *tyra-3::gfp* transgene were digested with 5 U SbfI and 5 U AfeI incubated at 37°C for 3 hours, the restriction digest was run on a 0.4% agarose gel at 57 V for 12 hours, and we had a shorter

31.5kb *tyra-3::gfp* transgene (Figure 2.8). We ran the 31.5kb *tyra-3::gfp* transgene on a 0.4% agarose gel to verify it is at the correct size (Figure 2.9). Microinjection of this transgene resulted in a TYRA-3::GFP transgenic strain.

Ten replicates of 3 µg of the 44.8kb *mgl-3::gfp* transgene was digested with 10 U PluTI and 10 U BmtI-HF incubated at 37°C for 2 hours, the restriction digest was run on a 0.4% agarose gel at 36 V for 14 hours, and we had a shorter 25.2kb *mgl-3::gfp* transgene (Figure 2.10). We did notice the presence of a 13kb product we did not expect from the restriction digest, but as our smaller products were 5kb and 8kb in size, the presence of this 13kb product was most likely due to an incomplete digest. We ran the 25.2kb *mgl-3::gfp* transgene on a 0.4% agarose gel to verify it is at the correct size (Figure 2.11). Microinjection of this transgene resulted in a MGL-3::GFP transgenic strain.

Ten replicates of 2.5 µg of the 44.6kb *dop-5::gfp* transgene was digested with 10 U AhdI and 10 U AvrII incubated at 37°C for 2 hours, the restriction digest was run on a 0.4% agarose gel at 57 V for 9 hours, and we had a shorter 25.4kb *dop-5::gfp* transgene (Figure 2.12). We did notice the presence of a 18kb product we did not expect from the restriction digest, but as our smaller products were 5.3kb, 5.8kb and 8kb in size, the presence of this 18kb product was most likely due to an incomplete digest. Interestingly, we also did not see an expected 8kb product, which might indicate there was an incomplete digest (Figure 2.12). We ran the 25.4kb *dop-5::gfp* transgene on a 0.4% agarose gel to verify it is at the correct size (Figure 2.13). Microinjection of this transgene resulted in a DOP-5::GFP transgenic strain.

For the *mgl-3::gfp* and *dop-5::gfp* transgene, we did see in Figure 2.10 and Figure 2.12, respectively that the restriction digest of the GPCR::GFP transgene yielded other products that may have been a result of an incomplete digest.

However, we wanted to confirm that we isolated the correct product for the *mgl-3::gfp* and *dop-5::gfp* transgene. We designed primers that amplified the ends for each of our transgene one kb away from the cut site, where the presence of a band indicates that we isolated the correct product. For the 25.19kb *mgl-3::gfp* transgene, we used two sets of primers to amplify a few hundred base pairs away from the PluTI cut site and BmtI cut site, we amplified both products indicating we did isolate the 25.19kb *mgl-3::gfp* transgene (Figure 2.14). For the 25.365kb *dop-5::gfp* transgene, we used two sets of primers to amplify a few hundred base pairs away from the AvrII cut site and AhdI cut site. However, we only saw a band for the AvrII cut site and no band was seen for the AhdI cut site (Figure 2.14). To confirm that the 25.365kb *dop-5::gfp* transgene actually had GFP present, we used two sets of primers that spanned the GFP site, and we saw a band present (data not shown), indicating that our isolated product is the correct 25.365kb *dop-5::gfp* transgene.

Neurotransmitter GPCR::GFP transgene	Neurotransmitter GPCR::GFP transgene size	Restriction enzymes	Expected products size
dop-3::gfp	45.442kb	NotI, AfeI	**28.66kb**, 9.277kb, 3.923kb, 3.575kb
tyra-2::gfp	53.802kb	SacII, StuI	**39.671kb**, 10.211kb, 3.229kb, 0.691kb
tyra-3::gfp	49.065kb	SbfI, AfeI	**31.481kb**, 10.644kb, 6.399kb, 0.541kb
mgl-3::gfp	44.849kb	BmtI, PluTI	**25.19kb**, 8.504kb, 5.706kb, 5.449kb
dop-5::gfp	44.624kb	AvrII, AhdI	**25.365kb**, 8.081kb, 5.795kb, 5.383kb

Table 2.1 Restriction digest of neurotransmitter GPCR::GFP transgenes. For the five neurotransmitter GPCR::GFP transgenes, we noted the size of the entire GPCR::GFP transgene, the restriction enzymes used to digest the GPCR::GFP transgene, and the size of the products after restriction digest. Our product of interest after restriction digest is bolded.

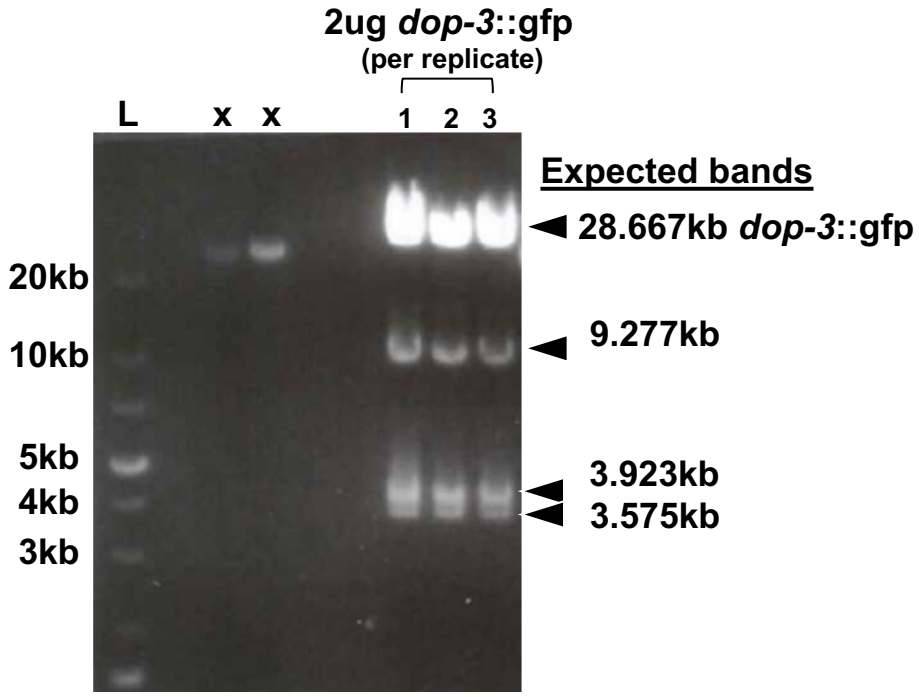

Figure 2.4 Restriction digest of the 45.442kb *dop-3::gfp* transgene. Three replicates of 2 ug of *dop-3::gfp* was incubated at 37°C for 2 hours with the restriction enzymes 10 U NotI and 10 U AfeI. The entire restriction digest was run on a 0.4% agarose gel at 36 V for 10 hours to ensure proper separation. Our product of interest (*dop-3::gfp*) is at 28.667kb and the size of the other products are listed next to the black triangles. L: GeneRuler 1kb Plus DNA Ladder; X: unrelated DNA band.

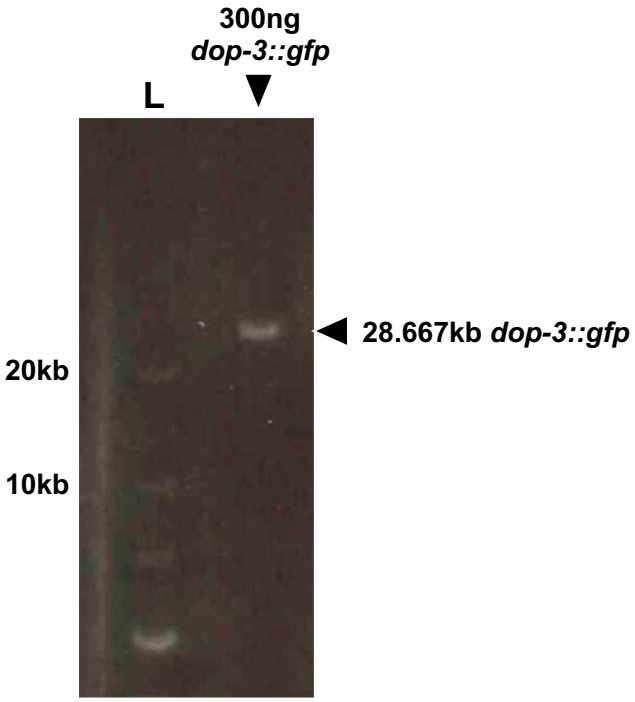

Figure 2.5 Confirming the gel purified *dop-3::gfp* transgene was at the expected size. After gel purification of the 28.667kb *dop-3::gfp* transgene, 300 ng of the *dop-3::gfp* transgene was run on a 0.4% agarose gel at 36 V for 10 hours to confirm the product was at the expected size. L: GeneRuler 1kb Plus DNA Ladder.

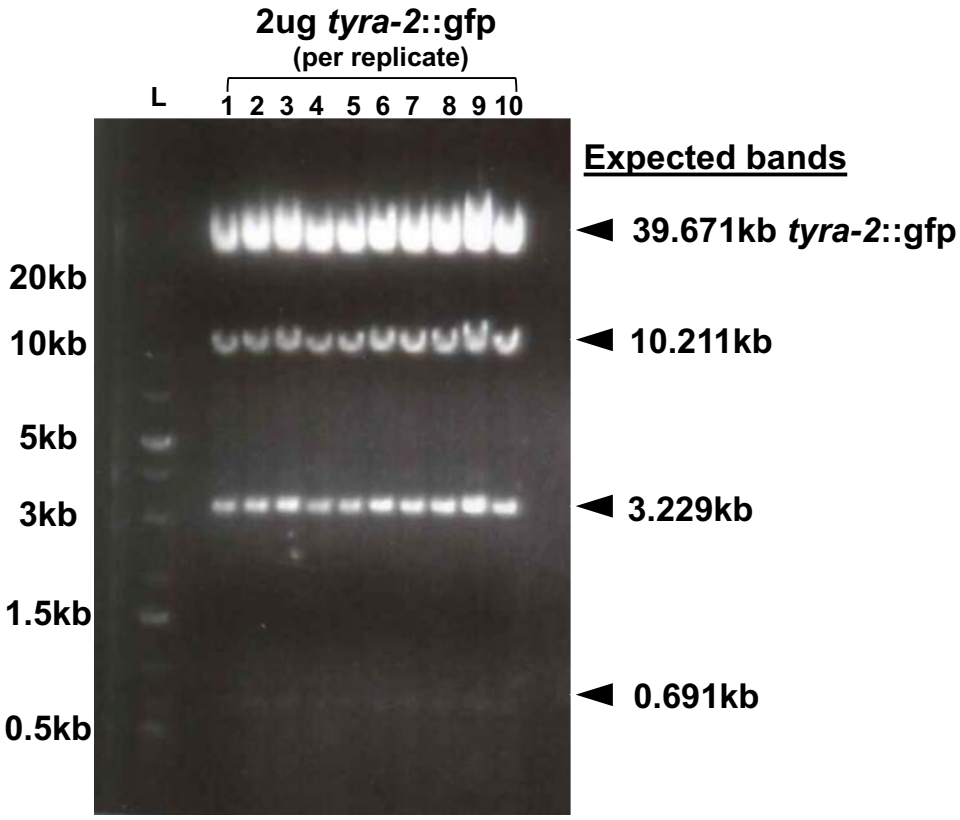

Figure 2.6 Restriction digest of the 53.802kb *tyra-2::gfp* transgene. Ten replicates of 2 ug of *tyra-2::gfp* was incubated at 37°C for 2 hours with the restriction enzymes 10 U SacII and 10 U StuI. The entire restriction digest was run on a 0.4% agarose gel at 57 V for 10hours to ensure proper separation. Our product of interest (*tyra-2::gfp*) is at 39.671kb and the size of the other products are listed next to the black triangles. L: GeneRuler 1kb Plus DNA Ladder.

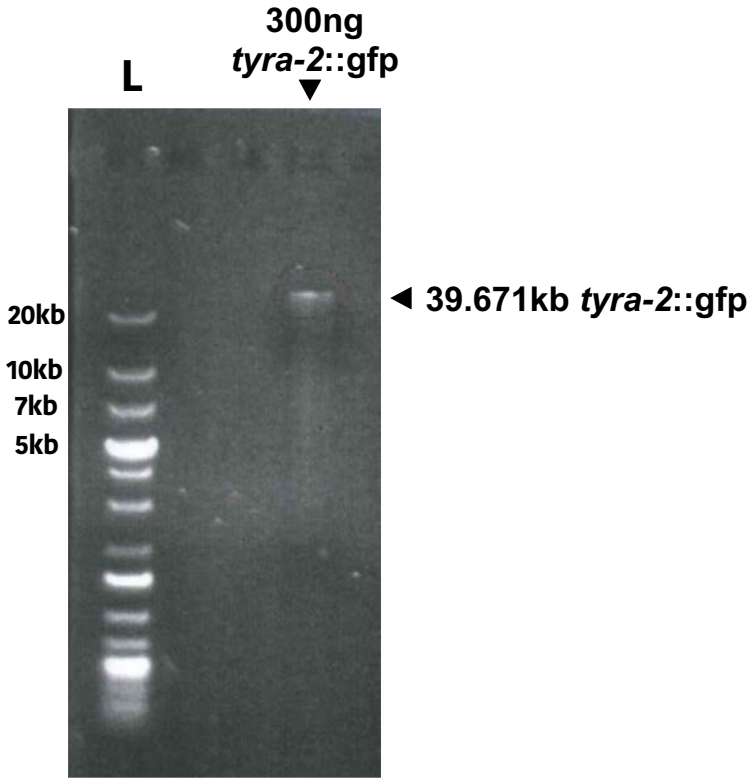

Figure 2.7 Confirming the gel purified *tyra-2::gfp* transgene was at the expected size. After gel purification of the 39.671kb *tyra-2::gfp* transgene, 300 ng of the *tyra-2::gfp* transgene was run on a 0.4% agarose gel at 57 V for 8 hours to confirm the product was at the expected size. L: GeneRuler 1kb Plus DNA Ladder.

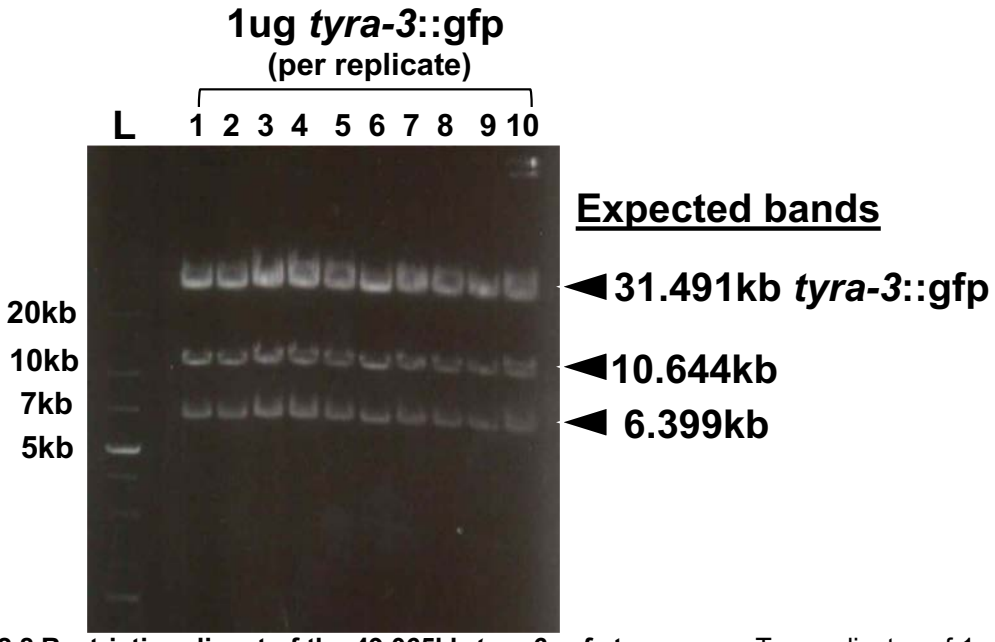

Figure 2.8 Restriction digest of the 49.065kb *tyra-3::gfp* transgene. Ten replicates of 1 ug of *tyra-3::gfp* was incubated at 37°C for 3 hours with the restriction enzymes 5 U SbfI and 5 U AfeI. The entire restriction digest was run on a 0.4% agarose gel at 57 V for 12 hours to ensure proper separation. Our product of interest (*tyra-3::gfp*) is at 31.491kb and the size of the other products are listed next to the black triangles. L: GeneRuler 1kb Plus DNA Ladder.

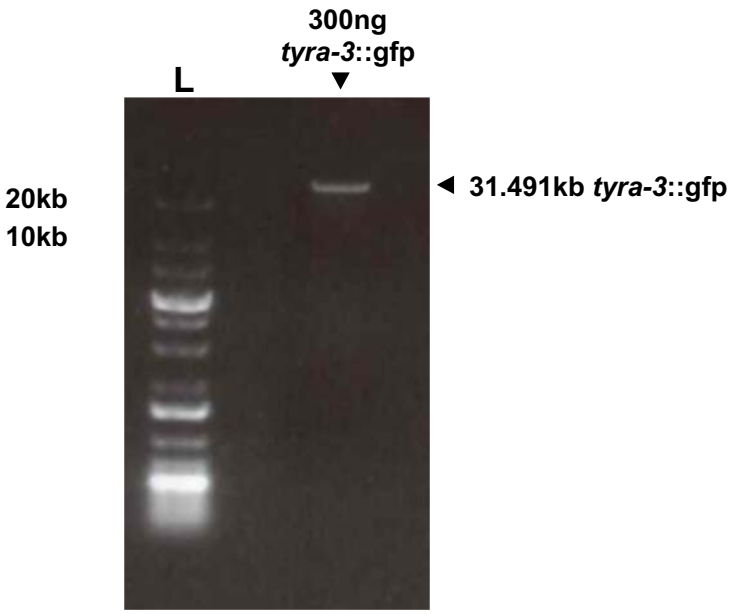

Figure 2.9 Confirming the gel purified *tyra-3::gfp* transgene was at the expected size. After gel purification of the 31.491kb *tyra-3::gfp* transgene, 300 ng of the *tyra-3::gfp* transgene was run on a 0.4% agarose gel at 36 V for 4 hours to confirm the product was at the expected size. L: GeneRuler 1kb Plus DNA Ladder.

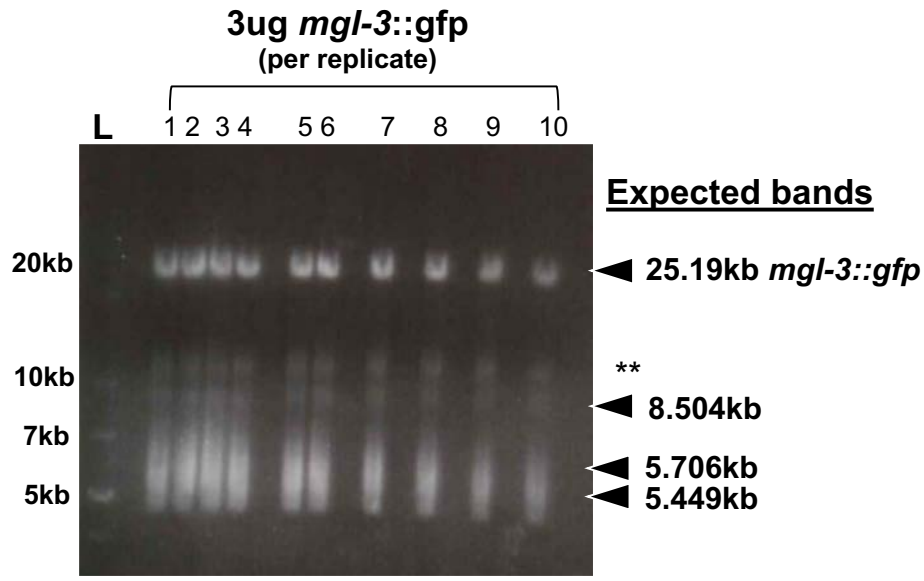

Figure 2.10 Restriction digest of the 44.894kb *mgl-3::gfp* transgene. Ten replicates of 3 ug of *mgl-3::gfp* was incubated at 37°C for 2 hours with the restriction enzymes 10 U BmtI and 10 U PluTI. The entire restriction digest was run on a 0.4% agarose gel at 36 V for 14hours to ensure proper separation. Our product of interest (*mgl-3::gfp*) is at 25.19kb and the size of the other products are listed next to the black triangles. L: GeneRuler 1kb Plus DNA Ladder. **: Products from an incomplete digest.

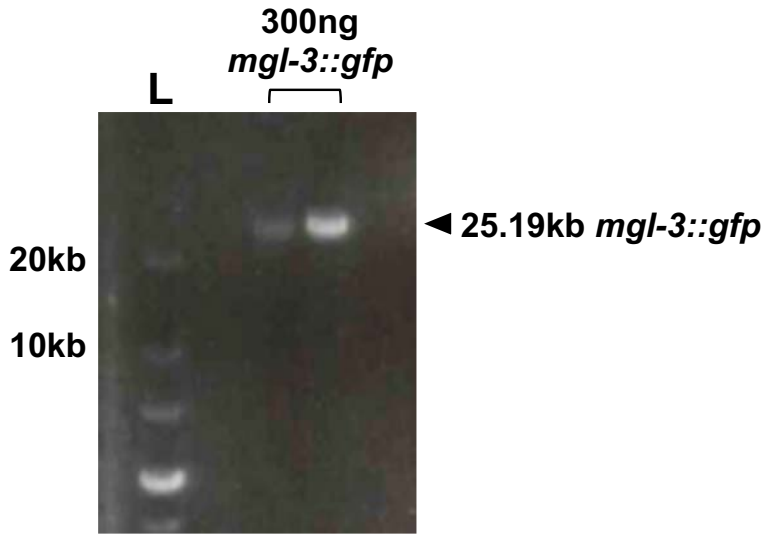

Figure 2.11 Confirming the gel purified *mgl-3::gfp* transgene was at the expected size. After gel purification of the 25.19kb *mgl-3::gfp* transgene, two replicates of 300 ng of the *mgl-3::gfp* transgene was run on a 0.4% agarose gel at 36 V for 10 hours to confirm the product was at the expected size. L: GeneRuler 1kb Plus DNA Ladder.

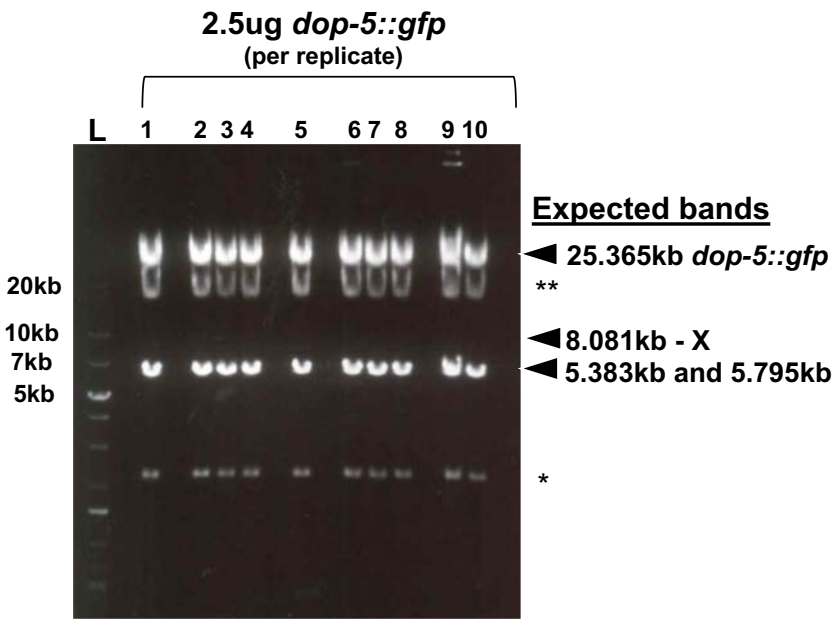

Figure 2.12 Restriction digest of the 44.624kb *dop-5::gfp* transgene. Ten replicates of 2.5 ug of *dop-5::gfp* was incubated at 37°C for 2 hours with the restriction enzymes 10 U AvrII and 10 U AhdI. The entire restriction digest was run on a 0.4% agarose gel at 57 V for 9.5 hours to ensure proper separation. Our product of interest (*dop-5::gfp*) is at 25.365kb and the size of the other products are listed next to the black triangles. L: GeneRuler 1kb Plus DNA Ladder. **: Products from an incomplete digest. *: Star activity. X: Product was not found.

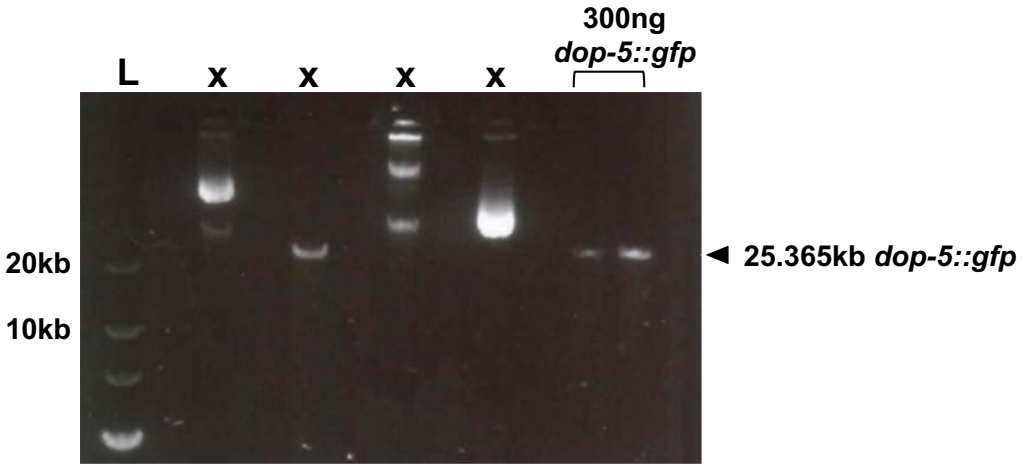

Figure 2.13 Confirming the gel purified *dop-5::gfp* transgene was at the expected size. After gel purification of the 25.365kb *dop-5::gfp* transgene, two replicates of 300 ng of the *dop-5::gfp* transgene was run on a 0.4% agarose gel at 36 V for 10 hours to confirm the product was at the expected size. L: GeneRuler 1kb Plus DNA Ladder. X: unrelated DNA bands.

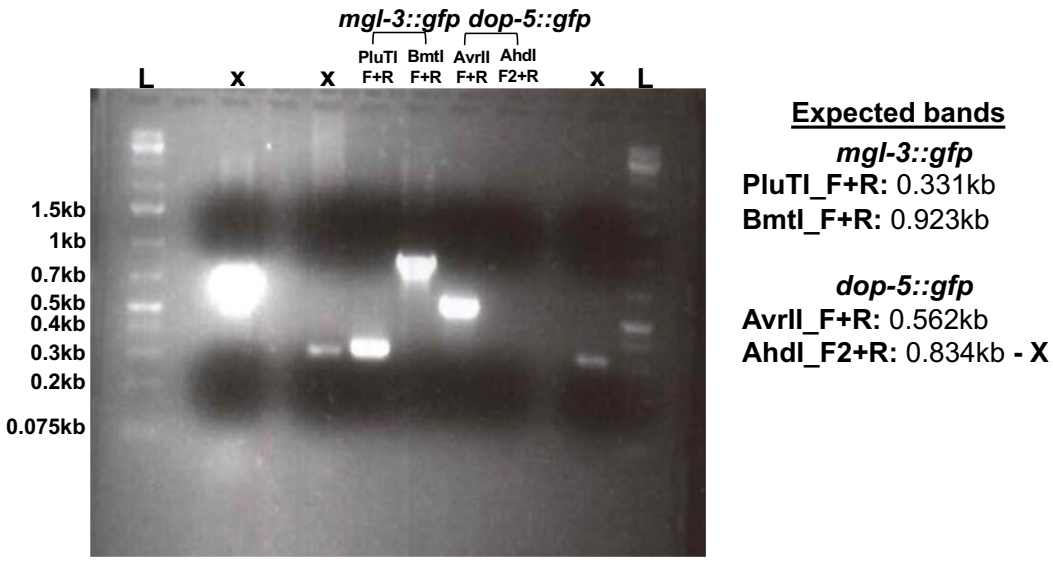

Figure 2.14 Confirming the ends of the purified *mgl-3::gfp* and *dop-5::gfp* transgene. To confirm that the 25.19kb *mgl-3::gfp* transgene was purified, two sets of primers were made that amplified a few hundred base pairs away from the PluTI cut site and BmtI cut site. The forward and reverse primer near the PluTI cut site yields a 0.331kb product and the forward and reverse primer near the BmtI cut site yields a 0.923kb product. To confirm that the 25.365kb *dop-5::gfp* transgene was purified, two sets of primers were made that amplified a few hundred base pairs away from the AvrII cut site and AhdI cut site. The forward and reverse primer near the AvrII cut site yields a 0.562kb product and the forward and reverse primer near the AhdI cut site yields a 0.834kb product (not found). L: GeneRuler 1kb Plus DNA Ladder. X: unrelated DNA bands.

2.5 Generating neurotransmitter GPCR::GFP transgenic strains

The 25 GFP reporter transgenes for neurotransmitter GPCRs, consisting of 20 C-terminal GFP reporters, four SL2::GFP reporters, and one promoter::GFP reporter were successfully microinjected to produce high-copy extrachromosomal transgenes. Further information on the concentration of the GFP reporter transgene used for microinjections along with co-injection markers are described in Table 2.2. and Chapter 5.2.2. The high-copy nature of the reporter transgenes means that they are expressed in the same cells as the corresponding endogenous genes (Serrano-Saiz et al., 2013; Pereira et al., 2016; Gendrel et al., 2016), but at increased levels, increasing the GFP fluorescence produced so that even cells that express a GPCR gene at low levels could be identified. Each of the extrachromosomal GFP reporter strains for the 25 neurotransmitter GPCRs were then chromosomally integrated (Figure 2.3 and described in Chapter 5.2.3). In addition to the integrated SER-4::GFP transgenic strain (Gürel et al., 2012), we have a total of 26 chromosomally integrated GFP reporters. For several neurotransmitter GPCR transgenes, we have several independent chromosomally integrated lines as listed in Table 2.2.

Neurotransmitter GPCR::GFP transgenes	Microinjection conditions to generate extrachromosomal GPCR::GFP lines	# of integrated GPCR::GFP lines
ser-1::gfp	*ser-1(fosmid)::GFP 60ng/uL + pLI15EK 50ng/uL + DH5α 25ng/uL*	3
ser-4(7.8kb)::gfp	N/A [Tsalik et al., 2003]	1
ser-5::gfp	*ser-5(fosmid)::gfp 50ng/uL + pLI15EK 50ng/uL + DH5α 25ng/uL*	1
ser-7::gfp	*ser-7(fosmid)::gfp 60ng/uL + pLI15EK 50ng/uL + DH5α 25ng/uL*	4
dop-1::SL2::NLS::gfp	*dop-1(fosmid)::SL2::NLS::gfp 60ng/uL + pLI15EK 50ng/uL + DH5α 25ng/uL*	3
dop-2::gfp	*dop-2(fosmid)::gfp + unc-119 (+) 50ng/uL + pLI15EK 50ng/uL*	3
dop-3::gfp	*dop-3(fosmid)::gfp 20ng/uL + pLI15EK 50ng/uL + DH5α 25ng/uL*	3
dop-4:SL2::NLS::gfp	*dop-4(fosmid)::SL2::NLS::gfp 60ng/uL + pLI15EK 50ng/uL + DH5α 25ng/uL*	6
octr-1::gfp	*octr-1(fosmid)::gfp + unc-119 (+) 100ng/uL*	1
ser-3::gfp	*ser-3(fosmid)::gfp + unc-119 (+) 100ng/uL*	2
ser-6::gfp	*ser-6(fosmid)::gfp + unc-119 (+) 100ng/uL*	1
ser-2::gfp	*ser-2(fosmid)::gfp + unc-119 (+) 100ng/uL*	1
tyra-2::gfp	*tyra-2(fosmid)::gfp 20ng/uL + pLI15EK 50ng/uL + DH5α 25ng/uL*	4
tyra-3::gfp	*tyra-3(fosmid)::gfp 20ng/uL + pLI15EK 50ng/uL + DH5α 25ng/uL*	1
gar-1::gfp	*gar-1(fosmid)::gfp + unc-119 (+) 100ng/uL*	1
gar-2::SL2::NLS::gfp	*gar-2(fosmid)::SL2::NLS::gfp 60ng/uL + pLI15EK 50ng/uL + DH5α 25ng/uL*	1
gar-3::gfp	*gar-3(fosmid)::gfp 60ng/uL + pLI15EK 50ng/uL + DH5α 25ng/uL*	4
gbb-1::gfp	*gbb-1(fosmid)::gfp + unc-119 (+) 100ng/uL*	2
gbb-2::gfp	*gbb-2(fosmid)::gfp 60ng/uL + pLI15EK 50ng/uL + DH5α 25ng/uL*	2
mgl-1::gfp	*mgl-1(fosmid)::gfp + unc-119 (+) 100ng/uL*	4
mgl-2(7.9kb)::gfp	*mgl-2(7.9kb)::gfp 30ng/uL + pLI15EK 50ng/uL + DH5α 25ng/uL*	1
mgl-3::gfp	*mgl-3(fosmid)::gfp 20ng/uL + pLI15EK 50ng/uL + DH5α 25ng/uL*	1
ador-1::gfp	*ador-1(fosmid)::gfp + unc-119 (+) 100ng/uL*	4
F35H10.10::GFP	*F35H10.10(fosmid)::SL2::NLS::gfp 60ng/uL + pLI15EK 50ng/uL + DH5α 25ng/uL*	6
dop-5::gfp	*dop-5(fosmid)::gfp 20ng/uL + pLI15EK 50ng/uL + DH5α 25ng/uL*	3
dop-6::gfp	*dop-6(fosmid)::gfp 60ng/uL + pLI15EK 50ng/uL + DH5α 25ng/uL*	2

Table 2.2 Neurotransmitter GPCR::GFP transgenic strains. For each neurotransmitter GPCR::GFP transgene, the concentrations used for microinjection of the GPCR::GFP transgene and co-injection markers (*pLI15EK* and *DH5α*) are noted. The number of GPCR::GFP chromosomal integrants are listed. Further details are provided in Methods Chapter 5.2.

2.6 mCherry markers to identify cells of the *C. elegans* egg-laying system

To accurately identify the cells of the egg-laying system that our 26 neurotransmitter GPCRs are expressed in, we obtained chromosomally-integrated transgenes that express mCherry in each cell type of the egg-laying system (Figure 2.15). Neurons of the egg-laying system are labeled by the *ida-1::mCherry* marker (Figures 2.15A). These neurons are: 1) the HSN neurons, which promote egg-laying events by releasing serotonin and neuropeptides (Waggoner et al., 1998; Shyn et al., 2003; Hapiak et al., 2009; Emtage et al., 2012; Brewer et al., 2019); 2) the uv1 neuroendocrine cells, which release tyramine and neuropeptides to inhibit egg-laying (Collins et al., 2016; Banerjee et al., 2017); and 3) the VC4/5 neurons, which release acetylcholine via synapses onto the vm2 egg-laying muscles (Collins et al., 2016). The *unc-103e::mCherry* marker labels the vm1 and vm2 vulval muscles and was also used as a landmark to identify the um1 and um2 uterine muscles (Figure 2.15B). Eggs are laid when vm1 and vm2 muscle cells open up the vulva and the um1 and um2 muscles squeeze eggs out the uterus through the vulva to the outside of the animal (Kim et al., 2001; Waggoner et al., 2001; Bany et al., 2003; Ringstad et al., 2008; Collins et al., 2016). There are also body wall muscle cells (bwms; not shown in Figure 2.15) surrounding the egg-laying system. The *ajm-1::mCherry* marker labels the junctions between most of the cells that make up the uterus and vulva (Figure 2.15C). Eggs are fertilized in the spermatheca (sp), and enter the uterus via the spermatheca-uterine (sp-ut) valve. The uterus itself comprises the ut1-ut4 uterine toroid cells and dorsal uterine (du) cells that together form a tube to hold

eggs. Eggs pass from the uterus into the vulva through a junction comprising the uterine seam (utse) and uterine-ventral (uv1, uv2, uv3) cells, and the vulva itself comprises several types of vulval toroid (vt) cells (Schindlet and Sherwood, 2014; Ghosh and Sternberg, 2014; Ecsedi et al., 2015).

For each of our GFP reporters for the 26 neurotransmitter GPCRs, we genetically crossed them to the *ida-1::mCherry* strain that labels the egg-laying neurons and if we saw expression in the egg-laying muscles or other cells near the egg-laying circuit, they were also crossed to the *unc-103e::mCherry* or *ajm-1::mCherry*, respectively (Figure 2.3). A complete list of all of the double-labeled strains for the 26 neurotransmitter GPCRs are listed in Appendix Chapter 5.

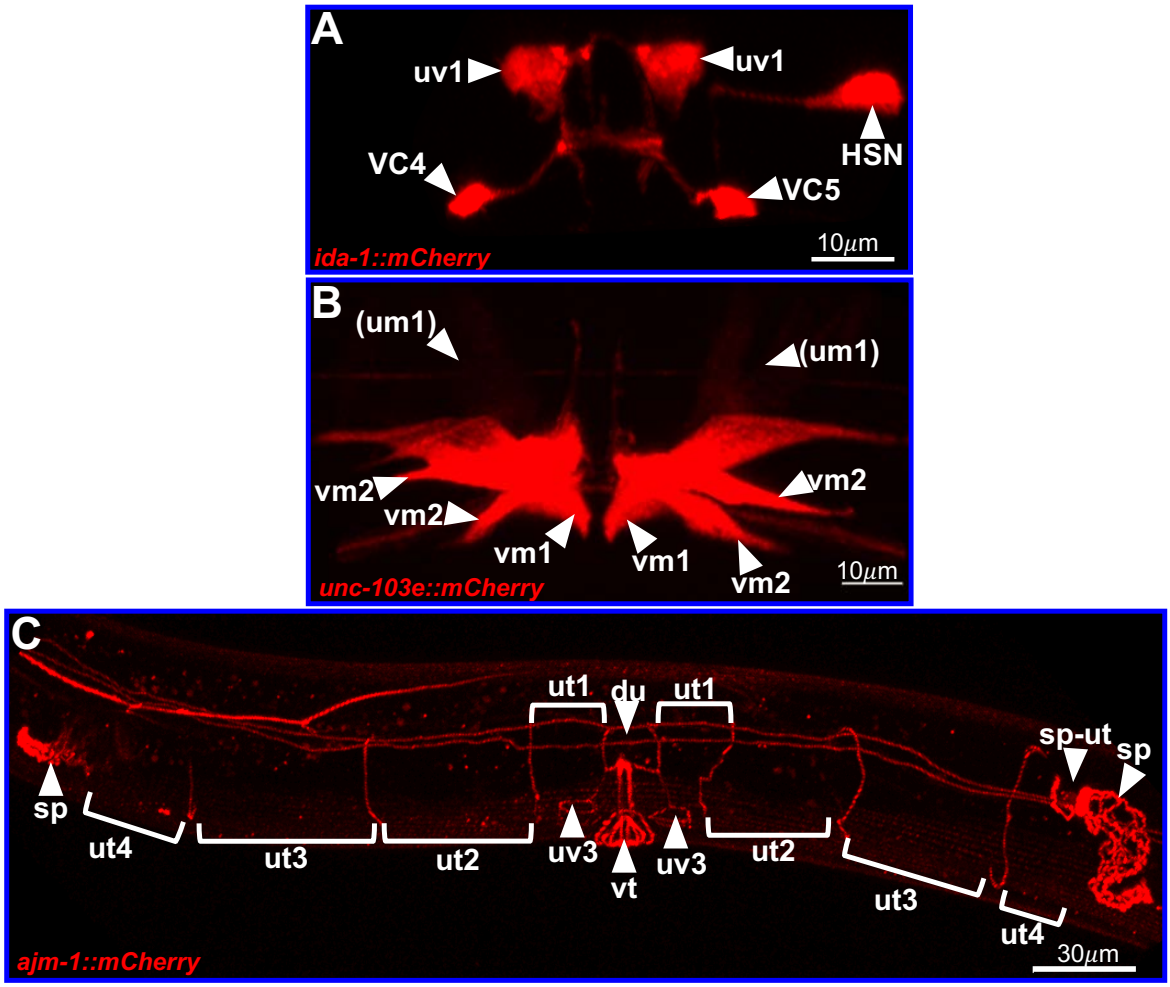

Figure 2.15 mCherry markers that label subsets of the *C. elegans* egg-laying system. **A**) Two-dimensional renderings of a confocal image of *C. elegans* egg-laying neurons labeled by the *ida-1::mCherry* marker. Scale: 10μm. For this panel and the next, white triangles or brackets point to the cells that are labeled. **B**) Two-dimensional renderings of a confocal image of *C. elegans* egg-laying muscles labeled by the *unc-103e::mCherry* marker. Scale: 10μm. The parenthesis indicates that the uterine muscles um1 are difficult to see in the *unc-103e::mCherry* marker without rendering at a higher mCherry intensity. **C**) Two-dimensional renderings of a confocal image of other cells near the *C. elegans* egg-laying circuit labeled by the *ajm-1::mCherry* marker. Scale: 30μm. Cell types are denoted by the following abbreviation: du: dorsal uterine cell; HSN: hermaphrodite-specific neuron; sp: spermatheca; sp-ut: spermatheca-uterine valve; um: uterine muscle; ut: uterine toroid cell; uv: uterine ventral cell; VC: ventral cord type C neuron; vm: vulval muscle; vt: vulval toroid cells.

2.7 Strategy to identify GPCR::GFP expression in cells of the *C. elegans* egg-laying system

As our GFP reporters for the 26 neurotransmitter GPCRs were genetically crossed to at most three different egg-laying mCherry markers strains, we sought to 1) accurately identify every cell of the egg-laying system that expresses each of the 26 neurotransmitter GPCR::GFP transgenes; 2) qualitatively record the GFP expression levels for each reporter in each cell, which may reflect expression levels of the endogenous receptors; and 3) record animal-to animal variability in GFP expression levels from these reporters, which may reflect variability in expression of the endogenous receptors.

For all 26 neurotransmitter GPCR::GFP transgenes, three-dimensional confocal images of the egg-laying system were collected for at least 10 young adult animals per double-labeled strain. The process for identifying GFP-expressing cells and qualitatively scoring GFP levels is illustrated for the octopamine receptor OCTR-1 in Figure 2.16. Each image was analyzed in three dimensions using rotations, cuts through the image volumes, and mCherry markers to reveal and identify internal features. We scored the strongest GFP expressing cells in a strain as “+++”, those with GFP that was easily detectable as “++”, and those with GFP just above background as “+” as seen in Figure 2.16. For example, *octr-1::gfp* expression in the uterine toroid cells ut2 and ut3 as well as the uv1s were scored as “+++” (Figure 2.16B and Figure 2.16D). *octr-1::gfp* expression in the HSN were scored as “++” while *octr-1::gfp* expression in vulval muscles were scored as “+” (Figure 2.16F).

We next went on to record animal-to animal variability in GFP expression levels, and we noticed that *octr-1::gfp* expression in the uv1s were consistent across different three different animals (Figure 2.17). Interestingly, we noticed that even though each GPCR::GFP transgene is stably chromosomally integrated, a number of these transgenes show variation in the intensity and even presence of GFP expression in individual cell types. For example, *octr-1::gfp* expression in the HSN range from "++" to completely absent across three different animals (Figure 2.18); this was also consistent with *octr-1::gfp* expression in VC4 and VC5 neurons, which ranged from "++" to completely absent (Figure 2.19). We proceeded to do qualitatively record the GFP expression levels and record animal to animal variability in the GFP expression levels for all 26 neurotransmitter GPCRs in different egg-laying mCherry markers.

As a side-note, we note that for reporters that express a receptor with GFP fused to its C-terminus, the fusion proteins were sometimes subcellularly localized. An example is seen for *octr-1::gfp* in the uterine toroid cells ut2 in Figure 2.16. Because these are fusion proteins and are overexpressed due to the high-copy number of the transgenes, it is unclear if such subcellular localization might reflect a similar localization of the corresponding endogenous receptors. Thus, we chose not to try to interpret such subcellular localization in this work.

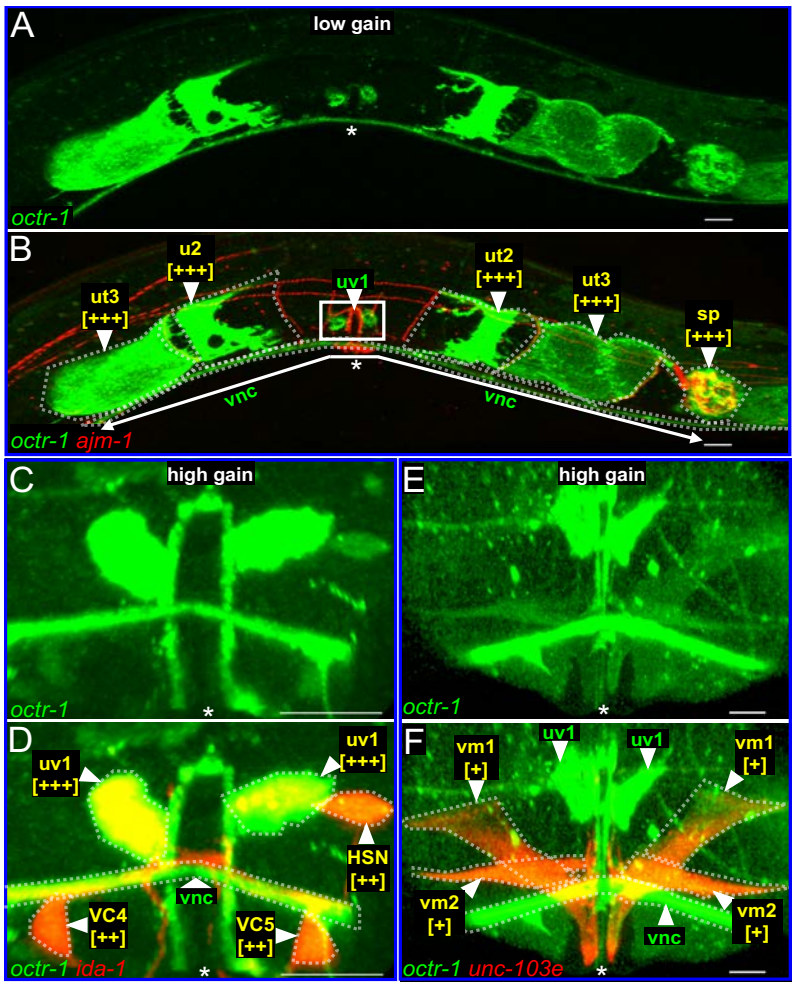

Figure 2.16: Identification of cells of the *C. elegans* egg-laying system expressing the octopamine GPCR OCTR-1. (A and B) Two-dimensional renderings of a confocal image of the egg-laying system in a chromosomally integrated *octr-1::gfp; ajm-1::mCherry* young adult showing GFP (A) or GFP and mCherry fluorescence (B). The uterine toroid cells ut2 and ut3 and the spermatheca (sp) are identified as GFP positive as these cells are outlined by the *ajm-1::mCherry* marker, despite the fact that *octr-1::gfp* does not uniformly fill out ut2. In these and other panels, white asterisks indicate position of the vulval opening, yellow text indicates names of cells labeled with both GFP and mCherry, green text indicates cells labeled with GFP but not mCherry, the number of "+" symbols after a cell name indicate relative intensity of GFP labeling, text names are accompanied by dotted lines outlining corresponding cells, and scale bars are 10 µm. "vnc" in green indicates that GFP but not mCherry labels the ventral nerve cord, a bundle of axons from neurons with cell bodies outside the egg-laying system that run past the vulva. White box in (B) indicates region shown at higher magnification in (C-F). **(C and D)** An *octr-1::gfp; ida-1::mCherry* animal with GFP fluorescence displayed at high gain to show saturated GFP labeling in the neuroendocrine cells uv1s, GFP labeling in the HSN and VC4/5 neurons, which are above background when viewed at higher gain and in three dimensions. All these neurons are double-labeled by the *ida-1::mCherry* marker in (D). **(E and F)** An *octr-1::gfp; unc-103e::mCherry* animal with GFP fluorescence displayed at high gain to show GFP labeling in vm1 and vm2 egg-laying muscles, which are barely above background in (E) and double-labeled in (F). HSN: hermaphrodite-specific neuron; sp: spermatheca; ut: uterine toroid cell; uv: uterine ventral cell; VC: ventral cord type C neuron; vm: vulval muscle; vnc: ventral nerve cord.

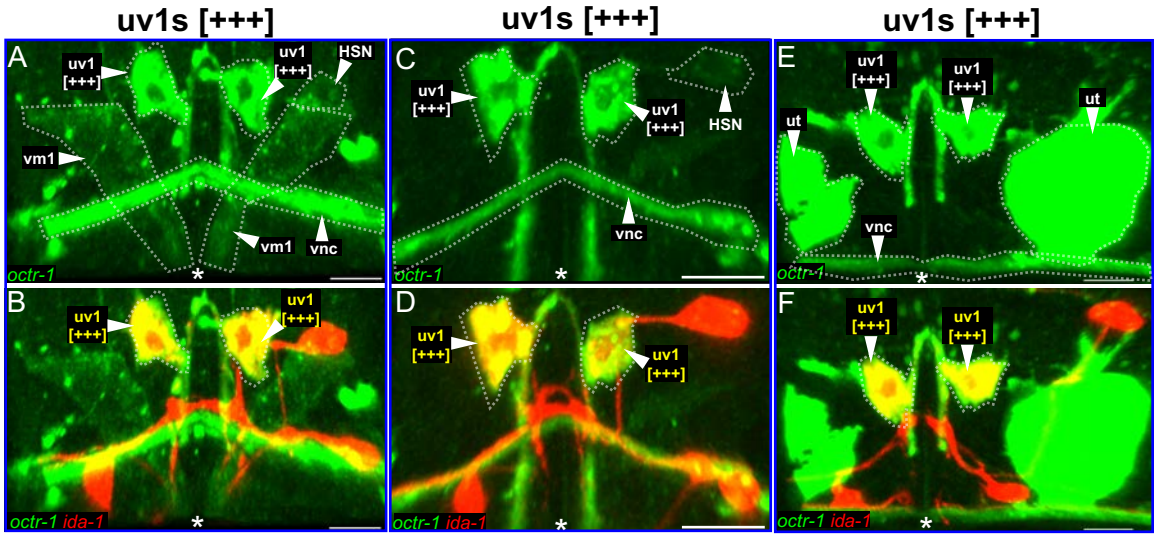

Figure 2.17 Consistent strong GFP expression in the uv1s from a chromosomally integrated *octr-1::gfp* transgene. (A-F) Strong expression of *octr-1::gfp* in uv1 cells is consistent from animal to animal. Confocal images of *octr-1::gfp; ida-1::mCherry* in the GFP channel (A, C, E) and GFP plus mCherry channel (B, D, F) for three different young adult animals. White asterisks indicate position of the vulval opening, yellow text indicates the uv1s labeled with both GFP and mCherry, white text indicates (A, C, F) all the cells labeled with GFP, the number of "+" symbols after a cell name indicate relative intensity [+++ (among the strongest cells labeled), ++ (easily detectable), + (slightly above background)] of GFP labeling, text names are accompanied by dotted lines outlining corresponding cells, and scale bars are 10 μm. HSN: hermaphrodite-specific neuron; ut: uterine toroid cell; uv: uterine ventral cell; VC: ventral cord type C neuron; vm: vulval muscles; vnc: ventral nerve cord.

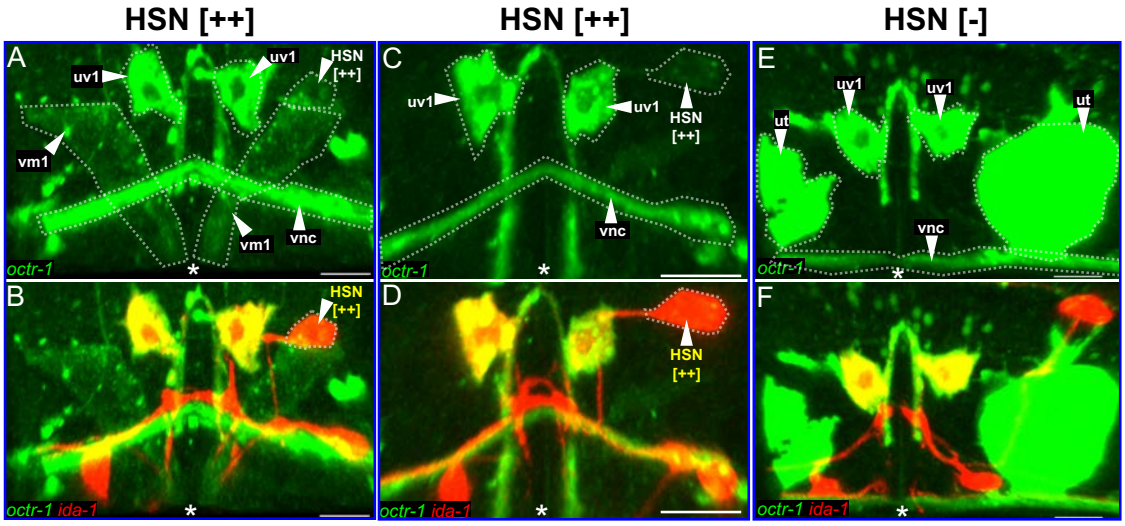

Figure 2.18 Animal to animal variation in GFP expression in the HSN from a chromosomally integrated *octr-1::gfp* transgene. (A-F) GFP expression of *octr-1::gfp* in the HSN varies from moderate to undetectable in different animals. Confocal images of *octr-1::gfp; ida-1::mCherry* in the GFP channel (A, C, E) and GFP plus mCherry channel (B, D, F) for three different young adult animals. GFP is expressed at a moderate level in two animals shown (A and C) but not detectable above background in a third (E). White asterisks indicate position of the vulval opening, yellow text indicates the HSN labeled with both GFP and mCherry, white text indicates (A, C, F) all the cells labeled with GFP, the number of "+" symbols after a cell name indicate relative intensity [+++ (among the strongest cells labeled), ++ (easily detectable), + (slightly above background)] of GFP labeling, text names are accompanied by dotted lines outlining corresponding cells, and scale bars are 10 μm. HSN: hermaphrodite-specific neuron; ut: uterine toroid cell; uv: uterine ventral cell; VC: ventral cord type C neuron; vm: vulval muscles; vnc: ventral nerve cord.

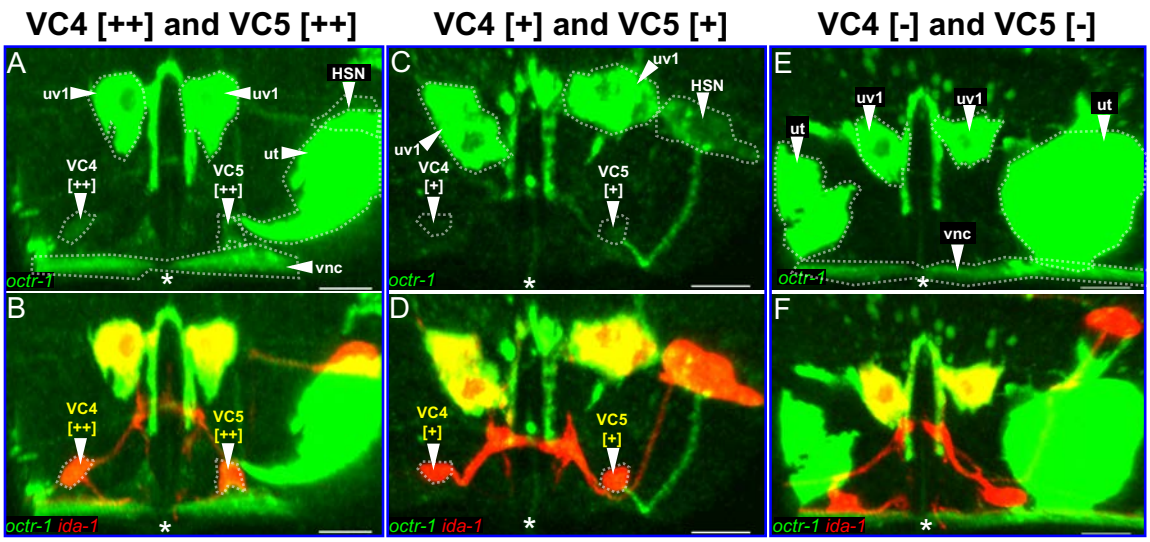

Figure 2.19 Animal to animal variation in GFP expression in VC4 and VC5 from a chromosomally integrated *octr-1::gfp* transgene. (A-F) GFP expression of *octr-1::gfp* in VC4 and VC5 varies from moderate to undetectable in different animals. Confocal images of *octr-1::gfp; ida-1::mCherry* in the GFP channel (A, C, E) and GFP plus mCherry channel (B, D, F) for three different young adult animals. GFP is expressed at a moderate level (A), just above background (C) but not detectable above background in a third (E). White asterisks indicate position of the vulval opening, yellow text indicates the HSN labeled with both GFP and mCherry, white text indicates (A, C, F) all the cells labeled with GFP, the number of "+" symbols after a cell name indicate relative intensity [+++ (among the strongest cells labeled), ++ (easily detectable), + (slightly above background)] of GFP labeling, text names are accompanied by dotted lines outlining corresponding cells, and scale bars are 10 μm. HSN: hermaphrodite-specific neuron; ut: uterine toroid cell; uv: uterine ventral cell; VC: ventral cord type C neuron; vnc: ventral nerve cord.

2.8 Discussion and Conclusion

In summary, we have generated chromosomally integrated strains for all 26 neurotransmitter GPCRS. These neurotransmitter GPCR::GFP transgenic strains were crossed to different mCherry marker strains to accurately identify GPCR::GFP expression in the egg-laying neurons, egg-laying muscles, and other cells such as non-neuronal cells i.e. uterine toroid cells near the *C. elegans* egg-laying system. In addition to identifying GFP expression in different egg-laying cells for all 26 neurotransmitter GPCRs, we also qualitatively record the GFP expression levels for each reporter in each cell and recorded animal-to animal variability in GFP expression levels from these reporters. As we only imaged young adult animals for our analysis of GPCR::GFP expression in different egg-laying cells, perhaps the animal-to-animal variability in GFP expression seen in the case of the HSN, VC4 and VC5 are dependent on the age of the worm. Future studies will have to be done to determine if the animal-to-animal variability in GFP expression is age dependent or whether variation in GFP expression in chromosomally integrated GPCR::GFP worms has a biological meaning.

Chapter 3: An atlas of neurotransmitter GPCRs expression in the *C. elegans* egg-laying circuit

Some text, figures, and captions in Chapter 3 adapted from those submitted as:

Fernandez, R.W., Wei, K., Wang, E.Y., Mikalauskaite, D., Olson, A., Pepper, J., Kim, S., Christie, N., Hasse, S., Sarov, M., and Koelle, M.R. Cellular expression and functional roles of 26 neurotransmitter GPCRs in the *C. elegans* egg-laying circuit. (2020)

The confocal imaging of the GFP reporters for the Neurotransmitter GPCRs in the different mCherry marker strains for the egg-laying cells, cell identification of GPCR::GFP transgenic strains in different egg-laying cells, and the analysis based on the cellular expression patterns of the Neurotransmitter GPCRs in the C. elegans egg-laying circuit were all done by Robert W. Fernandez.

3.1 Introduction

In this chapter, we describe the cellular expression patterns for all 26 neurotransmitter GPCRs, which include serotonin, dopamine, octopamine, tyramine, acetylcholine, GABA, glutamate, and orphan GPCRs. We discuss the possible role of these neurotransmitter GPCRs in the *C. elegans* egg-laying system. Taking into account the frequency and GFP intensity for each reporter for the 26 neurotransmitter GPCRs expressed in the egg-laying cells, we catalogued neurotransmitter GPCR expression for all cells of the *C. elegans* egg-laying system. Key discoveries include: 1) some neurons express many neurotransmitter GPCRs, for example, the HSN expresses a total of 14

neurotransmitter GPCRs. 2) There is a lot of weak, variable GFP expression in neurons while there is prominently strong GFP expression in egg-laying muscles and non-neuronal cells. 3) Neurotransmitter GPCRs are often expressed in non-neuronal cells such as the uterine toroid cells, vulval toroid cells, and the spermatheca which are not known to regulate the egg-laying circuit. Furthermore, we compared our neurotransmitter GPCR expression patterns in the *C. elegans* egg-laying system to that in previous publications, and we showed that 82% cell identifications were all new findings, 13% of the cell identifications confirmed previous publications, and the remaining 6% of cell identifications could not be confirmed. Lastly, using the connectome, neurotransmitter map, and the Neurotransmitter GPCR Atlas of the *C. elegans* egg-laying system, we annotated cases where receptors in egg-laying cells are positioned to receive synaptic or extrasynaptic signals. We found that dopamine, octopamine, and tyramine may act extrasynaptically onto the *C. elegans* egg-laying circuit, while serotonin, GABA, and glutamate may mainly act synaptically onto this circuit; however, further experiments will have to be done to test these observations.

3.2 Serotonin GPCRs expressed in the *C. elegans* egg-laying circuit

Serotonin GPCRs are expressed in egg-laying neurons of the *C. elegans* egg-laying circuit. Some notable findings seen in Figure 3.1 include: 1) Three serotonin GPCRs (SER-1, SER-5, and SER-7) have weak, variable to strong, variable GFP expression in the HSN (Figure 3.1B, 3.1L, 3.1P). As serotonin is released from the HSN to modulate egg-laying events by acting on the vulval muscles (Desai et al., 1988, Shyn et al., 2003, Carnell et al., 2005; Hobson et at.

2006; Hapiak et al., 2009), perhaps serotonin signaling in the egg-laying circuit is an example of autocrine signaling, where serotonin can either excite or inhibit the serotonin-releasing egg-laying neuron, HSN, through the serotonin receptors it expresses. 2) The serotonin receptor SER-7, a receptor that has been extensively studied (Hobson et at. 2006; Hapiak et al., 2009), was found in VC4 and VC5 (Figure 3.1P). Further studies will have to be done to determine whether SER-7 mediates the ability to excite the activity of VC4 and VC5 (Collins et al., 2016).

Serotonin GPCRs are strongly expressed in the egg-laying muscles of the *C. elegans* egg-laying circuit. Some interesting findings include: 1) We found consistent, weak expression for the serotonin receptor SER-4 in the vulval muscles vm1 (Figure 3.1J), which was previously thought to only be expressed in the vulval muscle vm2 (Gürel et al., 2012). 2) We confirmed the expression of the serotonin receptor SER-7 in the vulval muscles vm1 as well as three serotonin receptors (SER-1, SER-4, SER-7) in the vulval muscles vm2 (Cho et al., 2000; Carnell et al., 2005; Carre-Pierrat et al., 2006; Dempsey et al., 2005; Gürel et al., 2012) as seen in Figure 3.1. 3) We could not confirm expression of the serotonin receptor SER-1 in the vulval muscles vm1 (Cho et al., 2000; Carnell et al., 2005; Dempsey et al., 2005) or SER-5 expression in both of the vulval muscles (Hapiak et al. 2009). This may be due to very weak, variable GFP expression that we were unable to detect or that vulval muscle expression for these serotonin receptors are more prominent in different stages of development in adults.

We also examined whether serotonin receptors are expressed in the uterine muscles, which are thought to contract to cause egg laying and are directly or indirectly gap junctioned to vm1 and to each other (White et al., 1986). In addition to confirming SER-1 expression in the uterine muscles um1 and um2 (Carnell et al., 2005), we also found SER-7 expression in both of the uterine muscles (Figure 3.1R). As the serotonin receptors SER-1 and SER-7 that couple to $G\alpha_q$ and $G\alpha_s$, respectively, are known to stimulate egg-laying are mostly co-expressed in the HSN, vulval muscles and uterine muscles, this provides further evidence (Hapiak et al., 2009) that co-expression of these serotonin receptors in similar egg-laying cells perhaps positions them to play an excitatory role throughout the egg-laying circuit.

Serotonin GPCRs are expressed in non-neuronal and non-muscle cells near the egg-laying circuit. Some interesting findings include: 1) We found the serotonin GPCRs SER-1 and SER-5 expressed in different subsets of the uterine toroid cells (Figure 3.1F, 3.1N), epithelial cells that form the tube that holds unlaid egs, which were not previously known to respond to neurotransmitters. 2) We found three serotonin GPCRs SER-1, SER-5, and SER-7 expressed in the spermatheca, a structure that holds sperm and through which eggs pass to be fertilized (Figure 3.1F, 3.1N, 3.1T). The role of serotonin GPCRs in these non-neuronal cells, whether these cells receive signals via the serotonin receptors they express and whether these cells can modulate the activity of the egg-laying circuit will have to be further investigated.

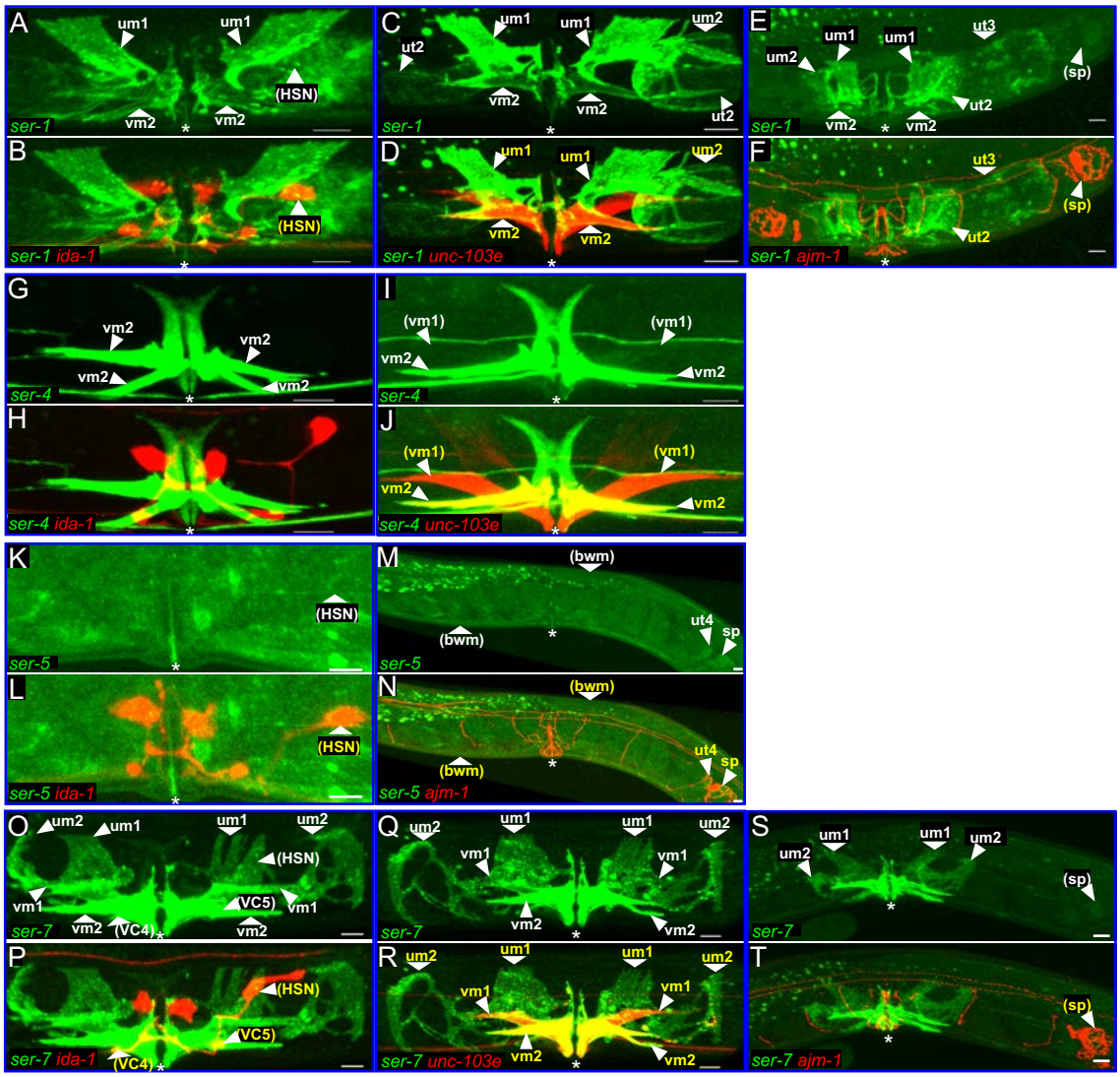

Figure 3.1. Serotonin GPCRs expressed in the *C. elegans* egg-laying circuit. Two-dimensional rendering of confocal images of young adult animals for serotonin GPCR::GFP reporters in different mCherry markers that label subsets of the egg-laying system. The top panel shows GFP fluorescence and the bottom panel shows both GFP and mCherry fluorescence for young adult animals for serotonin GPCR::GFP in the *ida-1::mCherry*, *unc-103e::mCherry*, or *ajm-1::mCherry* background. (**A-F**) *ser-1*::gfp expression patterns. A-B: *ser-1::gfp ida-1::mCherry*; C-D: *ser-1::gfp unc-103e::mCherry*; E-F: *ser-1::gfp ajm-1::mCherry*. (**G-J**) *ser-4*::gfp expression patterns. G-H: *ser-4::gfp ida-1::mCherry*; I-J: *ser-4::gfp unc-103e::mCherry*. (**K-N**) *ser-5*::gfp expression patterns. K-L: *ser-5::gfp ida-1::mCherry*; M-N: *ser-5::gfp ajm-1::mCherry*. (**O-T**) *ser-7*::gfp expression patterns. O-P: *ser-7::gfp ida-1::mCherry*; Q-R: *ser-7::gfp unc-103e::mCherry*; S-T: *ser-7::gfp ajm-1::mCherry*. For all panels, white asterisks indicate position of the vulval opening, yellow text indicates names of cells labeled with both GFP and mCherry, white text indicates all GFP expressing cells, parenthesis indicates GPCR::GFP expressing cell is difficult to see without rendering at a higher GFP intensity or viewing the image at different orientations, and scale bars are 10 μm. bwm: body wall muscle; HSN: hermaphrodite-specific neuron; sp: spermatheca; um: uterine muscle; ut: uterine toroid cell; uv: uterine ventral cell; VC: ventral cord type C neuron; vm: vulval muscle.

3.3 Dopamine GPCRs expressed in the *C. elegans* egg-laying circuit

Dopamine GPCRs are expressed in egg-laying neurons and muscles of the *C. elegans* egg-laying circuit. Some interesting findings include: 1) We found the dopamine GPCR DOP-2, a $G\alpha_o$-coupled neurotransmitter GPCR, is expressed in the uv1s (Figure 3.2F), which are known to inhibit egg-laying. As the G protein $G\alpha_o$ is involved in inhibiting egg-laying (Tanis et al. 2008), perhaps DOP-2 is receiving signals that regulate activity of the uv1s. 2) We found the dopamine GPCR DOP-3 expressed in the egg-laying neurons: HSN, VC4, and VC5 (Figure 3.2J). As this dopamine receptor is also a $G\alpha_o$-coupled neurotransmitter GPCR, perhaps it is involved in the inhibition of the activity of these egg-laying neurons. 3) Only one dopamine GPCR DOP-4 is expressed in the vulval muscles of the egg-laying circuit, specifically in the vm1s (Figure 3.2P). Similar to serotonin, dopamine may be acting on these vulval muscles to modulate egg-laying. While the role of the dopamine in modulating the egg-laying circuit is unclear as previous studies have shown that endogenous dopamine promotes egg-laying (Nagashima et al., 2016) and exogenous dopamine has been reported to both promote and inhibit egg-laying (Schafer and Kenyon, 1995; Vidal-Gadea et al., 2012), the expression of dopamine receptors in the egg-laying circuit is a starting point to study where dopamine acts in the cells of the egg-laying circuit to regulates egg-laying.

Dopamine GPCRs are expressed in several non-neuronal cells near the egg-laying circuit. Some notable findings include: 1) DOP-1 and DOP-2 expressed in different subsets of the uterine toroid cells (Figure 3.2D, 3.2H). 2) DOP-1 and DOP-3 expressed in the vulval toroid cells, epithelial cells form the opening through which eggs are laid (Figure 3.2D, 3.2L). 3) DOP-2 expressed in the utse (Figure 3.2H), an H-shaped uterine seam cell that attaches the uterus to the lateral epidermis, which functions as a hymen that is broken during the first egg-laying event (Collins et al., 2016). 4) All four dopamine receptors were expressed in the spermatheca (Figure 3.2D, 3.2H, 3.2L, 3.2R). Further studies will have to be done to determine whether the presence of several dopamine receptors in non-neuronal cells indicates these receptors are receiving signals that modulates the egg-laying circuit.

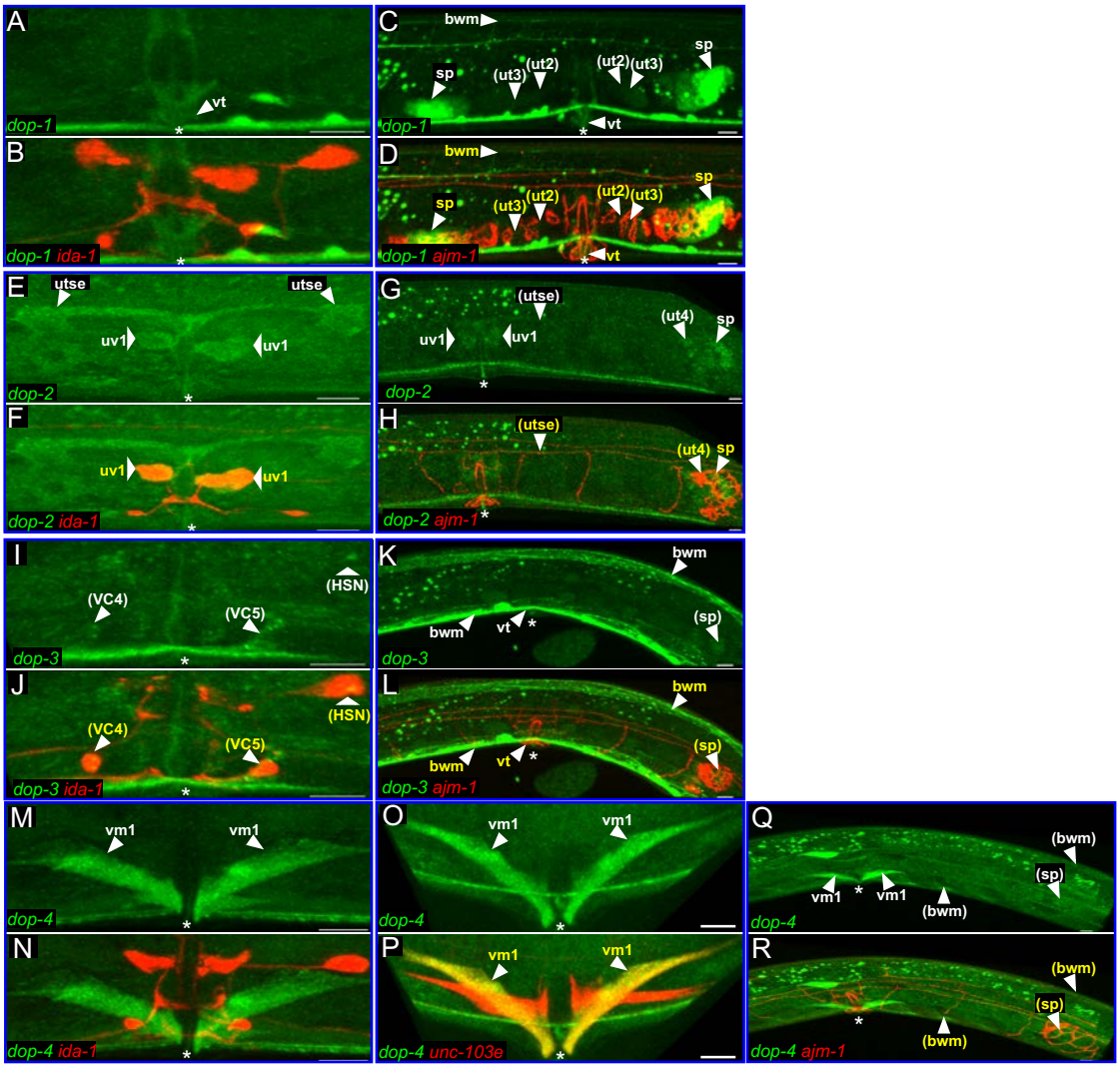

Figure 3.2. Dopamine GPCRs expressed in the *C. elegans* egg-laying circuit. Two-dimensional rendering of confocal images of young adult animals for dopamine GPCR::GFP reporters in different mCherry markers that label subsets of the egg-laying system. The top panel shows GFP fluorescence and the bottom panel shows both GFP and mCherry fluorescence for young adult animals for dopamine GPCR::GFP in the *ida-1::mCherry*, *unc-103e::mCherry*, or *ajm-1::mCherry* background.. (**A-D**) *dop-1*::gfp expression patterns. A-B: *dop-1::gfp ida-1::mCherry*; C-D: *dop-1::gfp ajm-1::mCherry*. (**E-H**) *dop-2*::gfp expression patterns. E-F: *dop-2::gfp ida-1::mCherry*; G-H: *dop-2::gfp ajm-1::mCherry*. (**I-L**) *dop-3*::gfp expression patterns. I-J: *dop-3::gfp ida-1::mCherry*; K-L: *dop-3::gfp ajm-1::mCherry*. (**M-R**) *dop-4*::gfp expression patterns. M-N: *dop-4::gfp ida-1::mCherry*; O-P: *dop-4::gfp unc-103e::mCherry*; Q-R: *dop-4::gfp ajm-1::mCherry*. For all panels, white asterisks indicate position of the vulval opening, yellow text indicates names of cells labeled with both GFP and mCherry, white text indicates all GFP expressing cells, parenthesis indicates GPCR::GFP expressing cell is difficult to see without rendering at a higher GFP intensity or viewing the image at different orientations, and scale bars are 10 μm. bwm: body wall muscle; HSN: hermaphrodite-specific neuron; sp: spermatheca; ut: uterine toroid cell; utse: uterine seam; uv: uterine ventral cell; VC: ventral cord type C neuron; vm: vulval muscle; vt: vulval toroid cells.

3.4 Octopamine GPCRs expressed in the *C. elegans* egg-laying circuit

Octopamine GPCRs are expressed in the *C. elegans* egg-laying neurons and muscles. Some notable discoveries include: 1) OCTR-1 is expressed in egg-laying neurons such as the HSN, VC4, and VC5 (Figure 3.3B). 2) All three octopamine GPCRs (OCTR-1, SER-3, and SER-6) are expressed in the uv1s (Figure 3.3B, 3.3H, 3.3L). 3) OCTR-1 is expressed in both of the vulval muscles (Figure 3.3D). These findings indicate octopamine may play a role in regulating egg laying as it is expressed in the entire circuit. Previous work has shown that octopamine inhibits egg-laying (Horvitz et al., 1982), even in the presence of exogenous serotonin; however, as no octopamine receptors were previously found in this circuit, where octopamine acts on to inhibit egg laying was unknown. Perhaps octopamine inhibits egg-laying by inhibiting the activity of the HSN, which is known to promote egg-laying.

Octopamine receptors are expressed in non-neuronal cells near the egg-laying circuit. Some notable findings include: 1) All three octopamine GPCRs are mainly expressed in the same subsets of the uterine toroid cells (Figure 3.3F, 3.3J, 3.3N). 2) SER-3 and SER-6 are expressed in the uterine-ventral cells, uv3 (Figure 3.3J, 3.3N), which has no known role of regulating egg-laying activity 3) SER-6 is expressed in the vulval toroid cells (Figure 3.3N). 4) All three octopamine GPCRs are found in the spermatheca (Figure 3.3F, 3.3J, 3.3N). Future studies will have to be done to determine the specific function of these octopamine GPCRs in these different non-neuronal cells and whether they modulate the activity of the egg-laying circuit.

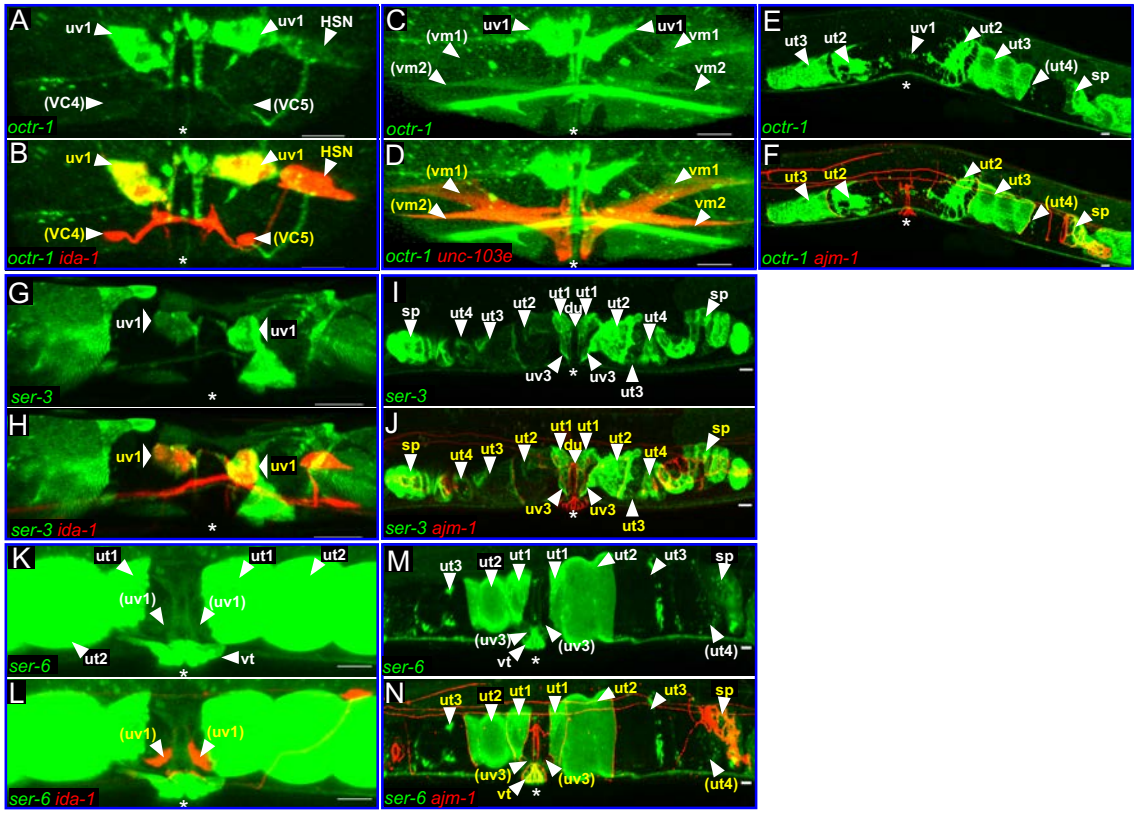

Figure 3.3. Octopamine GPCRs expressed in the *C. elegans* egg-laying circuit. Two-dimensional rendering of confocal images of young adult animals for octopamine GPCR::GFP reporters in different mCherry markers that label subsets of the egg-laying system. The top panel shows GFP fluorescence and the bottom panel shows both GFP and mCherry fluorescence for young adult animals for octopamine GPCR::GFP in the *ida-1::mCherry*, *unc-103e::mCherry*, or *ajm-1::mCherry* background. (**A-F**) *octr-1*::gfp expression patterns. A-B: *octr-1::gfp ida-1::mCherry*; C-D: *octr-1::gfp unc-103e::mCherry*; E-F: *octr-1::gfp ajm-1::mCherry*. (**G-J**) *ser-3*::gfp expression patterns. G-H: *ser-3::gfp ida-1::mCherry*; I-J: *ser-3::gfp ajm-1::mCherry*. (**K-N**) *ser-6*::gfp expression patterns. K-L: *ser-6::gfp ida-1::mCherry*; M-N: *ser-6::gfp ajm-1::mCherry*. For all panels, white asterisks indicate position of the vulval opening, yellow text indicates names of cells labeled with both GFP and mCherry, white text indicates all GFP expressing cells, parenthesis indicates GPCR::GFP expressing cell is difficult to see without rendering at a higher GFP intensity or viewing the image at different orientations, and scale bars are 10 μm. HSN: hermaphrodite-specific neuron; sp: spermatheca; ut: uterine toroid cell; uv: uterine ventral cell; VC: ventral cord type C neuron; vm: vulval muscle; vt: vulval toroid cells.

3.5 Tyramine GPCRs expressed in the *C. elegans* egg-laying circuit

Tyramine GPCRs are expressed in the *C. elegans* egg-laying neurons and muscles**.** Some notable findings include: 1) SER-2 and TYRA-3 are expressed in both the HSN and the uv1s (Figure 3.4B, 3.4L). 2) TYRA-3 is expressed in VC4 and VC5 (Figure 3.4L). 3) TYRA-3 was confirmed to be expressed in the vulval muscles, but also found it expressed in the uterine muscle um1 (Figure 3.4N). 4) SER-2 is expressed in the uterine muscle um2 (Figure 3.4D). These findings can help us generate several hypotheses on how tyramine regulates egg laying. As previous work has shown that uv1 releases tyramine to inhibit egg-laying by acting on a tyramine receptor LGC-55 on the HSN (Collins et al., 2016), the presence of several tyramine GPCRs throughout the egg-laying circuit, gives us further sites of action as to where tyramine acts to inhibit egg-laying. As tyramine is released by the uv1s to inhibit egg laying, perhaps tyramine is acting on SER-2 and TYRA-3 to autoregulate uv1 activity or tyramine may act through these receptors along with LGC-55 on the HSN to inhibit egg laying.

Tyramine GPCRs were expressed in non-neuronal cells near the egg-laying circuit: 1) TYRA-2 and TYRA-3 are expressed in uterine toroid cells (Figure 3.4J, 3.4P). 2) TYRA-3 is expressed in the uterine ventral cell uv3 (not shown). 3) SER-2 and TYRA-3 are expressed in the vulval toroid cells (Figure 3.4F, 3.4P). 4) SER-2 is expressed in the utse (Figure 3.4F). 5) All three tyramine GPCRs are expressed in the spermatheca (Figure 3.4F, 3.4J, 3.4P). Further studies will have to be done to determine why there is expression of several tyramine GPCRs in non-neuronal cells.

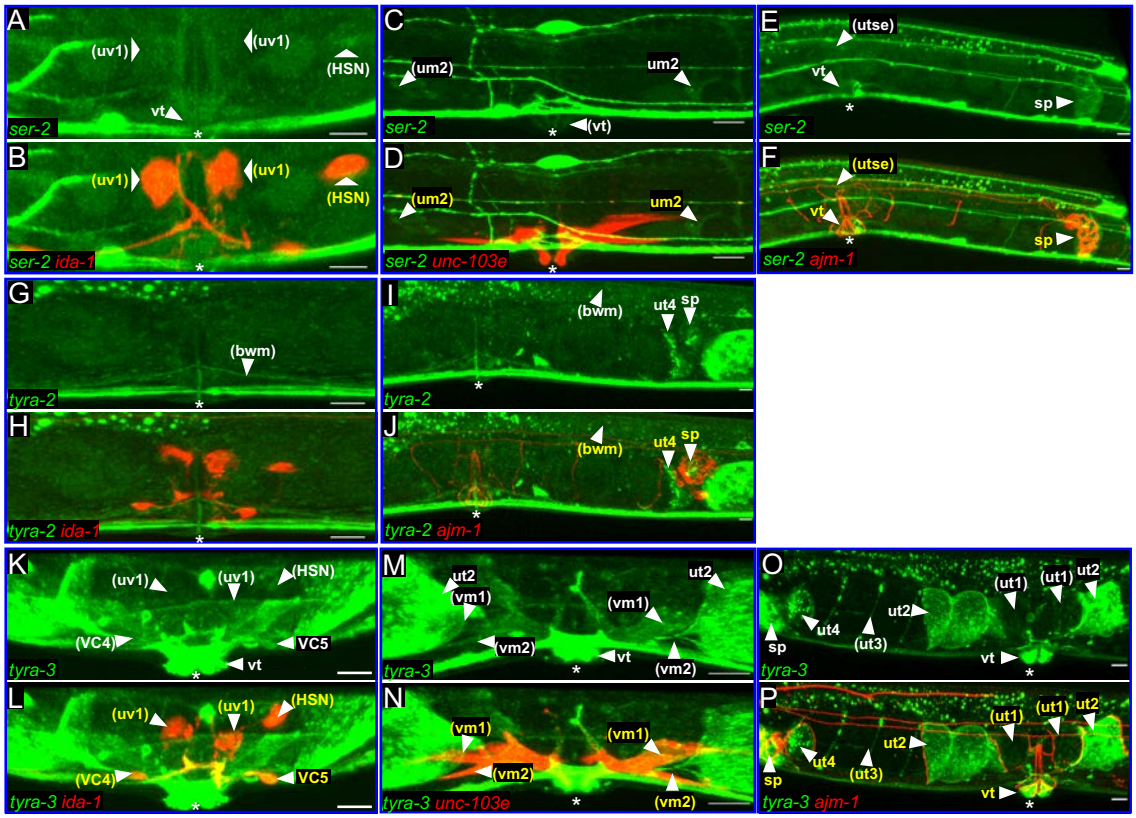

Figure 3.4. Tyramine GPCRs expressed in the *C. elegans* egg-laying circuit. Two-dimensional rendering of confocal images of young adult animals for tyramine GPCR::GFP reporters in different mCherry markers that label subsets of the egg-laying system. The top panel shows GFP fluorescence and the bottom panel shows both GFP and mCherry fluorescence for young adult animals for tyramine GPCR::GFP in the *ida-1::mCherry*, *unc-103e::mCherry*, or *ajm-1::mCherry* background. (**A-F**) *ser-2*::gfp expression patterns. A-B: *ser-2::gfp ida-1::mCherry*; C-D: *ser-2::gfp unc-103e::mCherry*; E-F: *ser-2::gfp ajm-1::mCherry*. (**G-J**) *tyra-2* gfp expression patterns. G-H: *tyra-2::gfp ida-1::mCherry*; I-J: *tyra-2::gfp ajm-1::mCherry*. (**K-P**) *tyra-3*::gfp expression patterns. K-L: *tyra-3::gfp ida-1::mCherry*; M-N: *tyra-3::gfp unc-103e::mCherry* O-P: *tyra-3::gfp ajm-1::mCherry*. For all panels, white asterisks indicate position of the vulval opening, yellow text indicates names of cells labeled with both GFP and mCherry, white text indicates all GFP expressing cells, parenthesis indicates GPCR::GFP expressing cell is difficult to see without rendering at a higher GFP intensity or viewing the image at different orientations, and scale bars are 10 µm. HSN: hermaphrodite-specific neuron; sp: spermatheca; um: uterine muscle; ut: uterine toroid cell; utse: uterine seam; uv: uterine ventral cell; VC: ventral cord type C neuron; vm: vulval muscle; vt: vulval toroid cells.

3.6 Acetylcholine GPCRs expressed in the *C. elegans* egg-laying circuit

Acetylcholine GPCRs are expressed in *C. elegans* egg-laying neurons and muscles. Some notable findings include: 1) GAR-1 and GAR-2 are expressed in the HSN (Figure 3.5B, 3.5H). 2) All three acetylcholine GPCRs are expressed in the uv1s (Figure 3.5B, 3.5H, 3.5L). 3) GAR-1 is expressed in both vulval muscles (Figure 3.5D), GAR-2 is expressed in the vulval muscle vm2 (Figure 3.5J), and GAR-3 is only expressed in the vulval muscle vm3 only (Figure 3.5N). As acetylcholine is known to be released by VC4 and VC5 to contract the vulval muscles (Collins et al., 2016) by acting on acetylcholine receptors (Waggoner et al., 2000; Kim et al., 2001), perhaps acetylcholine is also signaling to these acetylcholine GPCRs expressed in these vulval muscles. Further studies will have to be done to understand why acetylcholine GPCRs are expressed in the HSN and uv1s, whether they are involved in regulating the activity of these cells and if this is tied to the contraction of the vulval muscles before egg-laying events.

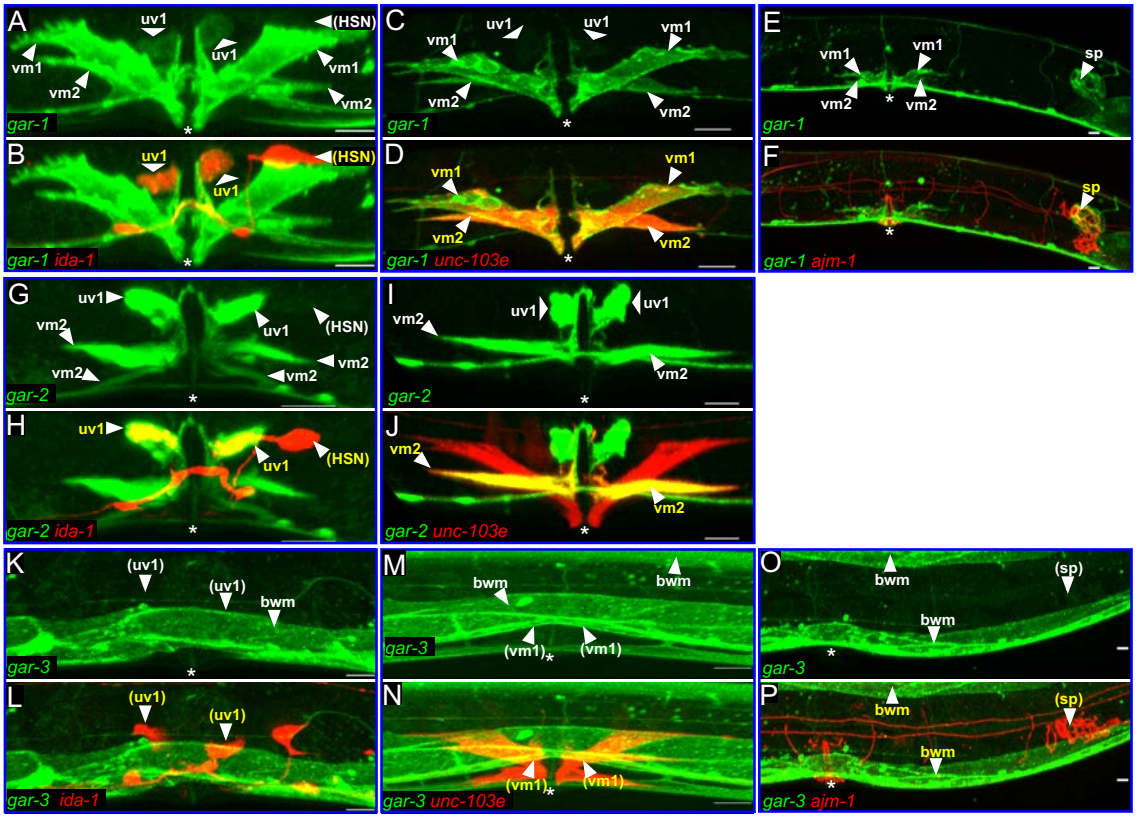

Figure 3.5. Acetylcholine GPCRs expressed in the *C. elegans* egg-laying circuit. Two-dimensional rendering of confocal images of young adult animals for acetylcholine GPCR::GFP reporters in different mCherry markers that label subsets of the egg-laying system. The top panel shows GFP fluorescence and the bottom panel shows both GFP and mCherry fluorescence for young adult animals for acetylcholine GPCR::GFP in the *ida-1::mCherry*, *unc-103e::mCherry*, or *ajm-1::mCherry* background. (**A-F**) *gar-1*::gfp expression patterns. A-B: *gar-1::gfp ida-1::mCherry*; C-D: *gar-1::gfp unc-103e::mCherry*; E-F: *gar-1::gfp ajm-1::mCherry*. (**G-J**) *gar-2*::gfp expression patterns. G-H: *gar-2::gfp ida-1::mCherry*; I-J: gar-*2::gfp unc-103e::mCherry*. (**K-P**) *gar-3*::gfp expression patterns. K-L: *gar-3::gfp ida-1::mCherry*; M-N: *gar-3::gfp unc-103e::mCherry* O-P: *gar-3::gfp ajm-1::mCherry*. For all panels, white asterisks indicate position of the vulval opening, yellow text indicates names of cells labeled with both GFP and mCherry, white text indicates all GFP expressing cells, parenthesis indicates GPCR::GFP expressing cell is difficult to see without rendering at a higher GFP intensity or viewing the image at different orientations, and scale bars are 10 μm. bwm: body wall muscle; HSN: hermaphrodite-specific neuron; sp: spermatheca; uv: uterine ventral cell; vm: vulval muscle.

3.7 GABA GPCRs expressed in the *C. elegans* egg-laying circuit

GABA GPCRs are expressed in *C. elegans* egg-laying system. Some notable findings include: 1) GBB-2 is expressed in the HSN (Figure 3.6F), however we could not confirm GBB-1 expression in the HSN. 2) GBB-2 is expressed in VC4 and VC5 (Figure 3.6F). 3) GBB-1 is expressed in several non-neuronal cells such as the uterine toroid cells ut1 and ut2, utse, vulval toroid cells, and dorsal uterine du (Figure 3.6D). The role of GABA in regulating the *C. elegans* egg-laying is unclear and the role of the GABA GPCRs in egg-laying neurons such as the HSN and VC4 and VC5 is a direction that will have to be further explored to determine whether GABA regulates egg laying.

With the expression pattern data of the GABA GPCRs in the *C. elegans* egg-laying circuit, we expected both of the GABA GPCRs to always be co-expressed as the G-protein coupled $GABA_B$ receptor is known to be an obligate heteromer between the two GPCRs (Bamber et al., 1999; Dittman and Kaplan, 2008). While GBB-1 and GBB-2 are both expressed in the uv1s, body wall muscles, and spermatheca (Figure 3.6D, 3.6H), they are not always co-expressed as GBB-2 is only expressed in VC4 and VC5 while GBB-1 is only expressed in the uterine toroid cells. It is surprising that the GABA GPCRs are not always co-expressed if they are obligate heteromers.

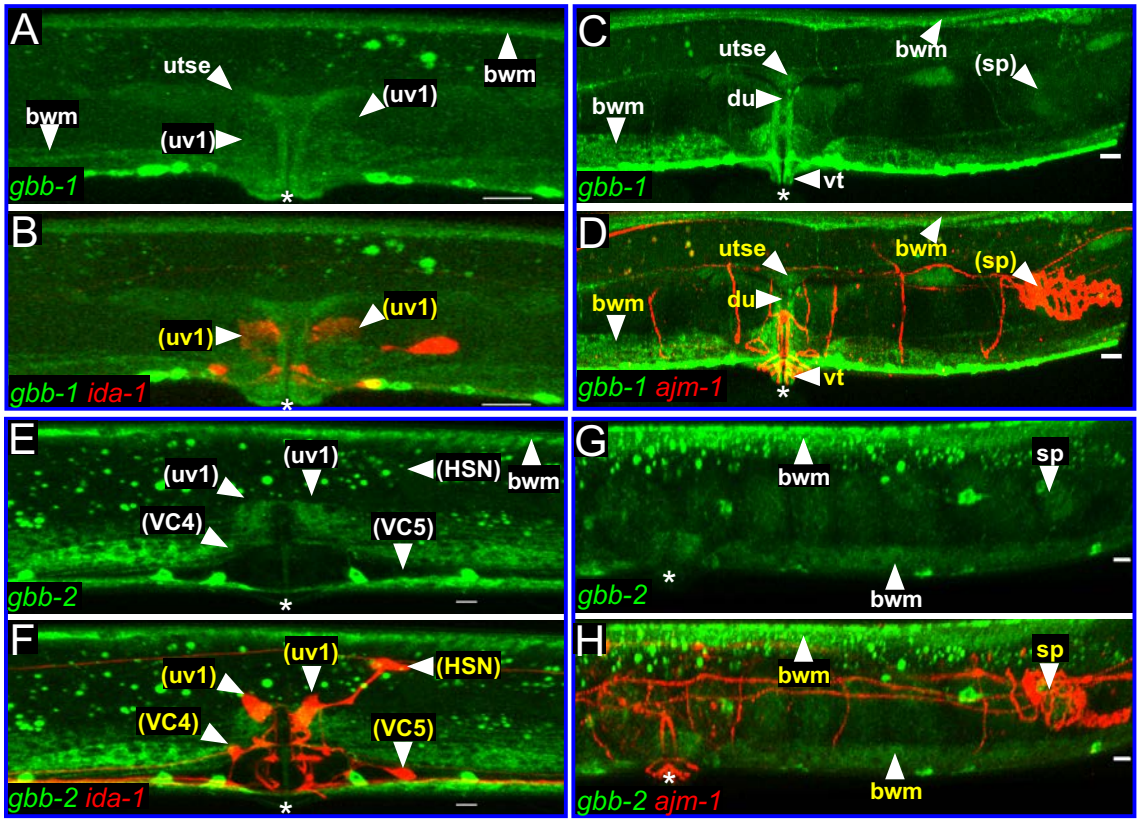

Figure 3.6. GABA GPCRs expressed in the *C. elegans* egg-laying circuit. Two-dimensional rendering of confocal images of young adult animals for GABA GPCR::GFP reporters in different mCherry markers that label subsets of the egg-laying system. The top panel shows GFP fluorescence and the bottom panel shows both GFP and mCherry fluorescence for young adult animals for GABA GPCR::GFP in the *ida-1::mCherry*, *unc-103e::mCherry*, or *ajm-1::mCherry* background. (**A-F**) *gbb-1*::gfp expression patterns. A-B: *gbb-1::gfp ida-1::mCherry*; C-D: *gbb-1::gfp unc-103e::mCherry*; E-F: *gbb-1::gfp ajm-1::mCherry*. (**G-J**) *gbb-2::gfp* expression patterns. G-H: *gbb-2::gfp ida-1::mCherry*; I-J: *gbb-2::gfp ajm-1::mCherry*. For all panels, white asterisks indicate position of the vulval opening, yellow text indicates names of cells labeled with both GFP and mCherry, white text indicates all GFP expressing cells, parenthesis indicates GPCR::GFP expressing cell is difficult to see without rendering at a higher GFP intensity or viewing the image at different orientations, and scale bars are 10 μm. bwm: body wall muscle; HSN: hermaphrodite-specific neuron; sp: spermatheca; ut: uterine toroid cell; utse: uterine seam; uv: uterine ventral cell; VC: ventral cord type C neuron; vt: vulval toroid cells.

3.8 Glutamate GPCRs expressed in the *C. elegans* egg-laying circuit

Glutamate GPCRs are expressed in *C. elegans* egg-laying system. Some notable findings include: 1) MGL-1 and MGL-2 are both expressed in the HSN (Figure 3.7B, 3.7F). 2) MGL-1 and MGL-3 are both expressed in the uv1s (Figure 3.7B,3.7H). 3) MGL-3 is expressed in both VC4 and VC5 (Figure 3.7H). 4) MGL-1 is expressed in several non-neuronal cells such as the uv3, utse, spermatheca, and subcellularly localized to the uterine toroid cell ut4 (Figure 3.7D). The neurotransmitter glutamate is not known to regulate egg laying, yet glutamate GPCRs are expressed in all egg-laying neurons; perhaps, glutamate has a role in regulating activity of this circuit.

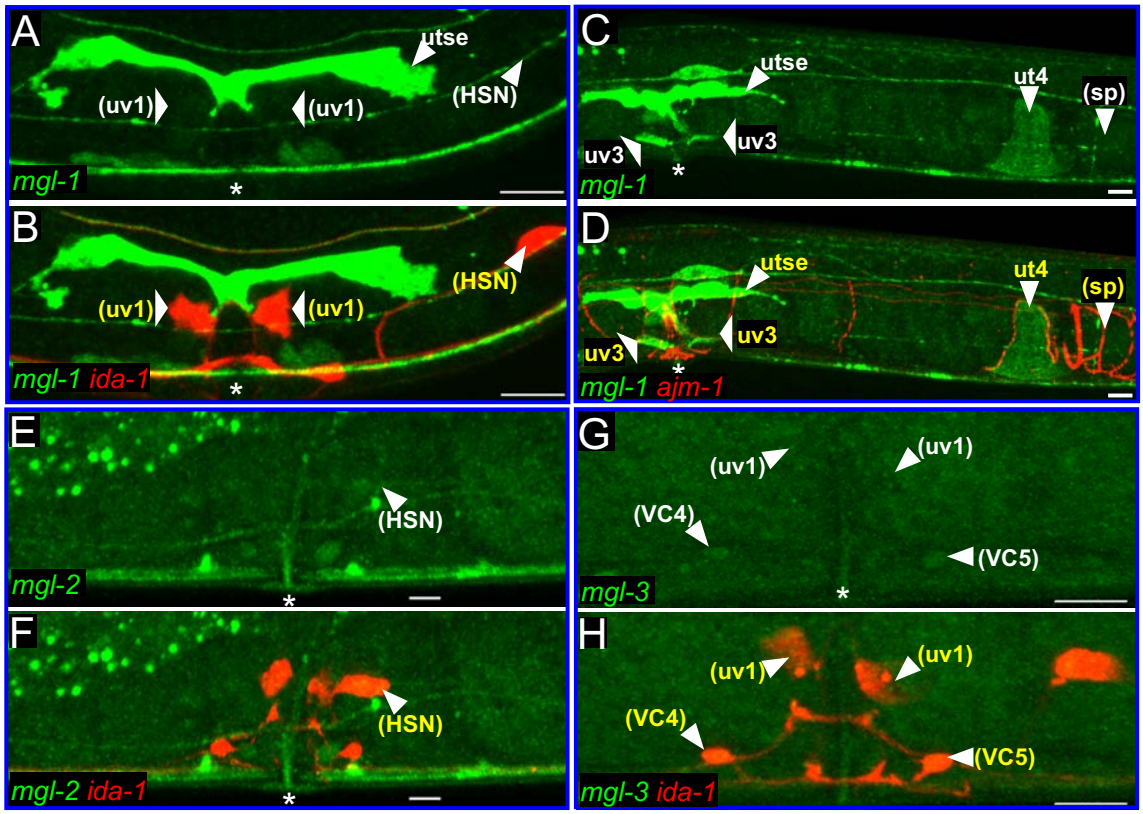

Figure 3.7. Glutamate GPCRs expressed in the *C. elegans* egg-laying circuit. Two-dimensional rendering of confocal images of young adult animals for glutamate GPCR::GFP reporters in different mCherry markers that label subsets of the egg-laying system. The top panel shows GFP fluorescence and the bottom panel shows both GFP and mCherry fluorescence for young adult animals for glutamate GPCR::GFP in the *ida-1::mCherry*, *unc-103e::mCherry*, or *ajm-1::mCherry* background. (**A-D**) *mgl-1*::gfp expression patterns. A-B: *mgl-1::gfp ida-1::mCherry*; C-D: *mgl-1::gfp ajm-1::mCherry*. (**E-F**) *mgl-2::*gfp expression patterns. E-F: *mgl-2::gfp ida-1::mCherry*; (**G-H**) *mgl-3*::gfp expression patterns. G-H: *mgl-3::gfp ida-1::mCherry*. For all panels, white asterisks indicate position of the vulval opening, yellow text indicates names of cells labeled with both GFP and mCherry, white text indicates all GFP expressing cells, parenthesis indicates GPCR::GFP expressing cell is difficult to see without rendering at a higher GFP intensity or viewing the image at different orientations, and scale bars are 10 μm. HSN: hermaphrodite-specific neuron; sp: spermatheca; ut: uterine toroid cell; utse: uterine seam; uv: uterine ventral cell; VC: ventral cord type C neuron.

3.9 Orphan GPCRs expressed in the *C. elegans* egg-laying circuit

We have found several orphan GPCRs expressed in the *C. elegans* egg-laying system. Some interesting findings include: 1) ADOR-1 is expressed in the HSN and vulval muscles (Figure 3.8B, 3.8D). 2) DOP-5 is expressed in the uv1s (Figure 3.8J). 3) DOP-6 is expressed in the HSN, uv1s, and vulval muscles vm2 (Figure 3.8N,3.8P). 4) DOP-5 is expressed in the uterine toroid cell ut4 (Figure 3.8L). 5) F35H10.10 is expressed in vulval toroid cells (Figure 3.8H). As the ligand that acts on these orphan GPCRs is unknown, it is difficult to ascertain the meaning behind these expression patterns in the *C. elegans* egg-laying system, however, perhaps there are other ligands besides the seven neurotransmitters involved in regulating egg-laying.

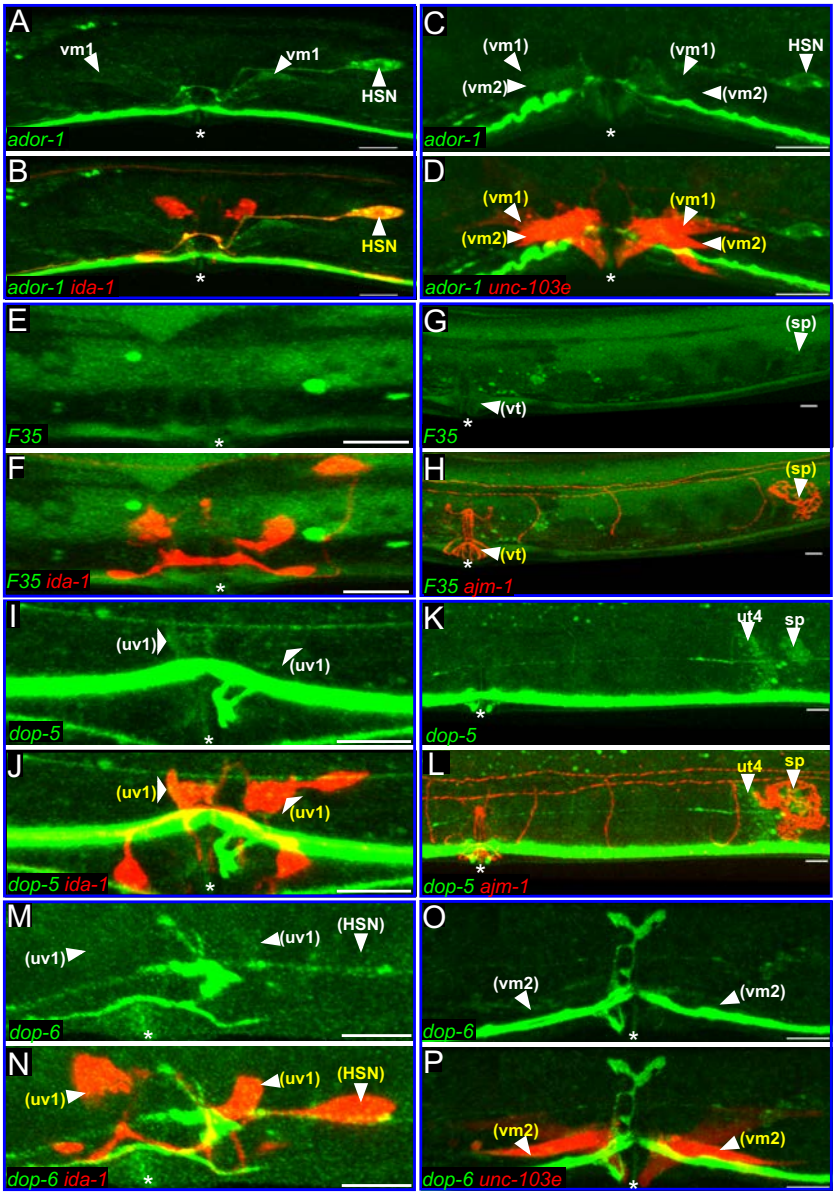

Figure 3.8. Orphan GPCRs expressed in the *C. elegans* egg-laying circuit. Two-dimensional rendering of confocal images of young adult animals for orphan GPCR::GFP reporters in different mCherry markers that label subsets of the egg-laying system. The top panel shows GFP fluorescence and the bottom panel shows both GFP and mCherry fluorescence for young adult animals for orphan GPCR::GFP in the *ida-1::mCherry*, *unc-103e::mCherry*, or *ajm-1::mCherry* background. (**A-D**) *ador-1*::gfp expression patterns. A-B: *ador-1::gfp ida-1::mCherry*; C-D: *ador-1::gfp unc-103e::mCherry* (**E-H**) *F35H10.10::*gfp expression patterns. E-F: *F35H10.10::gfp ida-1::mCherry*; G-H: *F35H10.10::gfp ajm-1::mCherry*. (**I-L**) *dop-5*::gfp expression patterns. I-J: *dop-5::gfp ida-1::mCherry*; K-L: *dop-5::gfp ajm-1::mCherry*. (**M-P**) *dop-6*::gfp expression patterns. M-N: *dop-6::gfp ida-1::mCherry*; O-P: *dop-6::gfp unc-103e::mCherry*. For all panels, white asterisks indicate position of the vulval opening, yellow text indicates names of cells labeled with both GFP and mCherry, white text indicates all GFP expressing cells, parenthesis indicates GPCR::GFP expressing cell is difficult to see without rendering at a higher GFP intensity or viewing the image at different orientations, and scale bars are 10 μm. HSN: hermaphrodite-specific neuron; sp: spermatheca; ut: uterine toroid cell; uv: uterine ventral cell; vm: vulval muscle.

3.10 Analysis of neurotransmitter GPCR cellular expression patterns in the *C. elegans* egg-laying circuit

We created a Neurotransmitter GPCR Atlas of the *C. elegans* egg-laying system by combining the following: 1) The cellular expression patterns of the neurotransmitter GPCRs expressed in the *C. elegans* egg-laying system. 2) The GFP expression levels for each neurotransmitter GPCR reporter in each cell. 3) Animal-to animal variability in GFP expression levels from these reporters (Figure 3.9). Figure 3.10 summarizes the cellular expression patterns for all neurotransmitter GPCRs expressed in the different cells of the *C. elegans* egg-laying system taking into account strong and weak GPCR::GFP expression in these cells. A further breakdown as to the number of neurotransmitter GPCRs in a specific egg-laying cell is shown in Figure 3.11.

Our Neurotransmitter GPCR Atlas gives us a starting point to determine the function of neurotransmitter GPCRs in these egg-laying cells as we can make testable hypotheses as to the function of a receptor based on the identity of the egg-laying cell it is expressed in. For example, the presence of several neurotransmitter GPCRs expressed in the HSN, may indicate that they are involved in promoting or inhibiting egg-laying, possibly by affecting HSN activity. We can test single knockouts for the receptors expressed in the HSN to screen for egg-laying defects. If the single knockouts do not display a strong egg-laying phenotype, using our Neurotransmitter GPCR Atlas of the *C. elegans* egg-laying system, we know the other neurotransmitter receptors expressed in the HSN. Therefore, we have a starting point as to what combination of neurotransmitter

receptor knockouts to generate in order to screen for egg-laying defects. Furthermore, we can test these neurotransmitter receptor knockouts and compare how HSN activity is affected in different neurotransmitter receptor knockouts compared to wild-type HSN activity using GCAMP calcium reporters established in our lab.

Using the neurotransmitter receptor expression patterns of the *C. elegans* egg-laying circuit, we derived key insights regarding neurotransmitter signaling that may extend beyond this circuit. Many neurotransmitter GPCRs are expressed in a single neuron. 54% (14 out of 26) of all neurotransmitter GPCRs are expressed in the HSN, the command neuron of the *C. elegans* egg-laying circuit that promotes egg-laying events (Figure 3.10 and Figure 3.11). Similarly, 58% (15 out of 26) of all neurotransmitter GPCRs are expressed in the uv1s, which inhibits egg-laying events (Figure 3.10 and Figure 3.11). Perhaps, this observation of many neurotransmitter GPCRs expressed in a single neuron is widespread to all neural circuits. Interestingly, only 23% (6 out of 26) neurotransmitter receptors are expressed in each VC4 and VC5 (Figure 3.10 and Figure 3.11), which may indicate how these neurons aid in the function of the circuit, but are not required for proper egg-laying events. Interestingly, there is a lot of weak, variable GPCR::GFP expression in neurons and further studies will have to be done to test if these receptors are functionally relevant.

Many neurotransmitter GPCR::GFP are strongly expressed in the egg-laying muscles of the circuit. Including serotonin and acetylcholine GPCR expression in the vulval muscles, we have also found the other classes of

neurotransmitter receptors (dopamine, octopamine, tyramine) expressed in the vulval muscles. Specifically, 31% (8 out of 26) of the neurotransmitter GPCRs are expressed in vm1 and 35% (9 out of 26) of the neurotransmitter GPCRs are expressed in vm2 (Figure 3.10 and Figure 3.11). There are cases of subcellular expression in the vulval muscles: the dopamine receptor DOP-4 and acetylcholine receptor GAR-3 are only expressed in the vm1, the serotonin receptor SER-1, acetylcholine receptor GAR-2, and the orphan receptor DOP-6 are only expressed in the vm2 (Figure 3.10 and Figure 3.11). This might indicate how certain neurotransmitter receptors might be involved in specifically regulating part of the vulval muscles. Furthermore, we also found few, 12% (3 out of 26), neurotransmitter receptors expressed in the uterine muscles, which might indicate they play a specialize role in egg-laying. While not egg-laying muscles, we also found 31% (8 out of 26) of neurotransmitter receptors in the body wall muscles (Figure 3.10 and Figure 3.11) and perhaps these receptors contribute to how locomotion modulates egg-laying activity (Collins et al., 2016).

Neurotransmitter GPCR::GFP are strongly expressed in non-neuronal and non-muscles of the *C. elegans* egg-laying system. Five different classes of neurotransmitter GPCRs are expressed in subsets of the uterine toroid cells, which indicates that these epithelial cells may play a functional role beyond acting as a scaffold for holding eggs. There is also neurotransmitter GPCR expression in other cells not known to be involved with egg laying behavior: the dorsal uterine cell du, uterine ventral cells uv3, spermathecal-uterine valve, spermatheca, vulval toroid cells (Figure 3.10 and Figure 3.11), which may

indicate that neurotransmitters are acting on non-neuronal and non-muscle cells to directly or indirectly modulate the egg-laying circuit.

Lastly, based on our studies of cellular expression patterns for all 26 neurotransmitter GPCRs to previous studies, 81% of cell identifications were all new findings, 14% of the cell identifications confirmed previous publications, 5% of cell identifications could not be confirmed (Figure 3.12).

			+++				++				+													
			Egg-Laying Neurons				Egg-Laying Muscles				Other cells near the Egg-Laying Circuit													
Neurotransmiter GPCRs		G protein	HSN	uv1s	VC4	VC5	vm1	vm2	um1	um2	ut1	ut2	ut3	ut4	uv2	uv3	du	vt	utse	sp-ut	sp	bwm
Serotonin	*ser-1*	*Gαq*	6/12	0/12	1/12	1/12	0/14	14/14	14/14	14/14	0/10	9/10	2/10	0/10	0/10	0/10	0/10	0/10	0/10	0/10	5/10	0/10
	ser-4	*Gαo*	0/14	0/14	0/14	0/14	9/10	10/10	0/10	0/10												
	ser-5	*Gαs*	2/19	0/19	0/19	0/19	1/11	0/11	0/11	0/11	0/11	0/11	0/11	2/11	0/11	0/11	0/11	0/11	0/11	0/11	11/11	10/11
	ser-7	*Gαs*	4/27	0/27	24/27	26/27	10/10	10/10	7/10	10/10	0/10	0/10	0/10	1/10	0/10	0/10	0/10	0/10	0/10	0/10	4/10	0/10
Dopamine	*dop-1*	*Gαq*	0/12	0/12	0/12	0/12					0/11	2/11	2/11	0/11	0/11	0/11	0/11	9/11	0/11	0/11	9/11	2/11
	dop-2	*Gαo*	0/10	10/10	0/10	0/10					0/13	0/13	1/13	10/13	0/13	0/13	0/13	0/13	6/13	0/13	11/13	0/13
	dop-3	*Gαo*	8/10	0/10	7/10	7/10					0/11	0/11	0/11	0/11	0/11	0/11	0/11	5/11	0/11	0/11	4/11	11/11
	dop-4	*Gαs*	0/12	0/12	1/12	1/12	10/10	0/10	0/10	0/10	0/11	0/11	0/11	0/11	0/11	0/11	0/11	0/11	0/11	0/11	9/11	6/11
Octopamine	*octr-1*	*Gαo*	16/23	23/23	6/23	4/23	13/21	5/21	0/21	0/21	0/10	10/10	10/10	6/10	0/10	0/10	0/10	0/10	0/10	0/10	10/10	0/10
	ser-3	*Gαq*	0/11	11/11	0/11	0/11					13/13	11/13	12/13	10/13	0/13	9/13	11/13	0/13	0/13	0/13	13/13	0/13
	ser-6	*Gαs*	1/19	10/19	1/19	1/19					10/10	10/10	10/10	10/10	0/10	8/10	0/10	10/10	0/10	0/10	10/10	0/10
Tyramine	*ser-2*	*Gαo*	5/18	9/18	0/18	0/18	0/10	1/10	0/10	4/10	0/10	0/10	0/10	0/10	0/10	0/10	0/10	6/10	5/10	0/10	9/10	0/10
	tyra-2	*Gαo*	0/12	0/12	0/12	0/12					0/10	0/10	0/10	7/10	0/10	0/10	0/10	0/10	0/10	1/10	8/10	7/10
	tyra-3	*Gαq*	4/10	4/10	6/10	9/10	9/10	10/10	3/10	0/10	6/11	11/11	8/11	11/11	0/11	7/11	0/11	11/11	0/11	11/11	11/11	0/11
Acetylcholine	*gar-1*	*Gαo*	2/22	22/22	1/22	1/22	10/10	10/10	0/10	0/10	0/11	0/11	0/11	0/11	0/11	0/11	0/11	0/11	0/11	0/11	9/11	0/11
	gar-2	*Gαo*	2/15	15/15	0/16	0/16	0/10	10/10	0/10	0/10												
	gar-3	*Gαo; Gαq*	0/12	2/12	1/12	0/12	11/11	0/11	0/11	0/11	0/11	0/11	0/11	0/11	0/11	0/11	0/11	0/11	0/11	3/11	4/11	11/11
GABA	*gbb-1*	*Gαo*	0/15	9/15	0/15	0/15	0/12	0/12	0/12	0/12	9/10	7/10	0/10	0/10	0/10	0/10	10/10	10/10	2/10	2/10	8/10	10/10
	gbb-2	*Gαo*	9/26	3/26	3/26	3/26					0/11	0/11	0/11	0/11	0/11	0/11	0/11	0/11	0/11	0/11	8/11	11/11
Glutamate	*mgl-1*		3/11	5/11	0/11	0/11	1/11	1/11	0/11	0/11	0/11	0/11	0/11	11/11	0/11	11/11	0/11	0/11	11/11	0/11	9/11	0/11
	mgl-2	*Gαq*	2/14	0/14	0/14	0/14																
	mgl-3		0/10	2/10	2/10	2/10																
Orphan	*ador-1*		17/17	0/17	0/17	0/17	10/11	8/11	0/11	0/11												
	F35H10.10		0/14	1/14	1/14	1/14	0/11	0/11	0/11	0/11	0/11	0/11	0/11	1/11	0/11	0/11	0/11	9/11	0/11	3/11	4/11	0/11
	dop-5		0/11	5/11	0/11	0/11					0/11	0/11	1/11	7/11	0/11	0/11	0/11	0/11	0/11	0/11	10/11	0/11
	dop-6		2/10	3/10	1/10	1/10	0/10	7/10	0/10	0/10												

Figure 3.9. Raw data of neurotransmitter GPCRs expression in the *C. elegans* egg-laying system. For every double-labeled strain for all 26 neurotransmitter GPCRs, at least 10 young animals were imaged to identify GPCR::GFP expression in the different cells of the *C. elegans* egg-laying system. *ida-1::mCherry* was used as a marker to identify the HSN, uv1s, VC4, and VC5; *unc-103e::mCherry* was used as a marker to identify vm1, vm2, um1, and um2; *ajm-1::mCherry* was used as a marker to identify ut1, ut2, ut3, ut4, uv2, uv3, du, vt, utse, sp-ut, ut, and bwm. +++ as indicated by the dark grey indicates cells that express GFP are among the strongest cells labeled, ++ as indicated by the moderate grey indicates cells that express GFP that is easily detectable, + as indicated by the light gray indicates cells that express GFP that are slightly above background, and white indicates cells in which GFP was not reproducibly observed. Cell types are denoted by the following abbreviation: bwm: body wall muscles; du: dorsal uterine cell; HSN: hermaphrodite-specific neuron; sp: spermatheca; sp-ut: spermathecal-uterine valve; um: uterine muscle; ut: uterine toroid cell; uv: uterine ventral cell; VC: ventral cord type C neuron; vm: vulval muscle; vt: vulval toroid cells.

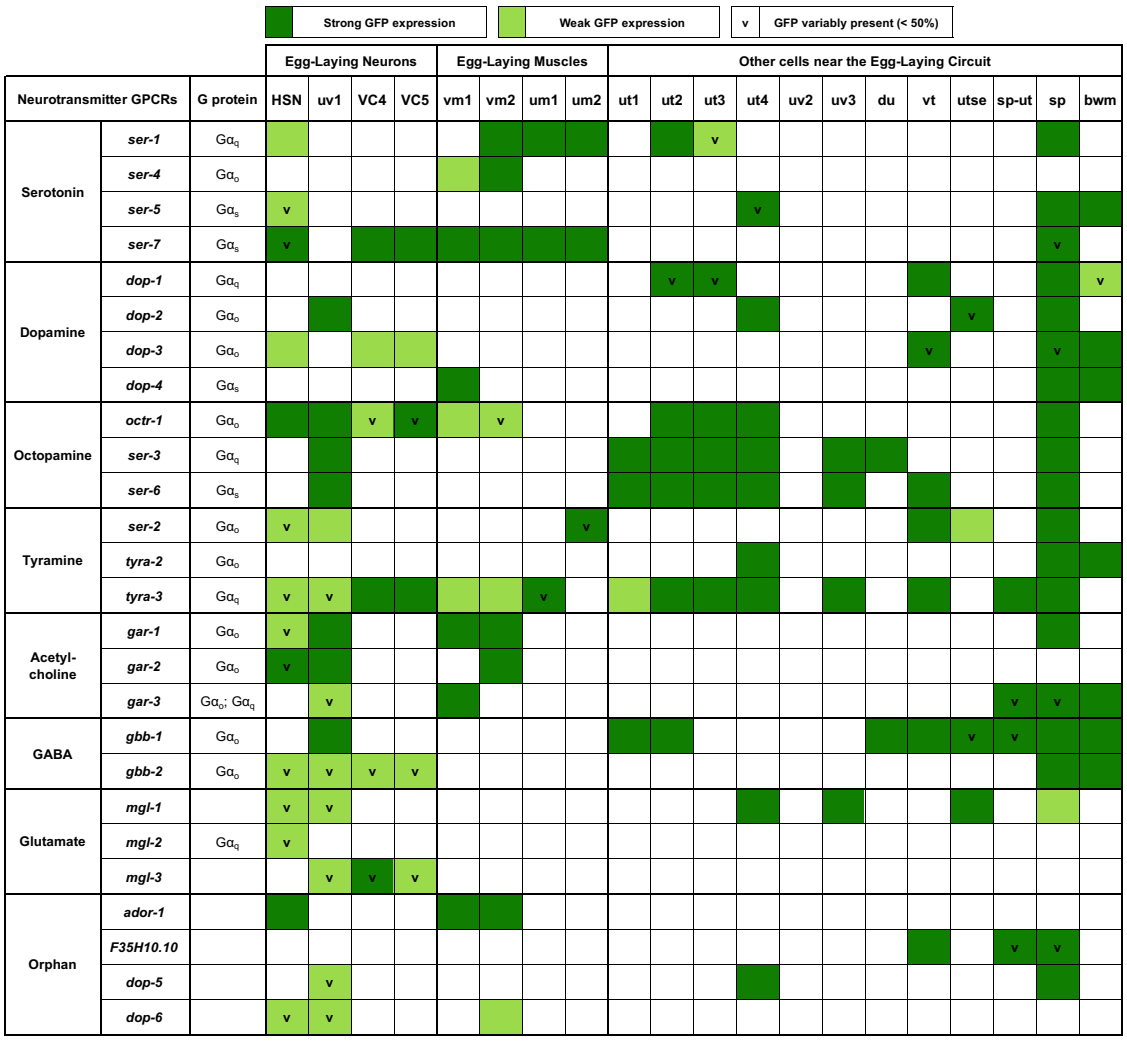

Figure 3.10. Summary of neurotransmitter GPCR expression in the *C. elegans* egg-laying system. For all 26 neurotransmitter GPCRs expressed in different cells of the *C. elegans* egg-laying system, we annotated the presence or absence of GFP expression. Dark green indicates the cells that express GFP are among the strongest cells labeled (+++) or easily detectable (++) levels, bright green indicates cells in which GFP is just above background (+) in at least two different animals, and white indicates cells in which GFP was not reproducibly observed. "v" further denotes cells in which GFP expressed, but was present in less than 50% of animals observed. Cell types are denoted by the following abbreviations: bwm: body wall muscles; du: dorsal uterine cell ; HSN: hermaphrodite-specific neuron; sp: spermatheca; sp-ut: spermathecal-uterine valve; um: uterine muscle; ut: uterine toroid cell; uv: uterine ventral cell; VC: ventral cord type C neuron; vm: vulval muscle; vt: vulval toroid cells.

		HSN	uv1	VC4	VC5	vm1	vm2	um1	um2	ut1	ut2	ut3	ut4	uv2	uv3	du	vt	utse	sp-ut	sp	bwm
# of GPCRs	**Strong**	4	7	3	3	5	6	3	3	3	7	5	9	0	4	2	7	3	4	19	7
	Weak	10	8	3	3	3	3	0	0	1	0	1	0	0	0	0	0	1	0	1	1
	TOTAL	**14**	**15**	**6**	**6**	**8**	**9**	**3**	**3**	**4**	**7**	**6**	**9**	**0**	**4**	**2**	**7**	**4**	**4**	**20**	**8**
$G\alpha_o$	**Strong**	2	5	0	1	2	3	0	1	1	2	1	3	0	0	1	3	2	2	9	5
	Weak	4	3	3	2	2	1	0	0	0	0	0	0	0	0	0	0	1	0	0	0
	TOTAL	**6**	**8**	**3**	**3**	**4**	**4**	**0**	**1**	**1**	**2**	**1**	**3**	**0**	**0**	**1**	**3**	**3**	**2**	**9**	**5**
$G\alpha_q$	**Strong**	0	1	1	1	1	1	2	1	1	4	3	2	0	2	1	2	0	2	5	1
	Weak	3	2	0	0	1	1	0	0	1	0	1	0	0	0	0	0	0	0	0	1
	TOTAL	**3**	**3**	**1**	**1**	**2**	**2**	**2**	**1**	**2**	**4**	**4**	**2**	**0**	**2**	**1**	**2**	**0**	**2**	**5**	**2**
$G\alpha_s$	**Strong**	1	1	1	1	2	1	1	1	1	1	1	2	0	1	0	1	0	0	4	2
	Weak	1	0	0	0	0	0	0	0	0	0	0	0	0	0	0	0	0	0	0	0
	TOTAL	**2**	**1**	**1**	**1**	**2**	**1**	**1**	**1**	**1**	**1**	**1**	**2**	**0**	**1**	**0**	**1**	**0**	**0**	**4**	**2**

Figure 3.11. Summary of neurotransmitters GPCRs cellular expression patterns in the *C. elegans* egg-laying system show neurotransmitter receptors are weakly and variably expressed in egg-laying neurons, yet strongly expressed in egg-laying muscles and other cells near the egg-laying circuit. For each egg-laying cell, the total number of receptors expressed are annotated along with breakdown of receptors that are strongly expressing GFP or weakly expressing GFP. The total number of the type of G protein-coupled receptor that is expressed in egg-laying cells along with a breakdown of receptors that are strongly expressing GFP or weakly expressing GFP are shown. Cell types are denoted by the following abbreviations: bwm: body wall muscles; du: dorsal uterine cell; HSN: hermaphrodite-specific neuron; sp: spermatheca; sp-ut: spermathecal-uterine valve; um: uterine muscle; ut: uterine toroid cell; uv: uterine ventral cell; VC: ventral cord type C neuron; vm: vulval muscle; vt: vulval toroid cells.

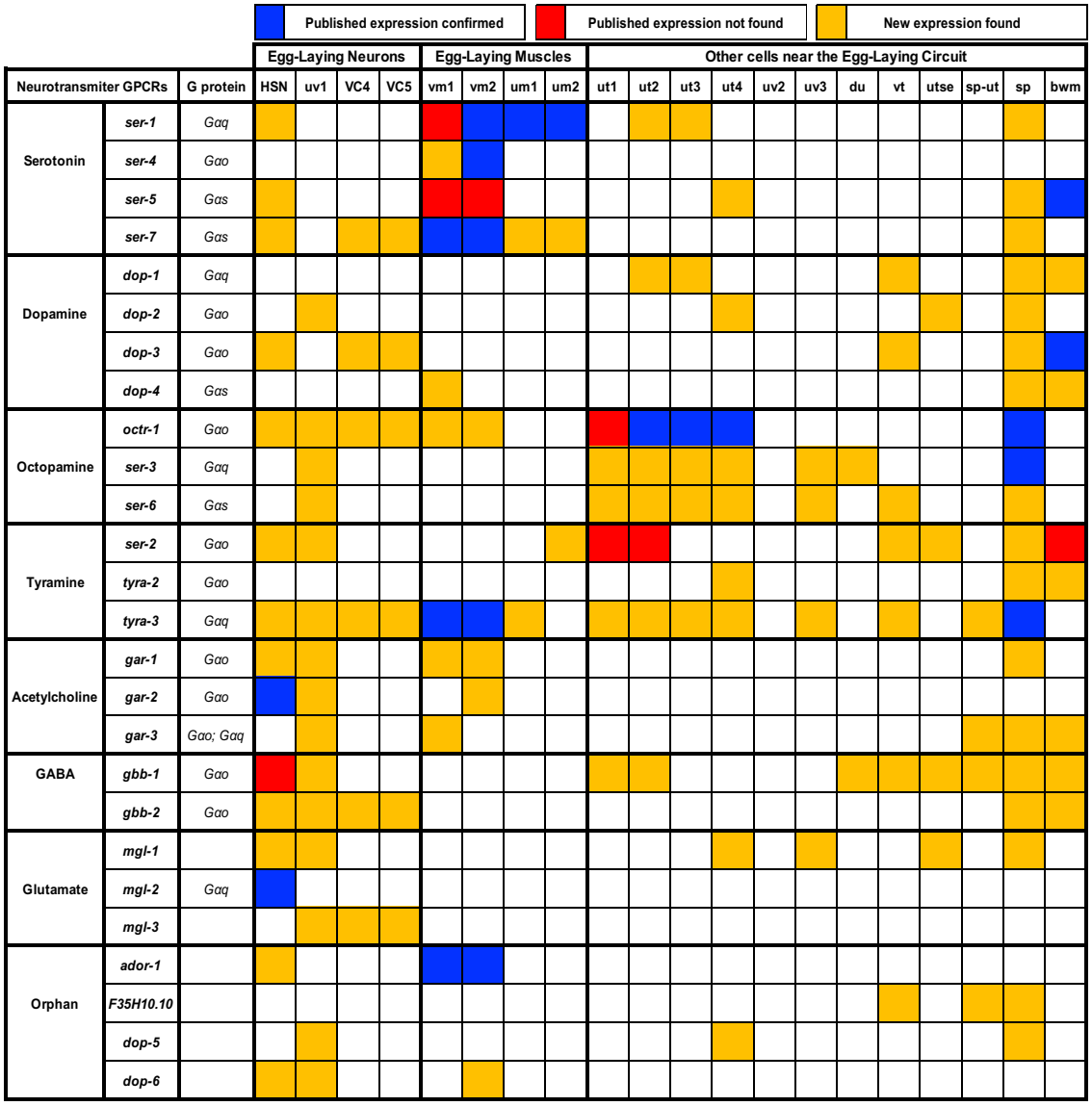

Figure 3.12. Comparison of neurotransmitter GPCR expression in the *C. elegans* egg-laying system based on previous publications. Examining neurotransmitter GPCR cellular expression patterns in *C. elegans* egg-laying neurons, egg-laying muscles, and other cells near the egg-laying circuit from our Neurotransmitter GPCR Atlas compared to previous studies. Blue indicates our studies have confirmed published expression patterns, red indicates our studies could not confirmed published expression patterns, and orange indicates our studies show novel expression patterns in the *C. elegans* egg-laying system. Cell types are denoted by the following abbreviations: bwm: body wall muscles; du: dorsal uterine cell; HSN: hermaphrodite-specific neuron; sp: spermatheca; sp-ut: spermathecal-uterine valve; um: uterine muscle; ut: uterine toroid cell; uv: uterine ventral cell; VC: ventral cord type C neuron; vm: vulval muscle; vt: vulval toroid cells.

3.11 Synaptic vs. extrasynaptic signaling in the *C. elegans* egg-laying circuit

Using the *C. elegans* connectome (Albertson & Thomas, 1976; White et al., 1986; Xu et al., 2013), neurotransmitter map (Serrano-Saiz et al., 2013; Pereira et al., 2016; Gendrel et al., 2016), and the neurotransmitter GPCR Atlas of the *C. elegans* egg-laying system, we sought to determine if the neurotransmitter receptors expressed in the egg-laying neurons or vulval muscles are positioned to receive synaptic or extrasynaptic signals. Synaptic signaling is defined as a neurotransmitter-releasing neuron making a synapse onto a neuron or muscles that expresses that type of neurotransmitter receptor. Extrasynaptic signaling occurs when there is no synapse between the neurotransmitter-releasing neuron and the neuron or muscles that expresses that cognate neurotransmitter receptor that may receive signals from that neurotransmitter-releasing neuron. For example, the serotonin receptor SER-7 is expressed in the HSN and receives synapse(s) from a serotonin-releasing neuron and might be subject to synaptic signaling (Table 3.1); in contrast, the octopamine receptor OCTR-1 is expressed in the HSN, yet no octopamine-releasing neuron synapses onto the HSN (Table 3.1), therefore it is subject to extrasynaptic signaling.

Combining the connectome, neurotransmitter map, and our Neurotransmitter GPCR Atlas, we knew what type of neurotransmitter-releasing neuron makes synapses on the HSN (Table 3.1), VC4 (Table 3.2), VC5 (Table 3.3), vulval muscle vm1 (Table 3.4), and vulval muscle vm2 (Table 3.5). We found that serotonin, acetylcholine, GABA, and glutamate-releasing neurons

primarily act synaptically (Table 3.6) onto the egg-laying neurons and muscles with the exception of vm1 and VC5 (Table 3.6), which receives no synapses from serotonin and GABA-releasing neurons, respectively. In contrast, dopamine, octopamine, and tyramine-releasing neurons may primarily act extrasynaptically on the egg-laying neurons and vulval muscles (Table 3.6) as there are no direct synapses between these neurotransmitter-releasing neurons and that of the egg-laying circuit. Future studies will have to be done to determine whether these extrasynaptic signals are functionally relevant.

Neurons sending input	# of Synapses	Neurotransmitter Released	Receptors expressed on the HSNL and HSNR
AIMR, HSNL, HSNR, VC5	13	Serotonin	SER-1, SER-5, SER-7
?	0	Dopamine	DOP-3
?	0	Tyramine	SER-2, TYRA-3
?	0	Octopamine	OCTR-1, SER-3
AVFL, AVFR, RIR, AVL	13	GABA	GBB-2
AWBL, AWBR, AVBR, ASJR, RIFR, HSNL, HSNR, ASJL, ASJR, AIYL, AIYR, AIAL, AVG, PVPR, PVNR, URXL, VC3, VC5	29	Acetylcholine	GAR-1, GAR-2
ASHL, ASHR, AIMR, PLML, PLMR, PVQL, ASKR	20	Glutamate	MGL-1, MGL-2

Table 3.1 Application of neurotransmitter signaling maps (connectome, neurotransmitter map, and neurotransmitter GPCR atlas in the *C. elegans* egg-laying system) to annotate cases of synaptic vs. extrasynaptic signaling in the HSN. HSN receives synaptic input from serotonin, GABA, Acetylcholine, and Glutamate-releasing neurons and expresses the corresponding neurotransmitter GPCRs. The HSN does not receive synaptic inputs from dopamine, tyramine, and octopamine-releasing neurons, yet it expresses the corresponding neurotransmitter GPCRs, indicating the HSN might be prone to extrasynaptic signaling from these neurotransmitter-releasing neurons. This connectivity information was derived from The Structure of the Nervous System of the Nematode Caenorhabditis elegans (The Mind of the Worm) on WormAtlas, WormWiring, and the Database of Synaptic Connectivity of C. elegans for Computation (Albertson & Thomas, 1976; White et al., 1986; Oshio et al., 2003; Xu et al., 2013). The neurotransmitter map that tells us the identity of every neurotransmitter expressed in every C. elegans neuron (Serrano-Saiz et al., 2013; Pereira et al., 2016; Gendrel et al., 2016). The Neurotransmitter GPCR Atlas of the *C. elegans* egg-laying system was used to annotate cases of neurotransmitter GPCR expression in the HSN.

Neurons sending input	# of Synapses	Neurotransmitter Released	Receptors expressed on VC4
HSNR, VC5	5	Serotonin	SER-7
?	0	Dopamine	DOP-3
?	0	Tyramine	TYRA-3
?	0	Octopamine	OCTR-1
AVF	1	GABA	GBB-2
HSNR, VC5	5	Acetylcholine	
?	0	Glutamate	MGL-3

Table 3.2 Application of neurotransmitter signaling maps (connectome, neurotransmitter map, and neurotransmitter GPCR atlas in the *C. elegans* egg-laying system) to annotate cases of synaptic vs. extrasynaptic signaling in VC4. VC4 receives synaptic input from serotonin and GABA-releasing neurons and expresses the corresponding neurotransmitter GPCRs. VC4 also receives synaptic input from acetylcholine-releasing neurons, yet expresses no acetylcholine GPCRs. VC4 does not receive synaptic inputs from dopamine, tyramine, and octopamine-releasing neurons, yet it expresses the corresponding neurotransmitter receptors, indicating VC4 might be prone to extrasynaptic signaling from these neurotransmitter-releasing neurons. This connectivity information was derived from The Structure of the Nervous System of the Nematode Caenorhabditis elegans (The Mind of the Worm) on WormAtlas, WormWiring, and the Database of Synaptic Connectivity of C. elegans for Computation (Albertson & Thomas, 1976; White et al., 1986; Oshio et al., 2003; Xu et al., 2013). The neurotransmitter map that tells us the identity of every neurotransmitter expressed in every C. elegans neuron (Serrano-Saiz et al., 2013; Pereira et al., 2016; Gendrel et al., 2016). The Neurotransmitter GPCR Atlas of the *C. elegans* egg-laying system was used to annotate cases of neurotransmitter GPCR expression in VC4.

Neurons sending input	# of Synapses	Neurotransmitter Released	Receptors expressed on VC5
HSNL, HSNR, VC4	12	Serotonin	SER-7
?	0	Dopamine	DOP-3
?	0	Tyramine	TYRA-3
?	0	Octopamine	OCTR-1
?	0	GABA	GBB-2
HSNL, HSNR, VC4	12	Acetylcholine	
?	0	Glutamate	MGL-3

Table 3.3 Application of neurotransmitter signaling maps (connectome, neurotransmitter map, and neurotransmitter GPCR Atlas in the *C. elegans* egg-laying system) to annotate cases of synaptic vs. extrasynaptic signaling in VC5. VC5 receives synaptic input from serotonin-releasing neurons and expresses serotonin GPCRs. VC5 also receives synaptic input from acetylcholine-releasing neurons, yet expresses no acetylcholine GPCRs. VC5 does not receive synaptic inputs from dopamine, tyramine, octopamine, GABA, and glutamate-releasing neurons, yet it expresses the corresponding neurotransmitter GPCRs, indicating that VC5 might be subject to extrasynaptic signaling from these neurotransmitter-releasing neurons. This connectivity information was derived from The Structure of the Nervous System of the Nematode Caenorhabditis elegans (The Mind of the Worm) on WormAtlas, WormWiring, and the Database of Synaptic Connectivity of C. elegans for Computation (Albertson & Thomas, 1976; White et al., 1986; Oshio et al., 2003; Xu et al., 2013). The neurotransmitter map that tells us the identity of every neurotransmitter expressed in every C. elegans neuron (Serrano-Saiz et al., 2013; Pereira et al., 2016; Gendrel et al., 2016). The Neurotransmitter GPCR Atlas of the *C. elegans* egg-laying system was used to annotate cases of neurotransmitter GPCR expression in VC5.

Neurons sending input	# of Synapses	Neurotransmitter Released	Receptors expressed on vm1R
?	0	Serotonin	SER-4, SER-7
?	0	Dopamine	DOP-4
?	0	Tyramine	TYRA-3
?	0	Octopamine	OCTR-1
VD7	1	GABA	
VA7, VB6	2	Acetylcholine	GAR-1, GAR-3
?	0	Glutamate	

Table 3.4 Application of neurotransmitter signaling maps (connectome, neurotransmitter map, and neurotransmitter GPCR atlas in the *C. elegans* egg-laying system) to annotate cases of synaptic vs. extrasynaptic signaling in the vulval muscle vm1. vm1 receives synaptic input from acetylcholine-releasing neurons and expresses acetylcholine GPCRs. vm1 also receives synaptic input from GABA-releasing neurons, yet expresses no GABA GPCRs. vm1 does not receive synaptic inputs from serotonin, dopamine, tyramine, octopamine, and glutamate-releasing neurons, yet it expresses the corresponding neurotransmitter GPCRs, indicating vm1 might be subject to extrasynaptic signaling from these neurotransmitter-releasing neurons. This connectivity information was derived from The Structure of the Nervous System of the Nematode Caenorhabditis elegans (The Mind of the Worm) on WormAtlas, WormWiring, and the Database of Synaptic Connectivity of C. elegans for Computation (Albertson & Thomas, 1976; White et al., 1986; Oshio et al., 2003; Xu et al., 2013). The neurotransmitter map that tells us the identity of every neurotransmitter expressed in every C. elegans neuron (Serrano-Saiz et al., 2013; Pereira et al., 2016; Gendrel et al., 2016). The Neurotransmitter GPCR Atlas of the *C. elegans* egg-laying system was used to annotate cases of neurotransmitter GPCR expression in vm1.

Neurons sending input	# of Synapses	Neurotransmitter Released	Receptors expressed on vm2R
VC4, VC5	2	Serotonin	SER-1, SER-4, SER-7
?	0	Dopamine	
?	0	Tyramine	TYRA-3
?	0	Octopamine	OCTR-1
?	0	GABA	
VC4, VC5	2	Acetylcholine	GAR-1, GAR-2
?	0	Glutamate	

Table 3.5 Application of neurotransmitter signaling maps (connectome, neurotransmitter map, and neurotransmitter GPCR atlas in the *C. elegans* egg-laying system) to annotate cases of synaptic vs. extrasynaptic signaling in vulval muscle vm2. vm2 receives synaptic input from serotonin and acetylcholine-releasing neurons and expresses the corresponding neurotransmitter GPCRs. vm2 does not receive synaptic inputs from tyramine or octopamine-releasing neurons, yet it expresses the corresponding neurotransmitter GPCRs, indicating that vm2 might be subject to extrasynaptic signaling from these neurotransmitter-releasing neurons. This connectivity information was derived from The Structure of the Nervous System of the Nematode Caenorhabditis elegans (The Mind of the Worm) on WormAtlas, WormWiring, and the Database of Synaptic Connectivity of C. elegans for Computation (Albertson & Thomas, 1976; White et al., 1986; Oshio et al., 2003; Xu et al., 2013). The neurotransmitter map that tells us the identity of every neurotransmitter expressed in every C. elegans neuron (Serrano-Saiz et al., 2013; Pereira et al., 2016; Gendrel et al., 2016). The Neurotransmitter GPCR Atlas of the *C. elegans* egg-laying system was used to annotate cases of neurotransmitter GPCR expression in vm2.

Neurotransmitter Released	Synaptic	Extrasynaptic
Serotonin	HSN, VC4, VC5, vm2	vm1
Dopamine		HSN, VC4, VC5, vm1
Octopamine		HSN, VC4, VC5, vm1, vm2
Tyramine		HSN, VC4, VC5, vm1, vm2
Acetylcholine	HSN, vm1, vm2	
GABA	HSN, VC4	VC5
Glutamate	HSN	

Table 3.6 Synaptic vs. extrasynaptic analysis of the *C. elegans* egg-laying system. Serotonin, acetylcholine, GABA, and glutamate-releasing neurons primarily act synaptically on the egg-laying system. Serotonin may act extrasynaptically onto vm1 and GABA might act extrasynaptically on VC5, as these cells receive no synapses from serotonin and GABA-releasing neurons, respectively. Dopamine, octopamine, and tyramine may primarily act extrasynaptically on the egg-laying system. This connectivity information was derived from The Structure of the Nervous System of the Nematode Caenorhabditis elegans (The Mind of the Worm) on WormAtlas, WormWiring, and the Database of Synaptic Connectivity of C. elegans for Computation (Albertson & Thomas, 1976; White et al., 1986; Oshio et al., 2003; Xu et al., 2013). The neurotransmitter map that tells us the identity of every neurotransmitter expressed in every C. elegans neuron (Serrano-Saiz et al., 2013; Pereira et al., 2016; Gendrel et al., 2016). The Neurotransmitter GPCR Atlas of the *C. elegans* egg-laying system was used to annotate cases of neurotransmitter GPCR expression in different cells of the *C. elegans* egg-laying system.

3.12 Discussion and Conclusion

In summary, all 26 neurotransmitter GPCRs, which includes serotonin, dopamine, octopamine, tyramine, acetylcholine, GABA, glutamate, and orphan GPCRs are expressed in different subsets of the *C. elegans* egg-laying circuit. The role of these neurotransmitter GPCRs in regulating the *C. elegans* egg-laying system will have to be further explored, but our Neurotransmitter GPCR Atlas which catalogues the cellular expression for all 26 neurotransmitter GPCR in the cells of the *C. elegans* egg-laying system can be used as a starting point to generate testable hypothesis. A few key discoveries include: 1) Some neurons express many neurotransmitter GPCRs, for example, the HSN expresses a total of 14 neurotransmitter GPCRs. 2) There is a lot of weak, variable GFP expression in neurons while there is prominently strong GFP expression in egg-laying muscles and non-neuronal cells. 3) Neurotransmitter GPCRs are often expressed in non-neuronal cells such as the uterine toroid cells, vulval toroid cells, and the spermatheca which are not known to regulate the egg-laying circuit. 4) Dopamine, octopamine, and tyramine may act extrasynaptically on the *C. elegans* egg-laying circuit, while serotonin, GABA, and glutamate may mainly act synaptically on this circuit. Further studies will have to be done to determine if these observations extend beyond the *C. elegans* egg-laying circuit to the rest of the nervous system.

Chapter 4: Functional role of neurotransmitter GPCRs in the *C. elegans* egg-laying circuit

Some text, figures, and captions in Chapter 4 adapted from those submitted as:

Fernandez, R.W., Wei, K., Wang, E.Y., Mikalauskaite, D., Olson, A., Pepper, J., Kim, S., Christie, N., Hasse, S., Sarov, M., and Koelle, M.R. Cellular expression and functional roles of 26 neurotransmitter GPCRs in the *C. elegans* egg-laying circuit. (2020)

This work was n in collaboration with undergraduate student Kimberly Wei, who helped in outcrossing single knockouts of $G\alpha_o$-coupled *neurotransmitter GPCRS, generating combination knockouts of* $G\alpha_o$-coupled *neurotransmitter GPCRS, and tested neurotransmitter GPCR knockout(s) and overexpressors in the unlaid egg assay and early-staged assay for Figure 4.1, 4.2, 4.4, 4.5, 4.7, 4.8, and 4.10.*

4.1 Introduction

In this chapter, we describe our approaches to lay the foundation for determining the function of neurotransmitter GPCRs in the *C. elegans* egg-laying system. Our initial approach was to test whole body single knockouts for all 26 neurotransmitter GPCRs to determine if there were any egg-laying defects. We used two established egg-laying assays, the unlaid egg assay, which measures the accumulation of unlaid eggs in the uterus of the worm. Egg-laying defective animals retain an abundance of eggs, while hyperactive egg-laying animals retain very few eggs. Our second assay is the early-staged egg-laying assay, which screens for hyperactive egg-laying animals, as determined by a high percentage of early-staged eggs laid (eggs that have < 8 cells), compared to

wild-type worms, which do not lay early-staged eggs, but instead lay late-staged eggs that have >8 cells. In addition to testing single neurotransmitter GPCR knockouts, we also went on to test a combination of $G\alpha_o$-coupled neurotransmitter GPCR knockouts to examine if these knockouts have a hyperactive egg-laying defect similar to the null mutant for the G protein $G\alpha_o$, which is a known hyperactive egg-laying animal.

As neurotransmitter receptor knockouts gave us no reproducible and strong egg-laying defects, our next approach was to overexpress neurotransmitter receptors, using our high-copy GPCR::GFP transgenes that have all the regulatory and coding sequences, to elucidate if these neurotransmitter GPCRs have any egg-laying defects. Our rationale was that overexpression of neurotransmitter GPCR::GFP transgenes should lead to increased receptor signaling, and in doing so, it may affect the activity of the egg-laying circuit. This approach has revealed egg-laying defects for several neurotransmitter GPCRs, which were validated.

4.2 Single knockouts of neurotransmitter GPCR genes does not reveal strong egg-laying defects

We sought to investigate whether neurotransmitter GPCRs expressed in the *C. elegans* egg-laying system are involved in regulating the egg-laying circuit. Even though a subset of neurotransmitter GPCR knockouts has been previously tested in egg-laying assays (Koelle, 2018), we sought to test single knockouts for all 26 neurotransmitter GPCR in these assays to determine if we could discover any new egg-laying defects. We collected neurotransmitter GPCR single knockouts

from the Caenorhabditis Genetics Center (CGC) and National BioResource Project (NBRP); most but not all of the neurotransmitter GPCR single knockouts were outcrossed, a detailed list can be found in Appendix Chapter 5.2. We first tested all of the 26 neurotransmitter GPCR single knockouts in the unlaid egg assay, which measures the accumulation of unlaid eggs in the uterus of the worm. We used two standard egg-laying defective mutants as controls for the unlaid egg assay, specifically *egl-10(md176) V* and *goa-1(n1134) I*, which accumulate an abundance or very few eggs in the uterus of the worm, respectively.

Compared to the controls, single knockouts of neurotransmitter GPCRs did not reveal egg-laying defects in the number of eggs accumulated in the uterus of the worm with the exception of *dop-4(tm1392) X*, a null allele for dopamine receptor DOP-4, (Figure 4.1). Unfortunately, there were no other *dop-4* null alleles preventing us from validating this egg-laying defect unless we generate another *dop-4* null allele through a CRISPR-based approach. Instead, we attempted to rescue the egg-laying defect of *dop-4(tm1392) X* by re-introducing the *dop-4* gene. While the standard strategy is microinjection of the *dop-4* gene in the *dop-4(tm1392) X* background to determine if we can rescue this egg-laying defect, we took an alternative approach. As we have generated high-copy GPCR::GFP transgenic strains, we decided to cross the chromosomally integrated *dop-4:SL2::NLS::GFP* into the *dop-4(tm1392) X* background. Unfortunately, in the *dop-4(tm1392) X*; *dop-4:SL2::NLS::GFP* construct, we were not able to rescue the egg-laying defect of *dop-4(tm1392) X*

(Figure 4.2). Validating the egg-laying defect of the dopamine receptor DOP-4 knockout will be left for future studies.

We next went on to test single knockouts for each of the 26 neurotransmitter GPCRs in the early-staged egg-laying assay, which measures the percentage of early-staged eggs laid. Hyperactive egg-laying animals lay a high percentage of early-staged eggs and we set a cut-off of 50% for hyperactive egg-laying animals, according to previous studies (Bany et al., 2003). Compared to our control, *goa-1(n1134) I* animals that are mutants known for having a strong hyperactive egg-laying phenotype, none of the single neurotransmitter GPCR knockouts displayed hyperactive egg-laying defects (Figure 4.3).

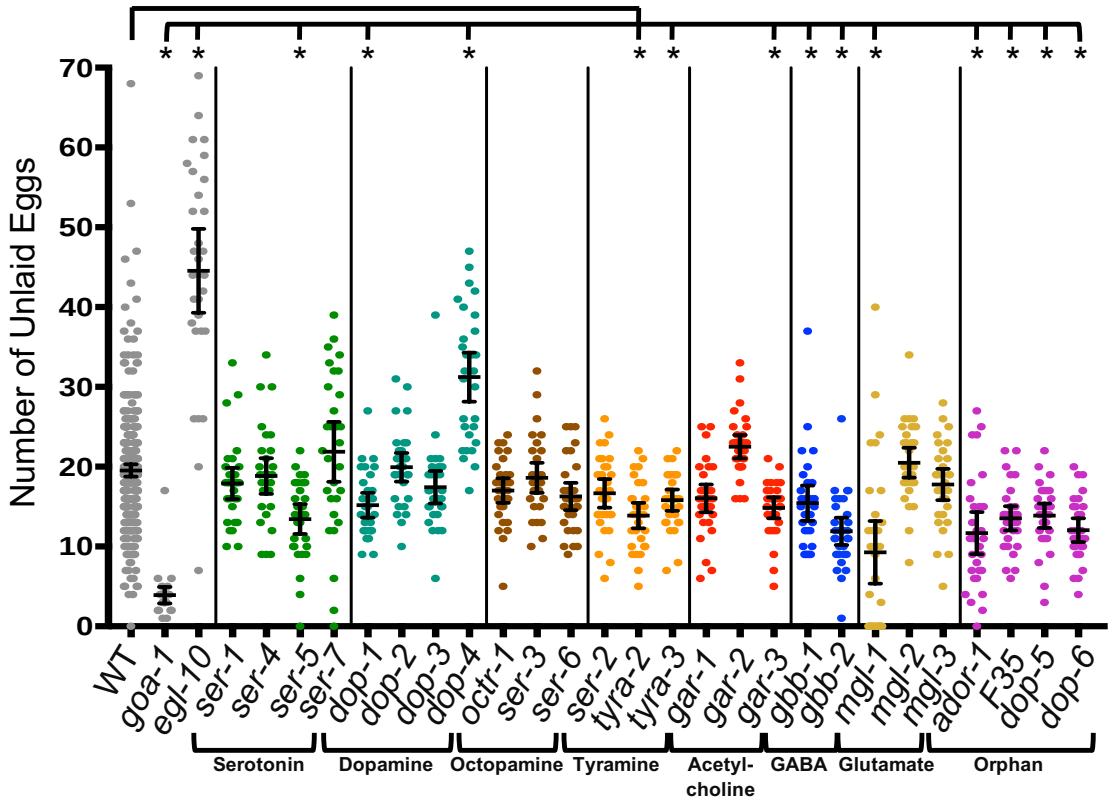

Figure 4.1 Only one neurotransmitter GPCR gene single knockout is egg-laying defective as seen by the accumulation of unlaid eggs in the uterus of the worm. WT: Wild-type; *egl-10(md176) V* and *goa-1(n1134) I* served as controls for strong egg-laying defects. Light gray: Controls; Dark green: serotonin GPCRs; light green: dopamine GPCRs; brown: octopamine GPCRs; orange: tyramine GPCRs; red: acetylcholine GPCRs; blue: GABA GPCRs; yellow: glutamate GPCRs; magenta: orphan GPCRs. n ≥ 30 for each strain. Statistical significance was tested using one-way ANOVA with Bonferroni correction for multiple comparisons for the Unlaid Egg Assay. p ≥0.05 was considered not significant (ns) and p <0.05 (*) was considered significant.

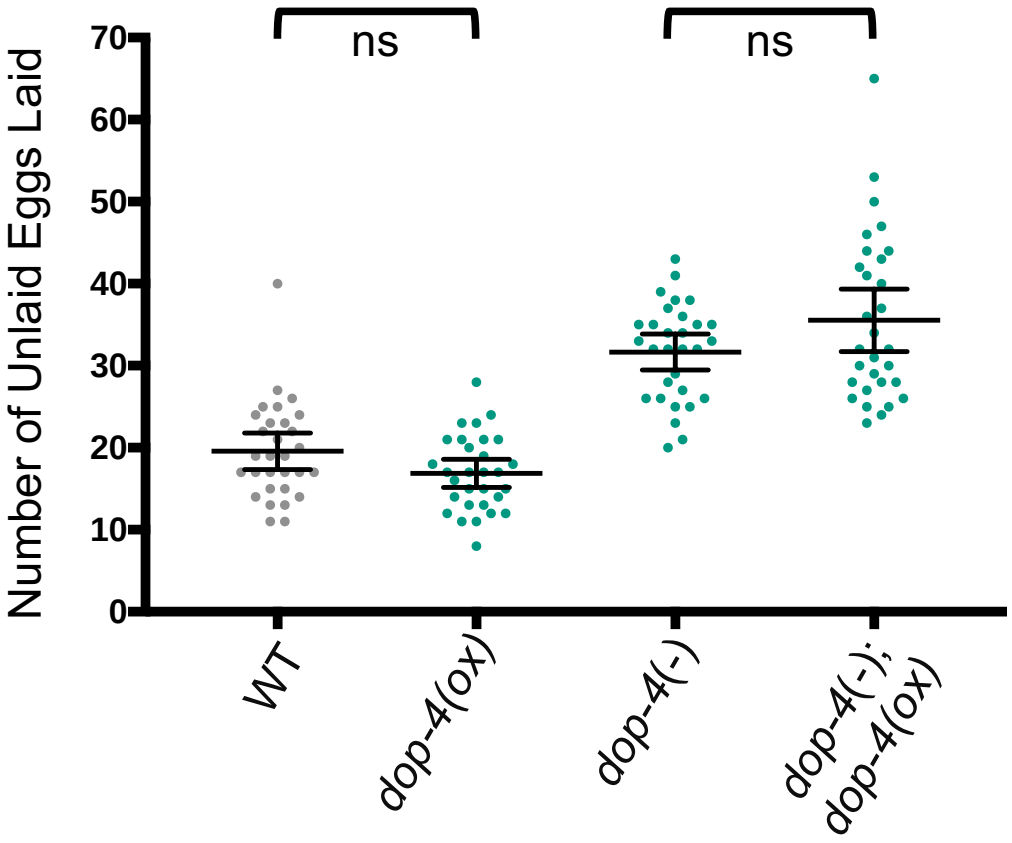

Figure 4.2. The egg-laying defective phenotype for the dopamine receptor DOP-4 knockout cannot be rescued by introduction of the chromosomally integrated DOP-4::SL2::NLS::GFP construct. WT: Wild-type; -: GPCR knockout; ox: overexpression of GPCR::GFP transgenic strain. Light gray: Controls; light green: dopamine GPCRs. n ≥ 30 for each strain. Statistical significance was tested using one-way ANOVA with a Tukey's test to determine statistical significance for multiple comparisons for the Unlaid Egg Assay. p ≥0.05 was considered not significant (ns) and p <0.05 (*) was considered significant.

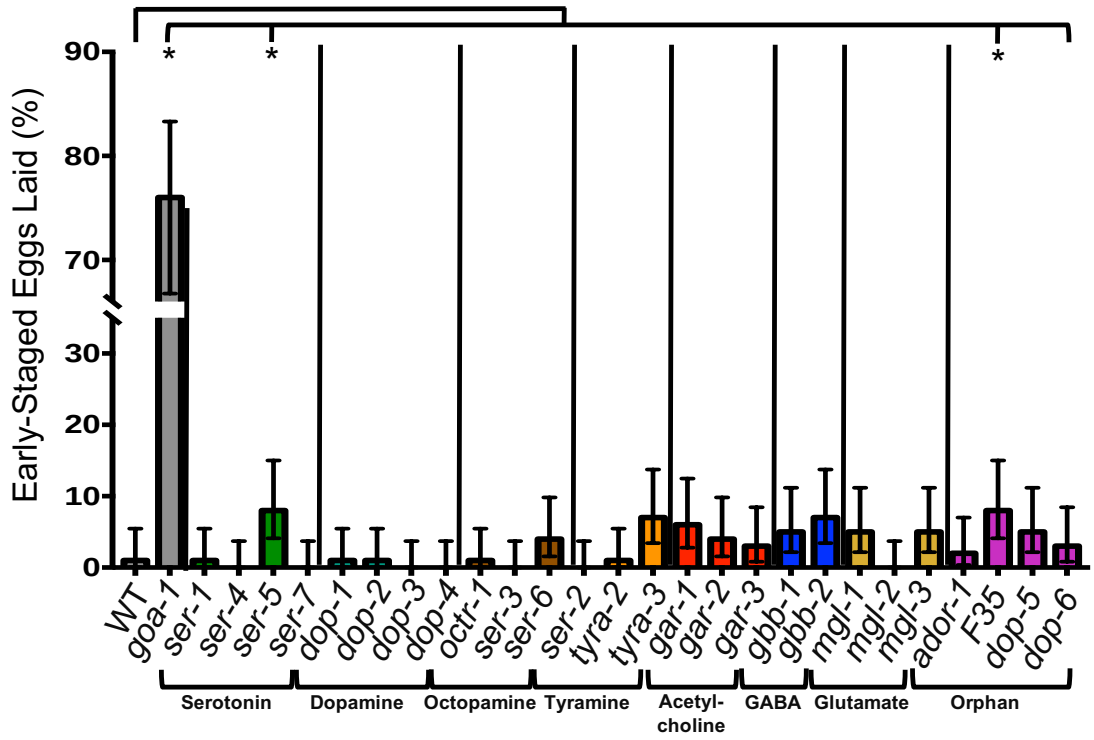

Figure 4.3 Neurotransmitter GPCR gene single knockout reveals no defect on the percentage of early-staged eggs laid. WT: Wild-type; *goa-1(n1134) I* served as a control for hyperactive egg-laying. Light gray: Controls; Dark green: serotonin GPCRs; light green: dopamine GPCRs; brown: octopamine GPCRs; orange: tyramine GPCRs; red: acetylcholine GPCRs; blue: GABA GPCRs; yellow: glutamate GPCRs; magenta: orphan GPCRs. n=100 eggs for each strain. Statistical significance was tested with the Fisher's exact test for the Early-Staged Egg-Laying Assay. The Wilson-Brown Method was used to determine the 95% C.I. for binomial data. $p \geq 0.05$ was considered not significant (ns) and $p < 0.05$ (*) was considered significant.

4.3 $G\alpha_o$-coupled neurotransmitter GPCR knockout does not reveal strong egg-laying defects

We rationalized that we did not see strong egg-laying defects, due to functional redundancy (Ringstad and Horvitz, 2008) where neurotransmitter GPCRs can compensate for the absence of a receptor, making it difficult to reveal egg-laying phenotypes. In order to overcome this functional redundancy, we decided to generate a series of neurotransmitter receptor knockouts.

Our strategy focused on *goa-1(n1134) I,* a null mutant for the G protein $G\alpha_o$, as the absence of this G protein in the worm leads to a strong hyperactive egg-laying phenotype (Mendel et al., 1995; Sègalat et al., 1995). As single knockouts for $G\alpha_o$-coupled neurotransmitter GPCRs revealed no hyperactive egg-laying phenotypes (Figure 4.3), we hypothesized that if we knocked out several $G\alpha_o$-coupled neurotransmitter GPCRs, we should see a strong hyperactive-egg-laying phenotype similar to knocking out the G protein $G\alpha_o$ in the entire animal. Table 4.1 shows all $G\alpha_o$-coupled neurotransmitter GPCRs that are expressed in different cells of the *C. elegans* egg-laying system. Out of the 11 $G\alpha_o$-coupled neurotransmitter GPCRs, we decided to generate receptor knockouts for most of the receptors that are expressed in the neuroendocrine cells uv1s. This includes the dopamine GPCR DOP-2, the octopamine GPCR OCTR-1, the acetylcholine GPCRs GAR-1 and GAR-2, and the GABA GPCR GBB-2; all of these single receptor knockouts were outcrossed. Using primers to genotype for the $G\alpha_o$-coupled neurotransmitter GPCRs deletion, we generated a

combination of receptor knockouts from double knockouts to a quintuple knockout.

We tested all of these $G\alpha_o$-coupled neurotransmitter GPCR knockouts in the early-staged egg-laying assay, using *goa-1(n1134) I*, as a control. We did not see a strong hyperactive egg-laying phenotype for the $G\alpha_o$-coupled neurotransmitter GPCRs knockouts (Figure 4.4), at most 25% early-staged eggs laid was seen in these receptor knockouts. We rationalized that this may be due to the presence of other $G\alpha_o$-coupled neurotransmitter GPCRs in the *C. elegans* egg-laying system compensating for the absence of these receptors. In addition, cell-specific knockouts of these receptors may reveal egg-laying phenotypes that are not observed when knocking out $G\alpha_o$-coupled neurotransmitter GPCRs in the whole animal.

Next, we decided to test these $G\alpha_o$-coupled neurotransmitter GPCRs knockouts in the unlaid egg assay to check if these combination knockouts had egg-laying defects in the accumulation of unlaid eggs in the uterus of the worm. Compared to our *egl-10(md176) V* control that is known to be egg-laying defective as it has ~45 eggs in the uterus of the worm, $G\alpha_o$-coupled neurotransmitter GPCRs knockouts did not have a strong egg-laying defect as only ~25 eggs were in the uterus of the worm for the quintuple knockout (Figure 4.5).

Neurotransmitter GPCRs	Cellular Expression Patterns		
$G\alpha_o$-coupled Receptors	**Egg-laying neurons**	**Egg-laying muscles**	**Other cells**
Serotonin GPCR, SER-4		vm1, vm2	
Dopamine GPCR, DOP-2	uv1		ut4, utse, sp
Dopamine GPCR, DOP-3	HSN, VC4, VC5		vt, sp, bwm
Octopamine GPCR, OCTR-1	HSN, uv1, VC4, VC5	vm1, vm2	ut2, ut3, ut4, sp
Tyramine GPCR, SER-2	HSN, uv1	um2	vt, utse, sp
Tyramine GPCR, TYRA-2			ut4, sp, bwm
Acetylcholine GPCR, GAR-1	HSN, uv1	vm1, vm2	sp
Acetylcholine GPCR, GAR-2	HSN, uv1	vm2	
Acetylcholine GPCR, GAR-3	uv1	vm1	sp-ut, sp, bwm
GABA GPCR, GBB-1	uv1		ut1, ut2, vt, utse, sp-ut, sp, bwm
GABA GPCR, GBB-2	HSN, uv1, VC4, VC5		sp, bwm

Table 4.1 $G\alpha_o$-coupled neurotransmitter GPCRs expressed in the *C. elegans* egg-laying system. $G\alpha_o$-coupled neurotransmitter GPCRs expressed in different cells of the egg-laying circuit. Cell types are denoted by the following abbreviations: bwm: body wall muscles; HSN: hermaphrodite-specific neuron; sp: spermatheca; sp-ut: spermathecal-uterine valve; um: uterine muscle; ut: uterine toroid cell; utse: uterine seam; uv: uterine ventral cell; VC: ventral cord type C neuron; vm: vulval muscle; vt: vulval toroid cells.

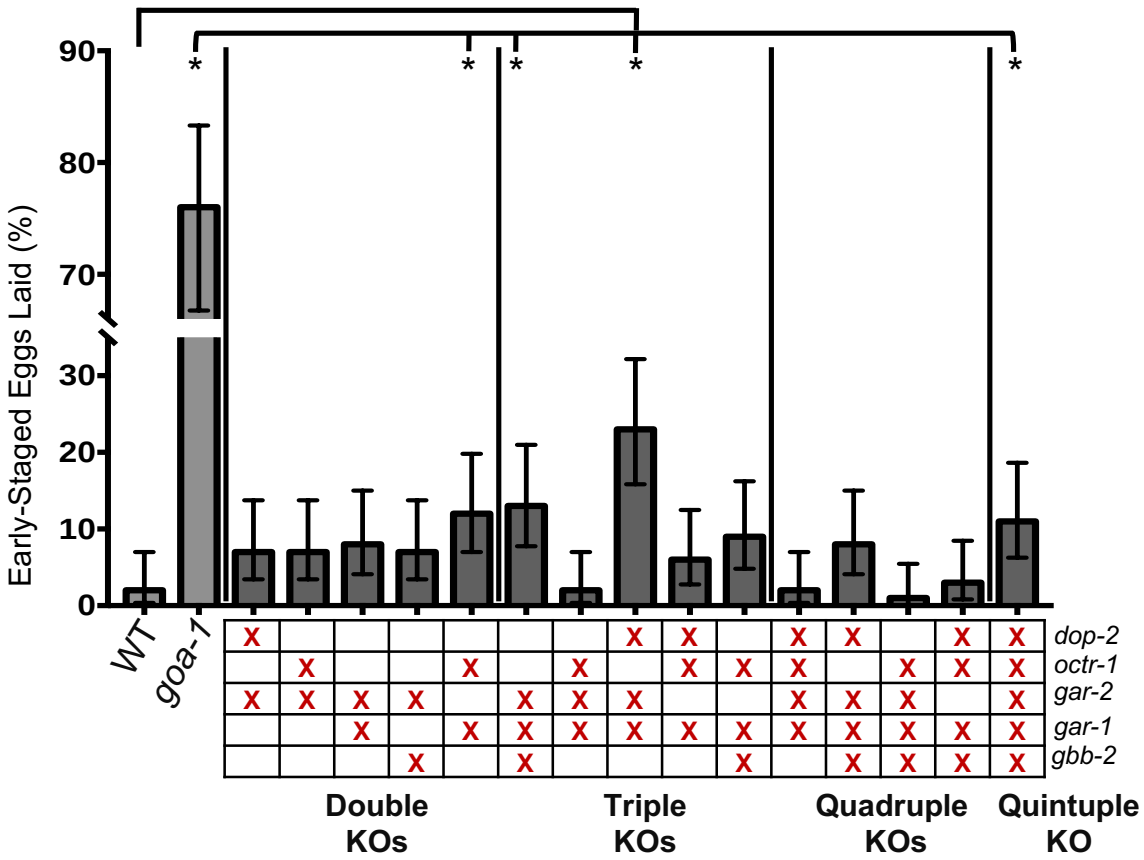

Figure 4.4 Combination knockouts of Gα$_o$-coupled neurotransmitter GPCRs expressed in the egg-laying system reveals no defect on the percentage of early-staged eggs laid. WT: Wild-type; *goa-1(n1134) I* served as a control for hyperactive egg-laying. Light gray: Controls; dark gray: Gα$_o$-coupled neurotransmitter GPCR knockout(s). In the table below graph, the red "X" signifies the combination of neurotransmitter Gα$_o$-coupled neurotransmitter GPCR genes knockout. n=100 eggs for each strain. Statistical significance was tested with the Fisher's exact test for the Early-Staged Egg-Laying Assay. The Wilson-Brown Method was used to determine the 95% C.I. for binomial data. p ≥0.05 was considered not significant (ns) and p <0.05 (*) was considered significant.

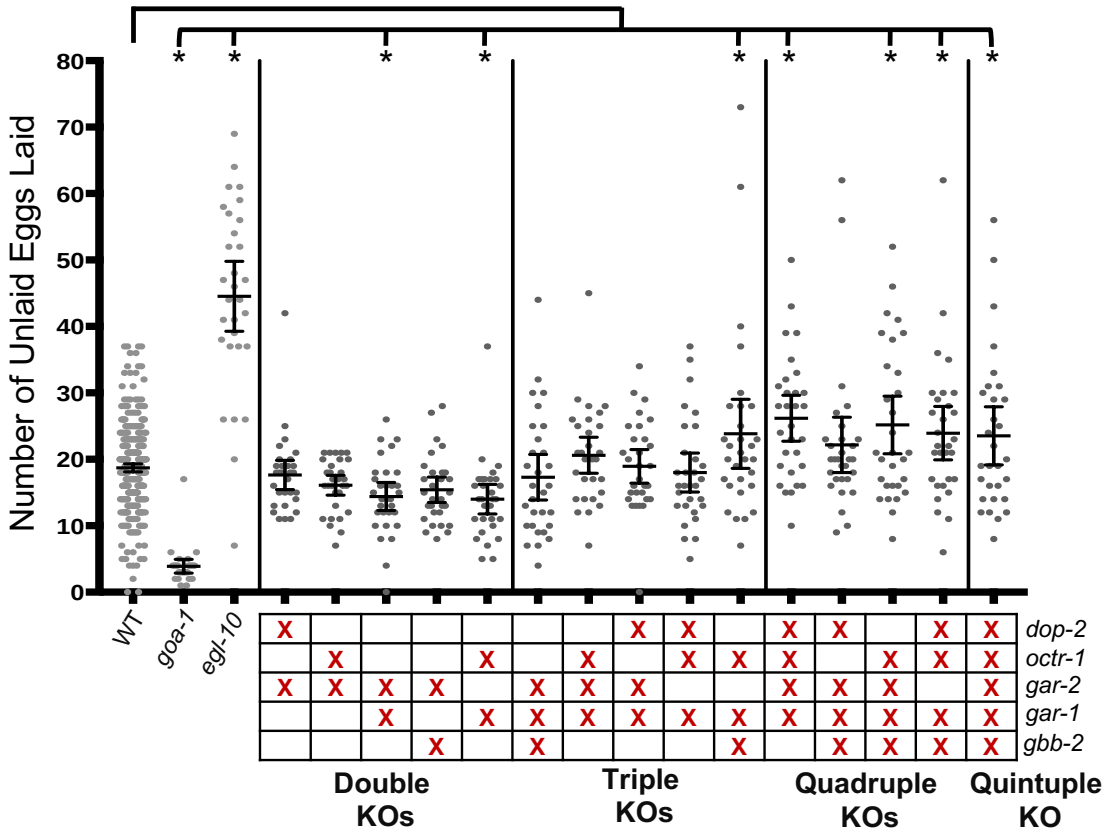

Figure 4.5 Combination knockouts of Gα$_o$-coupled neurotransmitter GPCRs expressed in the *C. elegans* egg-laying system reveals no strong egg-laying defects in the accumulation of unlaid eggs in the uterus. WT: Wild-type; *egl-10(md176) V* and *goa-1(n1134) I* served as controls for strong egg-laying defects. Light gray: Controls; dark gray: Gα$_o$-coupled neurotransmitter GPCR knockout(s). In the table below graph, the red "X" signifies the combination of neurotransmitter Gα$_o$-coupled neurotransmitter GPCR genes knockout. n ≥ 30 for each strain. Statistical significance was tested using one-way ANOVA with Bonferroni correction for multiple comparisons for the Unlaid Egg Assay. p ≥0.05 was considered not significant (ns) and p <0.05 (*) was considered significant.

4.4 Overcoming the absence of egg-laying phenotypes in neurotransmitter receptor knockout(s) through overexpression of the serotonin GPCR SER-1

As knocking out single or multiple neurotransmitter receptor(s) did not reveal egg-laying defects, our next approach was to overexpress neurotransmitter receptors, using our high-copy GPCR::GFP transgenes that have all the regulatory and coding sequences, to elucidate any egg-laying defects. As serotonin is well-known to regulate egg-laying behavior (Xiao et al., 2006; Hapiak et al., 2009; Brewer et al., 2019), we decided to pilot this strategy of overexpression of a neurotransmitter GPCR, with the extrachromosomal serotonin receptor *ser-1::gfp*. As seen in Figure 4.5, the extrachromosomal serotonin receptor *ser-1::gfp* has a strong hyperactive egg-laying defect. We also tested three independent integrated lines for the serotonin receptor *ser-1::gfp* and all independent lines had strong hyperactive egg-laying defects (Figure 4.5). The overexpression of the serotonin receptor, *ser-1(ox)*, indicated that this is a good approach to look for egg-laying defects.

Next, we wanted to confirm that this hyperactive egg-laying defect for *ser-1(ox)* is due to overexpression of the serotonin receptor SER-1 and not due to overexpression of the green fluorescent protein (GFP). We rationalized that the overexpression of the neurotransmitter receptor leads to an increase in receptor signaling that lead to the egg-laying defect. An increase in receptor signaling most likely resulted from neurotransmitters activating the cognate neurotransmitter receptor that is being overexpressed. Therefore, we hypothesized that if we knock out the neurotransmitter for the neurotransmitter

receptor being overexpressed with a known egg-laying defect, then in the absence of the neurotransmitter for that specific neurotransmitter receptor, the egg-laying defect should go back down to wild-type levels even though the neurotransmitter receptor is being overexpressed. In our case, serotonin is acting on the serotonin receptor SER-1 that is being overexpressed, which leads to an increase in SER-1 signaling, which resulted in the hyperactive egg-laying defect. If we knock out the serotonin biosynthetic enzyme TPH-1 that produces serotonin, in the background where SER-1 is being overexpressed, *ser-1(ox)*, we predict that the hyperactive egg-laying defect will be reduced similar to *tph-1(mg280) II*. As seen in Figure 4.7, the chromosomally integrated *ser-1(ox)* hyperactive egg-laying defect was rescued in the *tph-1(mg280) II*; *ser-1(ox)* background similar to *tph-1(mg280) II* levels. This validated that the *ser-1(ox)* hyperactive egg-laying defect was due to overexpression of the serotonin receptor SER-1 and not overexpression of GFP.

As previous studies have shown that serotonin release from the HSN is known to promote egg-laying (Desai et al., 1988, Shyn et al., 2003, Carnell et al., 2005; Hobson et at. 2006; Hapiak et al., 2009) by acting on the vulval muscles, the egg-laying defect seen when overexpressing the serotonin GPCR SER-1 was expected. However, SER-1 expression in the HSN (Table 4.2) is a new direction that we have not previously considered as we thought the serotonin receptors were only expressed in the vulval muscles and this discovery can further help us understand how egg laying is regulated.

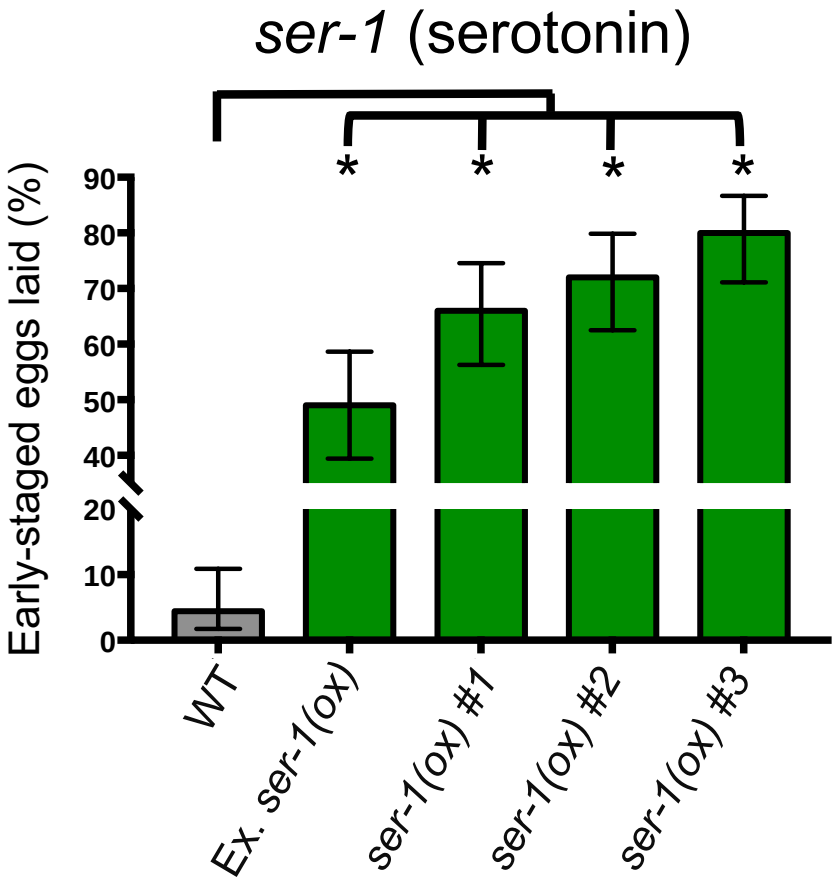

Figure 4.6 Overexpression of the serotonin GPCR SER-1 reveals strong hyperactive egg-laying defects that is validated by independent integrants and the extrachromosomal strain for SER-1. WT: Wild-type; Ex: extrachromosomal transgenic GPCR::GFP strain; ox: overexpression of GPCR::GFP transgenic strain. The number after (ox) indicates the independent line for the chromosomally integrated GPCR::GFP strains. *ser-1(ox)* #1 is 2x outcrossed while the other two independent lines are not outcrossed. Light gray: control; Dark green: serotonin GPCR. n=100 eggs for each strain. Statistical significance was tested with the Fisher's exact test for the Early-Staged Egg-Laying Assay. The Wilson-Brown Method was used to determine the 95% C.I. for binomial data. $p \geq 0.05$ was considered not significant (ns) and $p < 0.05$ (*) was considered significant.

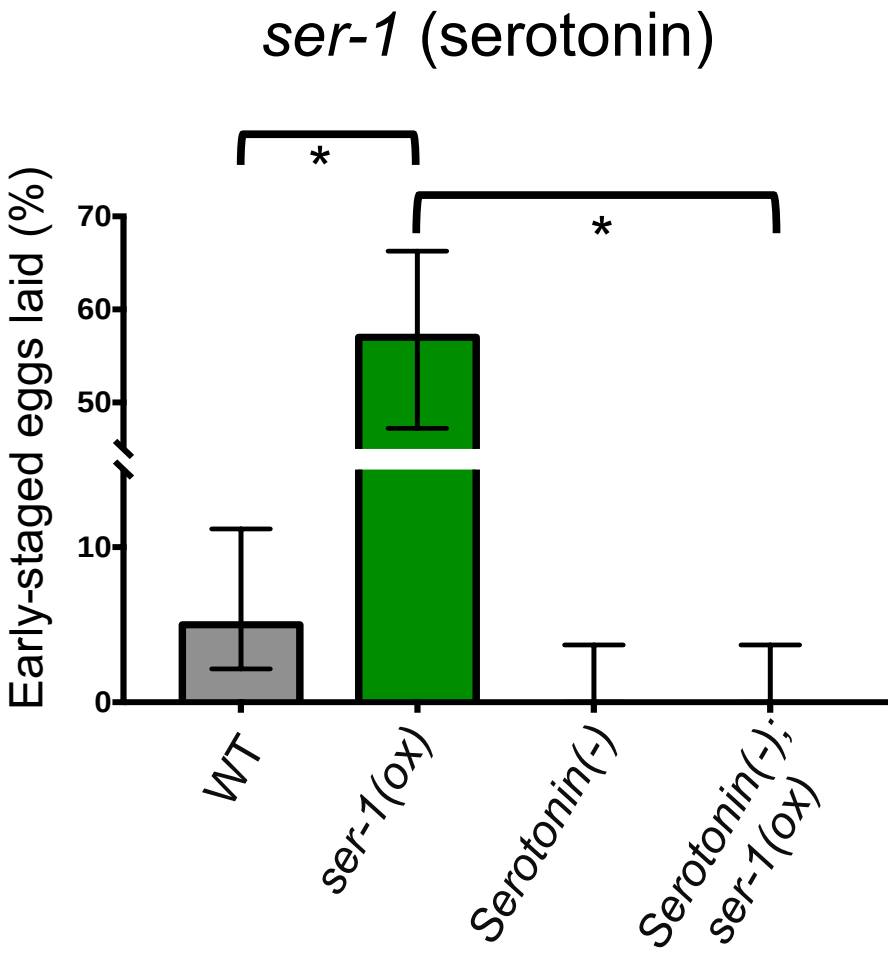

Figure 4.7 Overexpression of the serotonin GPCR SER-1 reveals strong hyperactive egg-laying defects that are rescued when you knock out the serotonin biosynthetic enzyme TPH-1. WT: Wild-type; -: knockout of the serotonin biosynthetic enzyme TPH-1 [*tph-1(mg280) II*]; ox: overexpression of GPCR::GFP transgenic strain. Light gray: control; Dark green: serotonin GPCR. n=100 eggs for each strain. Statistical significance was tested with the Fisher's exact test for the Early-Staged Egg-Laying Assay. The Wilson-Brown Method was used to determine the 95% C.I. for binomial data. $p \geq 0.05$ was considered not significant (ns) and $p < 0.05$ (*) was considered significant.

4.5 Overexpression of neurotransmitter GPCRs expressed in the *C. elegans* egg-laying system reveals strong egg-laying defects

The strategy of overexpressing neurotransmitter GPCRs to discover egg-laying defects is a good way to overcome the absence of egg-laying phenotypes seen in neurotransmitter receptor knockouts. Furthermore, we can validate that the egg-laying defects are due to increased receptor signaling by the overexpression of the neurotransmitter GPCR as knocking out the ligand for the specific receptor should rescue the egg-laying defect caused by overexpression of the neurotransmitter GPCR.

We went on to test chromosomally integrated neurotransmitter GPCR::GFP overexpressors for 24 neurotransmitter GPCRs in both egg-laying assays that were previously used to look for egg-laying defects in the neurotransmitter GPCR knockouts. However, we could not test overexpressors for the serotonin GPCR SER-4 and the glutamate GPCR MGL-2, as we did not have fosmid-based GFP reporter transgenes for these two receptors. We first tested the chromosomally integrated neurotransmitter GPCR::GFP overexpressors in the early-staged egg-laying assay (Figure 4.8) to look for hyperactive-egg laying defects. In addition to *ser-1(ox)*, the only other neurotransmitter GPCR that gave us a strong hyperactive egg-laying phenotype above the 50% cut-off for early-staged eggs laid was overexpression of the GABA receptor GBB-1, *gbb-1(ox)* (Figure 4.8). However, we were not able to validate the chromosomally integrated *gbb-1(ox)* hyperactive egg-laying phenotype in the extrachromosomal line for *gbb-1(ox)* or in a second

chromosomally integrated line for *gbb-1(ox)* (Figure 4.9). We tested four independent extrachromosomal lines for *gbb-1(ox)* (Figure 4.10) and could not replicate the egg-laying defect seen in one of the chromosomally integrated lines for *gbb-1(ox)*. We concluded that the egg-laying defect seen in one of the lines for the chromosomally integrated line for *gbb-1(ox)* may have been an artifact during the chromosomal integration process.

Next, we sought to test if overexpression of the neurotransmitter GPCRs resulted in egg-laying defects in the unlaid egg assay, specifically to determine if there is an increase in the accumulation of unlaid eggs, similar to the *egl-10(md176) V* control. As seen in Figure 4.11, overexpression of neurotransmitter GPCRs resulted in strong egg-laying defects as seen by a high number of eggs accumulated in the uterus of the worm for the following neurotransmitter GPCRS: the octopamine GPCR SER-6, the tyramine GPCR SER-2, the acetylcholine GPCR GAR-1, and the glutamate GPCRs MGL-1 and MGL-3.

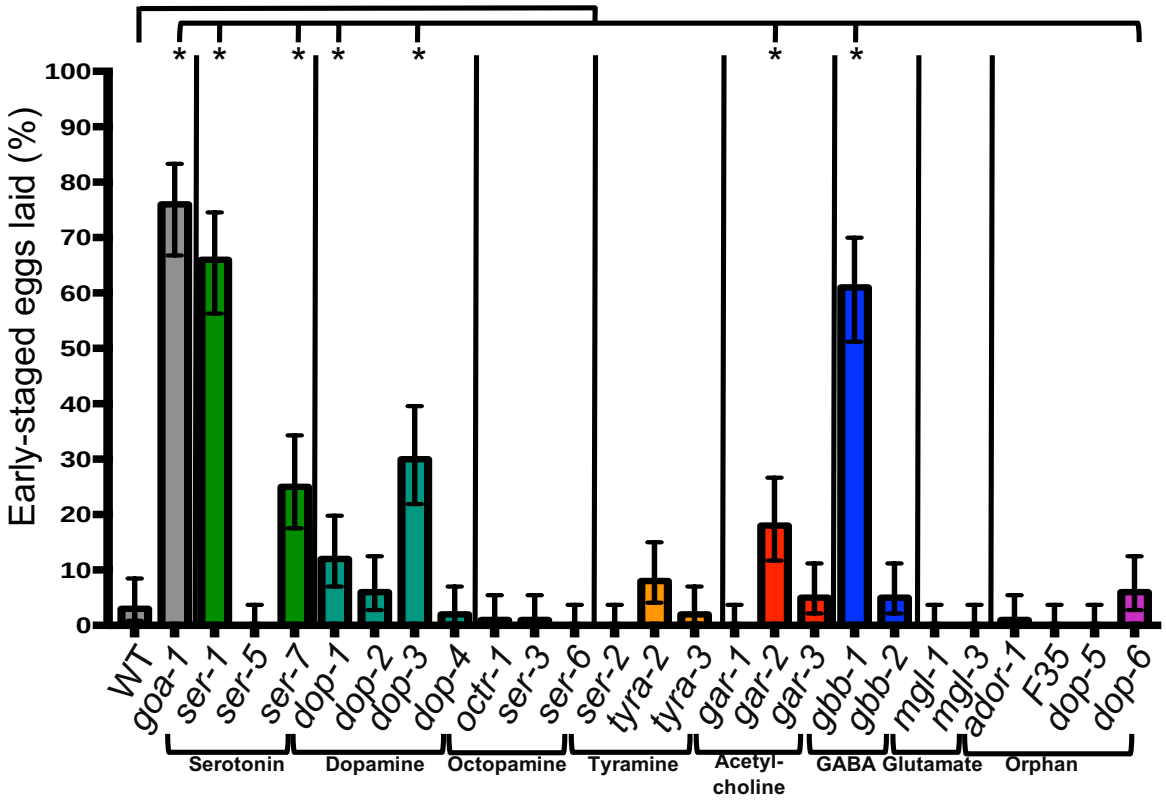

Figure 4.8 Overexpression of neurotransmitter GPCR gene reveals hyperactive egg-laying defect as seen by the high percentage of early-staged eggs laid for only two neurotransmitter GPCR genes, *ser-1* and *gbb-1*. WT: Wild-type; *goa-1(n1134) I* served as a control for hyperactive egg-laying. All of the neurotransmitter GPCR overexpressors are integrated neurotransmitter GPCR::GFP transgenic strains. The neurotransmitter GPCR::GFP overexpressors with hyperactive egg-laying defects are at least 2x outcrossed. Light gray: Controls; Dark green: serotonin GPCRs; light green: dopamine GPCRs; brown: octopamine GPCRs; orange: tyramine GPCRs; red: acetylcholine GPCRs; blue: GABA GPCRs; yellow: glutamate GPCRs; magenta: orphan GPCRs. n=100 eggs for each strain. Statistical significance was tested with the Fisher's exact test for the Early-Staged Egg-Laying Assay. The Wilson-Brown Method was used to determine the 95% C.I. for binomial data. $p \geq 0.05$ was considered not significant (ns) and $p < 0.05$ (*) was considered significant.

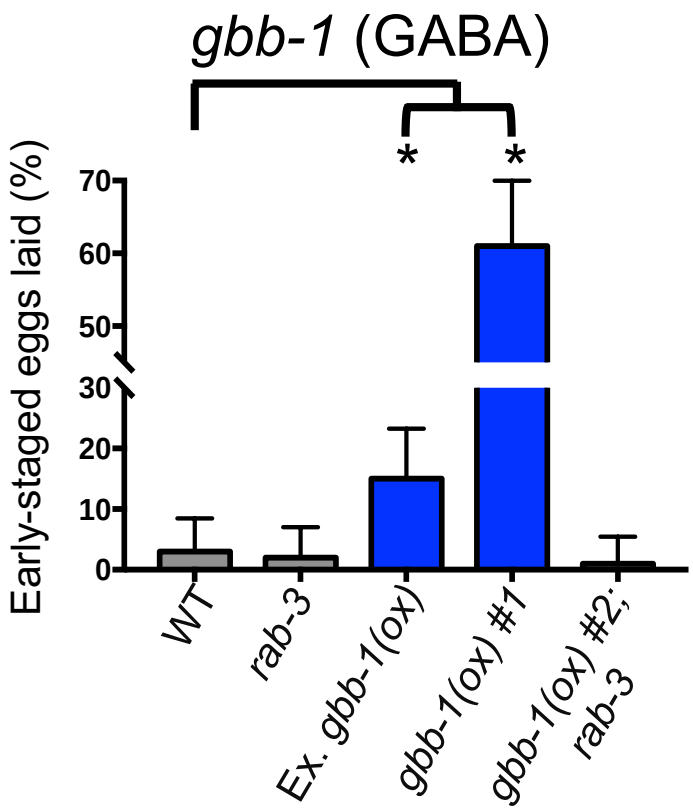

Figure 4.9 Overexpression of the GABA GPCR GBB-1 reveals strong hyperactive egg-laying defects that is not validated by a second integrant or the extrachromosomal strain for GBB-1. WT: Wild-type; *rab-3*: *rab-3p::NLS::TagRFP*; Ex: extrachromosomal transgenic GPCR::GFP strain; ox: overexpression of GPCR::GFP transgenic strain. The number after (ox) indicates the independent line number for the chromosomally integrated GPCR::GFP strains. *gbb-1(ox)* #1 is 4x outcrossed, while the other independent line for *gbb-1(ox)* in the *rab-3p::NLS::TagRFP* background is not outcrossed. Light gray: controls; Blue: GABA GPCR. n=100 eggs for each strain. Statistical significance was tested with the Fisher's exact test for the Early-Staged Egg-Laying Assay. The Wilson-Brown Method was used to determine the 95% C.I. for binomial data. $p \geq 0.05$ was considered not significant (ns) and $p < 0.05$ (*) was considered significant.

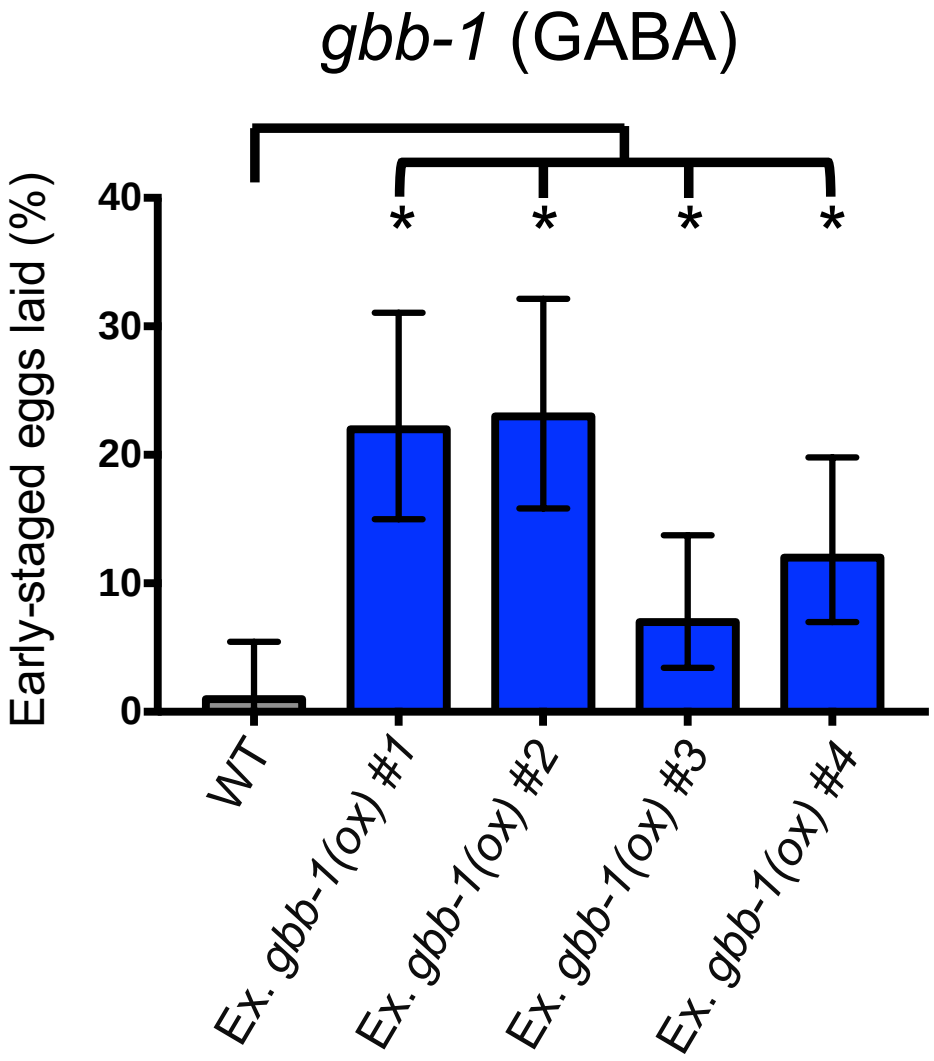

Figure 4.10 Overexpression of four independent extrachromosomal lines for the GABA GPCR GBB-1 does not reveal strong hyperactive egg-laying defects. WT: Wild-type; Ex: extrachromosomal transgenic GPCR::GFP strain; ox: overexpression of GPCR::GFP transgenic strain. The number after (ox) indicates the independent line number for the extrachromosomal GPCR::GFP strains. Light gray: controls; Blue: GABA GPCR. n=100 eggs for each strain. Statistical significance was tested with the Fisher's exact test for the Early-Staged Egg-Laying Assay. The Wilson-Brown Method was used to determine the 95% C.I. for binomial data. $p \geq 0.05$ was considered not significant (ns) and $p < 0.05$ (*) was considered significant.

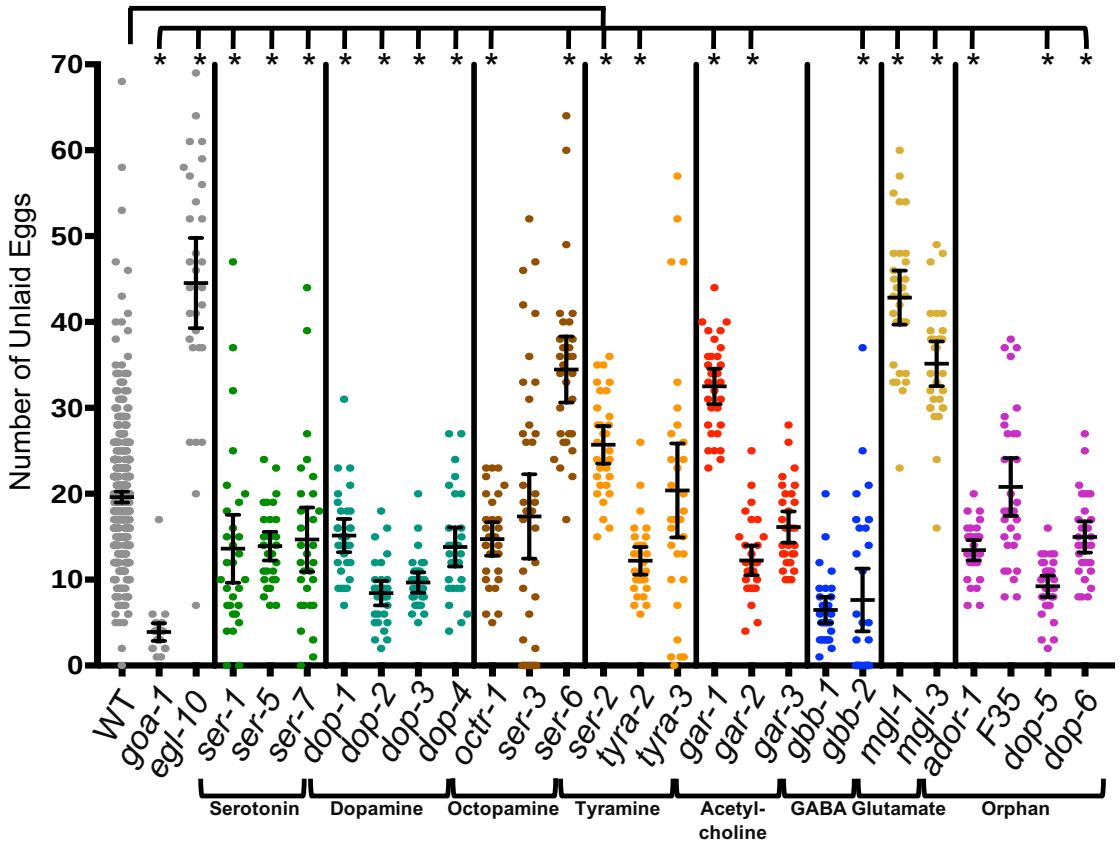

Figure 4.11 Overexpression of neurotransmitter GPCRs reveals strong egg-laying defects as seen by the accumulation of unlaid eggs in the uterus of the worm. WT: Wild-type; *egl-10(md176) V* and *goa-1(n1134) I* served as controls for strong egg-laying defects. All of the neurotransmitter GPCR overexpressors are integrated neurotransmitter GPCR::GFP transgenic strains. The neurotransmitter GPCR overexpressors with egg-laying defects were outcrossed at least twice. Light gray: Controls; Dark green: serotonin GPCRs; light green: dopamine GPCRs; brown: octopamine GPCRs; orange: tyramine GPCRs; red: acetylcholine GPCRs; blue: GABA GPCRs; yellow: glutamate GPCRs; magenta: orphan GPCRs. n ≥ 30 for each strain. Statistical significance was tested using one-way ANOVA with Bonferroni correction for multiple comparisons for the Unlaid Egg Assay. p ≥0.05 was considered not significant (ns) and p <0.05 (*) was considered significant.

4.6 Overexpression of the octopamine GPCR SER-6 reveals strong egg-laying defects

Overexpression of the octopamine receptor SER-6, *ser-6(ox)*, revealed a strong egg-laying defect (Figure 4.11), with an average of ~35 unlaid eggs. The egg-laying defect of the chromosomally integrated line *ser-6(ox)* was validated as the extrachromosomal line for *ser-6(ox)* and several other chromosomally integrated lines for *ser-6(ox)* also had a high number of unlaid eggs (Figure 4.12). We went on to determine whether the egg-laying defect seen in *ser-6(ox)* was due to an increase of octopamine receptor SER-6 signaling: If we knock out the octopamine biosynthetic enzyme, TBH-1, in the *ser-6(ox)* background, we expected this egg-laying defect to be reduced. Compared to the *ser-6(ox)* that on average has ~27 unlaid eggs, there is a statistically significant reduction in the number of unlaid eggs for the *tbh-1(n3247) X*; *ser-6(ox),* with an average of ~22 unlaid eggs. Interestingly, the number of unlaid eggs in the *tbh-1(n3247) X*; *ser-6(ox)* background is slightly higher than wild-type and *tbh-1(n3247) X*, which both have ~18 unlaid eggs (Figure 4.13).

Interestingly, the chromosomally integrated line for the octopamine receptor SER-3, *ser-3(ox)*, did not reveal a strong egg-laying defect (Figure 4.11) as it has on average 17 unlaid eggs, which is similar to wild-type. However, the extrachromosomal line for *ser-3(ox)* is egg-laying defective as it has on average ~48 unlaid eggs (Figure 4.14). We suspected that there was sterility in the chromosomally integrated line for *ser-3(ox)*, as several individual animals had no eggs in their uterus. Future studies include testing several independent

extrachromosomal lines for *ser-3(ox)* and generating new chromosomally integrated lines for *ser-3(ox)* to determine if there is an egg-laying defect for *ser-3(ox)*.

Further studies to determine the role of SER-6 and SER-3 in regulating egg-laying will have to be followed upon as previous studies have shown that exogenous octopamine inhibits egg-laying events (Horvitz et al., 1982), yet the receptor that octopamine acts on to inhibit egg laying remains unknown. Furthermore, as SER-6 and SER-3, are both expressed in the neuroendocrine cells uv1s that are known to inhibit egg-laying, these are good candidates to test if octopamine inhibits egg-laying through these receptors.

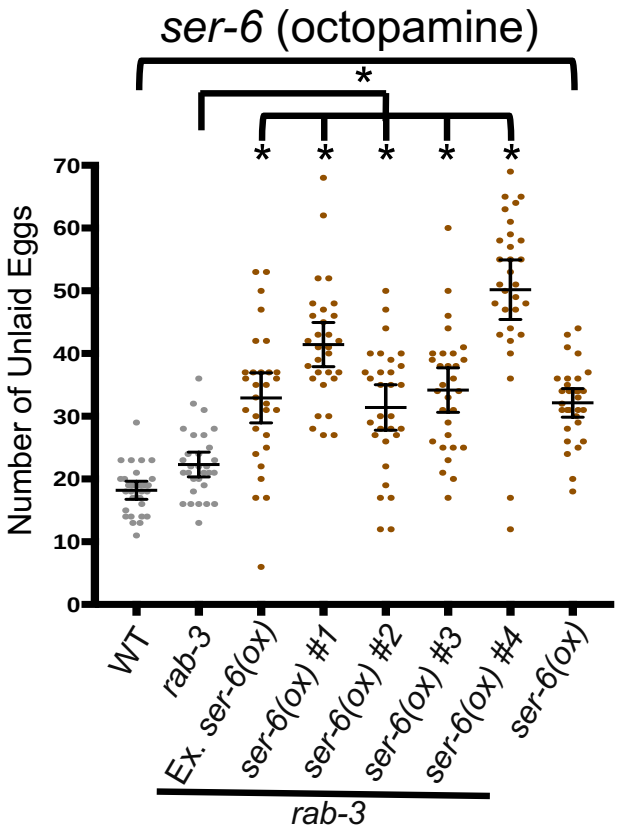

Figure 4.12 Overexpression of the octopamine GPCR SER-6 leads to an egg-laying defect that is validated by several independent integrants and the extrachromosomal strain for SER-6. WT: Wild-type; *rab-3*: *rab-3p::NLS::TagRFP*; Ex: extrachromosomal transgenic GPCR::GFP strain; ox: overexpression of GPCR::GFP transgenic strain. The number after (ox) indicates non-outcrossed independent lines for the chromosomally integrated GPCR::GFP strains. *ser-6(ox)* is the 2x outcrossed version derived from *ser-6(ox)* #1; *rab-3p::NLS::TagRFP*. Light gray: controls; Brown: Octopamine GPCR. n ≥ 30 for each strain. Statistical significance was tested using one-way ANOVA with a Tukey's test to determine statistical significance for multiple comparisons for the Unlaid Egg Assay. p ≥0.05 was considered not significant (ns) and p <0.05 (*) was considered significant.

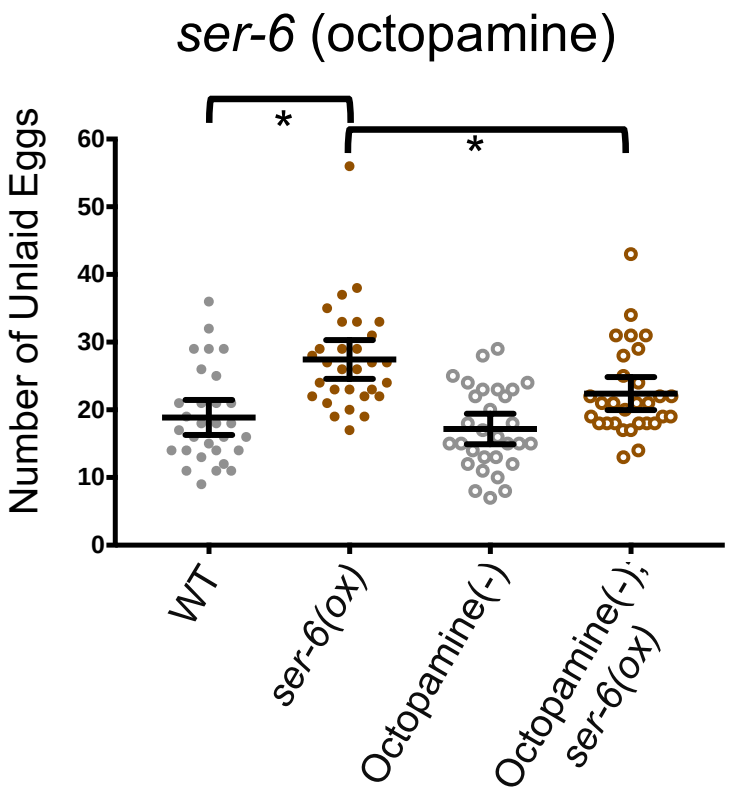

Figure 4.13 Overexpression of the octopamine GPCR SER-6 leads to a modest increase in the number of eggs retained in the uterus of the worm, which is partially rescued upon knock out of the octopamine biosynthetic enzyme TBH-1. WT: Wild-type; Open circle: knockout of the octopamine biosynthetic enzyme TBH-1 [*tbh-1(n3247) X*]; ox: overexpression of GPCR::GFP transgenic strain. *ser-6(ox)* is an integrated octopamine GPCR::GFP transgenic strain that is 2x outcrossed. Light gray: control; Brown: Octopamine GPCR. n ≥ 30 for each strain. Statistical significance was tested using one-way ANOVA with a Tukey's test to determine statistical significance for multiple comparisons for the Unlaid Egg Assay. p ≥0.05 was considered not significant (ns) and p <0.05 (*) was considered significant.

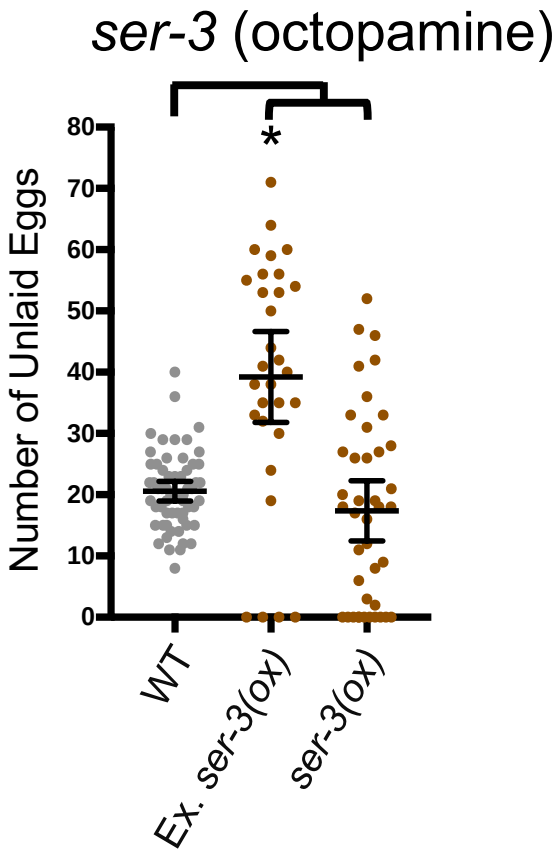

Figure 4.14 Overexpression of the extrachromosomal strain for the octopamine GPCR SER-3 reveals strong egg-laying defects that are not reproduced by the integrated strain for SER-3. WT: Wild-type; Ex: extrachromosomal transgenic GPCR::GFP strain; ox: overexpression of GPCR::GFP transgenic strain. *ser-3(ox)* is an integrated octopamine GPCR::GFP transgenic strain that is 4x outcrossed, which is partially sterile. Light gray: controls; Brown: Octopamine GPCR. n ≥ 30 for each strain. Statistical significance was tested using one-way ANOVA with a Tukey's test to determine statistical significance for multiple comparisons for the Unlaid Egg Assay. $p \geq 0.05$ was considered not significant (ns) and $p < 0.05$ (*) was considered significant.

4.7 Overexpression of the tyramine GPCR SER-2 reveals modest egg-laying defects

Overexpression of the tyramine receptor SER-2, *ser-2(ox)*, revealed a modest egg-laying defect (Figure 4.11), with on average of ~25 unlaid eggs. The egg-laying defect of the chromosomally integrated line for *ser-2(ox)* was validated as the extrachromosomal line for *ser-2(ox)* also had a high number of unlaid eggs (Figure 4.15). We went on to determine whether the egg-laying defect seen in *ser-2(ox)* was due to an increase of tyramine receptor SER-2 signaling: If we knock out the tyramine biosynthetic enzyme, TDC-1, in the *ser-2(ox)* background, we expected this egg-laying defect to be reduced. Compared to the *ser-2(ox)* that on average has ~25 unlaid eggs, there is a statistically significant reduction in the number of unlaid eggs for the *tdc-1(n3419) II*; *ser-2(ox),* with an average of ~14 unlaid eggs, similar to wild-type.

Further studies to determine the role of the tyramine GPCR SER-2 in regulating egg-laying will have to be followed upon. As previous studies have shown that the neuroendocrine cells uv1s are known to release tyramine to inhibit egg-laying by acting on a tyramine receptor, LGC-55, on the HSN (Collins et al., 2016), perhaps tyramine is also acting on SER-2 as it is expressed in the uv1s (Table 4.2). Furthermore, SER-2 is also expressed in the HSN (Table 4.2), which promotes egg-laying, and this could be another starting point to determine where SER-2 is regulating egg-laying behavior.

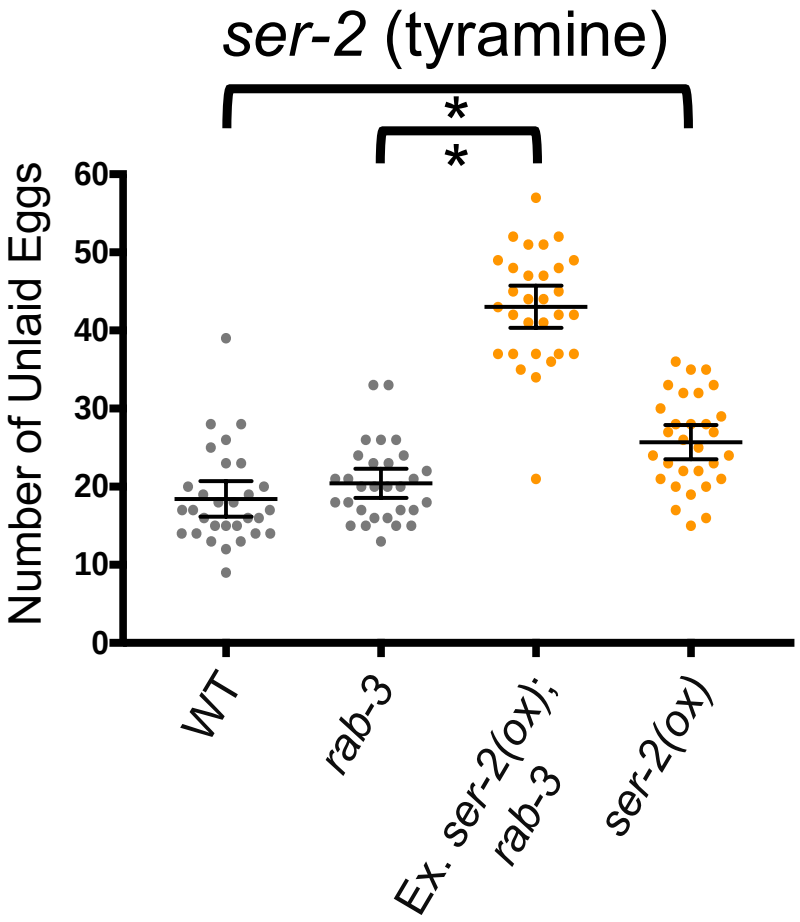

Figure 4.15 Overexpression of the tyramine GPCR SER-2 leads to an egg-laying defect that is reproduced by the extrachromosomal strain for SER-2. WT: Wild-type; *rab-3*: *rab3-p::NLS::TagRFP*; Ex: extrachromosomal transgenic GPCR::GFP strain; ox: overexpression of GPCR::GFP transgenic strain. *ser-2(ox)* is an integrated tyramine GPCR::GFP transgenic strain that is 2x outcrossed. Light gray: controls; Orange: Tyramine GPCR. n ≥ 30 for each strain. Statistical significance was tested using one-way ANOVA with a Tukey's test to determine statistical significance for multiple comparisons for the Unlaid Egg Assay. p ≥0.05 was considered not significant (ns) and p <0.05 (*) was considered significant.

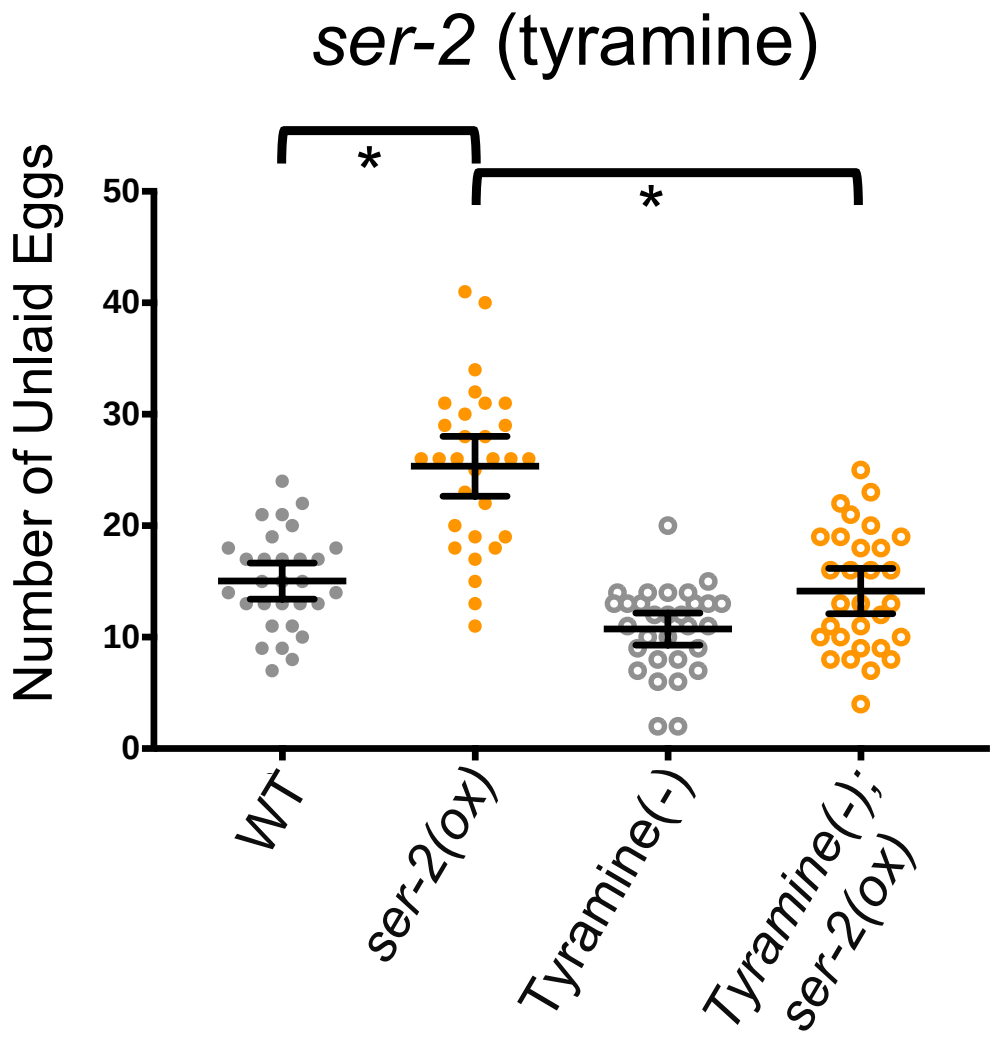

Figure 4.16 Overexpression of the tyramine GPCR SER-2 leads to a modest increase in the number of eggs retained in the uterus of the worm, which is rescued upon knock out of the tyramine biosynthetic enzyme TDC-1. WT: Wild-type; Open circle: knockout of the tyramine biosynthetic enzyme TDC-1 [*tdc-1(n3419) II*]; ox: overexpression of GPCR::GFP transgenic strain. *ser-2(ox)* is an integrated tyramine GPCR::GFP transgenic strain that is 2x outcrossed. Light gray: control; Orange: Tyramine GPCR. n ≥ 30 for each strain. Statistical significance was tested using one-way ANOVA with a Tukey's test to determine statistical significance for multiple comparisons for the Unlaid Egg Assay. p ≥0.05 was considered not significant (ns) and p <0.05 (*) was considered significant.

4.8 Overexpression of the acetylcholine GPCR GAR-1 reveals strong egg-laying defects

Overexpression of the acetylcholine GPCR GAR-1, *gar-1(ox)*, revealed a strong egg-laying defect (Figure 4.11), with an average of ~33 unlaid eggs. The egg-laying defect of the chromosomally integrated line for *gar-1(ox)* was validated as the extrachromosomal line for *gar-1(ox)* also had a high number of unlaid eggs (Figure 4.17). We were unable to rescue this egg-laying defect for *gar-1(ox)* as a null allele for the acetylcholine biosynthetic enzyme is lethal (Rand, 1989).

Further studies to determine the role of the acetylcholine GPCR GAR-1 in regulating egg-laying will have to be followed upon. As previous studies have shown that acetylcholine acts on acetylcholine receptors on the vulval muscles to regulate egg-laying activity (Waggoner et al., 2000; Kim et al., 2001), acetylcholine may also act on GAR-1 as it is also expressed in the vulval muscles (Table 4.2). Furthermore, GAR-1 is also expressed in the neuroendocrine cells uv1s (Table 4.2), which inhibit egg-laying, and this could be another starting point to determine where GAR-1 is regulating egg-laying behavior.

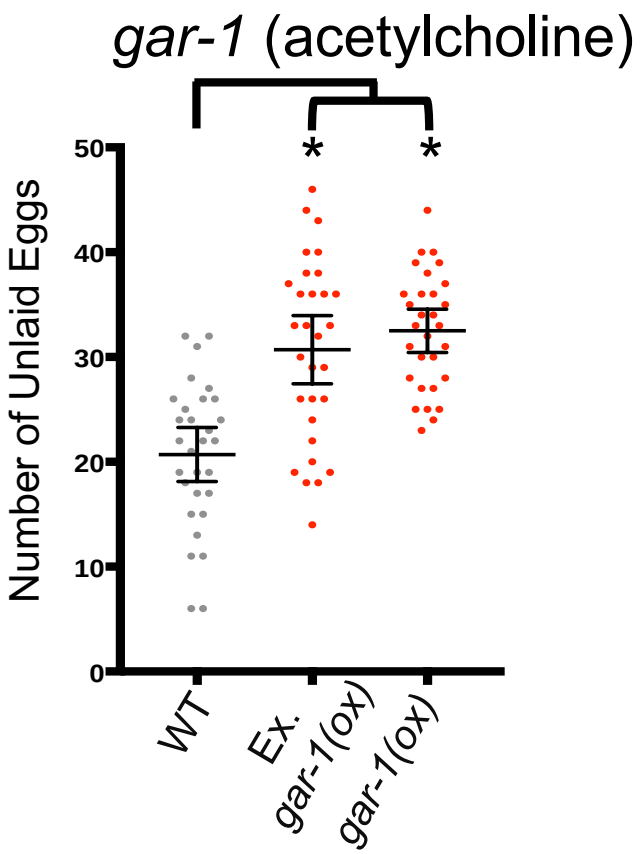

Figure 4.17 Overexpression of the acetylcholine GPCR GAR-1 leads to a modest increase in the number of eggs retained in the uterus of the worm that is reproduced by its extrachromosomal strain for GAR-1. WT: Wild-type; Ex: extrachromosomal transgenic GPCR::GFP strain; ox: overexpression of GPCR::GFP transgenic strain. *gar-1(ox)* is an integrated acetylcholine GPCR::GFP transgenic strain that is 2x outcrossed. Light gray: controls; Red: Acetylcholine GPCR. n ≥ 30 for each strain. Statistical significance was tested using one-way ANOVA with a Tukey's test to determine statistical significance for multiple comparisons for the Unlaid Egg Assay. p ≥0.05 was considered not significant (ns) and p <0.05 (*) was considered significant.

4.9 Overexpression of glutamate GPCRs, MGL-1 and MGL-3, reveals strong egg-laying defects

Overexpression of the glutamate GPCR MGL-1, *mgl-1(ox)*, revealed a strong egg-laying defect (Figure 4.11), with on average of ~43 unlaid eggs. The egg-laying defect of the chromosomally integrated line for *mgl-1(ox)* was validated as the extrachromosomal line for *mgl-1(ox)* also had a high number of unlaid eggs (Figure 4.18). We went on to determine whether the egg-laying defect in *mgl-1(ox)* was due to an increase of glutamate receptor MGL-1 signaling. However, as glutamate has four different glutamine synthetases (Hobert, 2013) in *C. elegans*, we decided to knock out the vesicular glutamate transporter EAT-4. We expected the egg-laying defect seen in *mgl-1(ox)* to be reduced in the *eat-4* knockout as there will be less glutamate present to signal onto MGL-1. Compared to *mgl-1(ox)* that on average has ~43 unlaid eggs, there is a statistically significant reduction in the number of unlaid eggs for the *eat-4(ky5) III*; *mgl-1(ox),* with an average of ~17 unlaid eggs, similar to wild-type.

Overexpression of the glutamate GPCR MGL-3, *mgl-3(ox)*, also revealed a strong egg-laying defect (Figure 4.11), with an average of ~35 unlaid eggs. The egg-laying defect of the chromosomally integrated line for *mgl-3(ox)* was validated as several extrachromosomal lines for *mgl-3(ox)* also had a high number of unlaid eggs (Figure 4.20). We went on to determine whether the egg-laying defect seen in *mgl-3(ox)* was due to an increase of glutamate receptor MGL-3 signaling: If we knock out the EAT-4 in the *mgl-3(ox)* background, we expected this egg-laying defect to be reduced. Compared to *mgl-3(ox)* that on

average has ~35 unlaid eggs, there is a statistically significant reduction in the number of unlaid eggs for the *eat-4(ky5) III*; *mgl-1(ox),* with an average of ~19 unlaid eggs, similar to wild-type (Figure 4.21). In summary, the glutamate receptors *mgl-1(ox)* and *mgl-3(ox)* both displayed a strong egg-laying defect, which is interesting as glutamate is not known to affect egg-laying and this can be a new direction to determine how the egg-laying circuit is regulated.

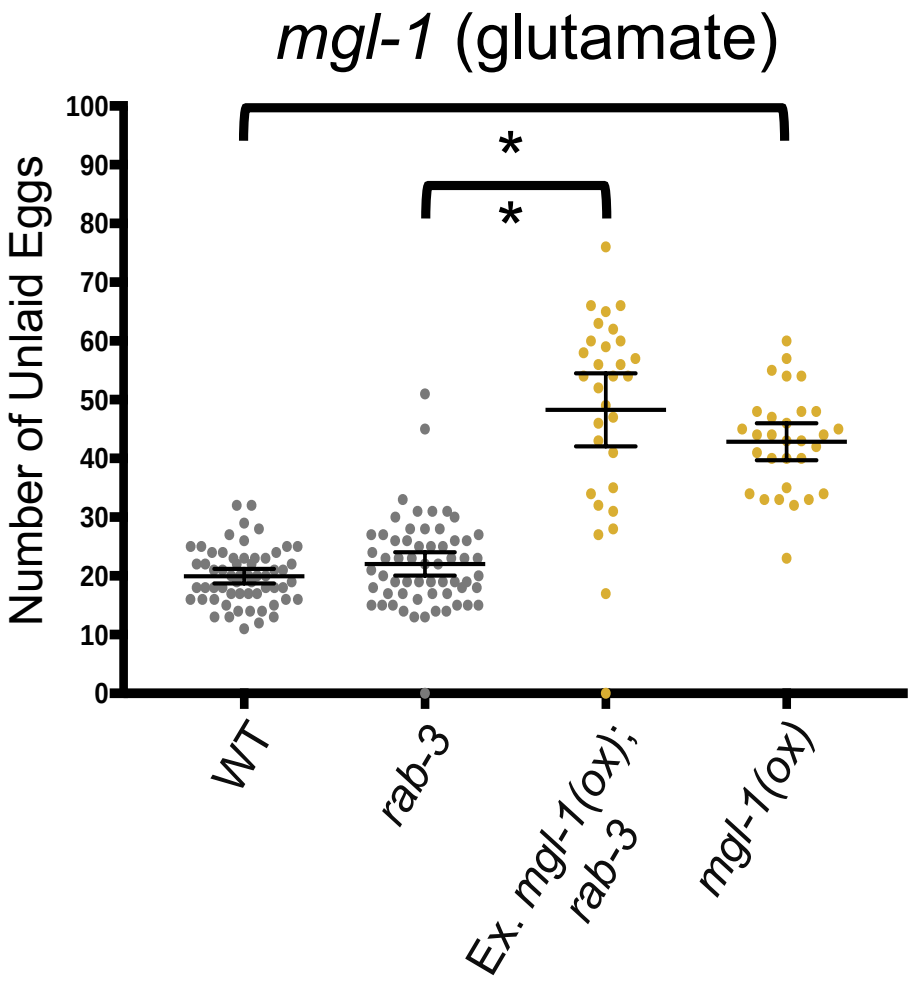

Figure 4.18 Overexpression of the glutamate GPCR MGL-1 reveals strong egg-laying defects as seen by the accumulation of unlaid eggs in the uterus of the worm that is validated by the extrachromosomal strain for MGL-1. WT: Wild-type; *rab-3*: *rab3-p::NLS::TagRFP*; Ex: extrachromosomal transgenic GPCR::GFP strain; ox: overexpression of GPCR::GFP transgenic strain. *mgl-1(ox)* is an integrated glutamate GPCR::GFP transgenic strain that is 2x outcrossed. Light gray: controls; Yellow: Glutamate GPCR. n ≥ 30 for each strain. Statistical significance was tested using one-way ANOVA with a Tukey's test to determine statistical significance for multiple comparisons for the Unlaid Egg Assay. p ≥0.05 was considered not significant (ns) and p <0.05 (*) was considered significant.

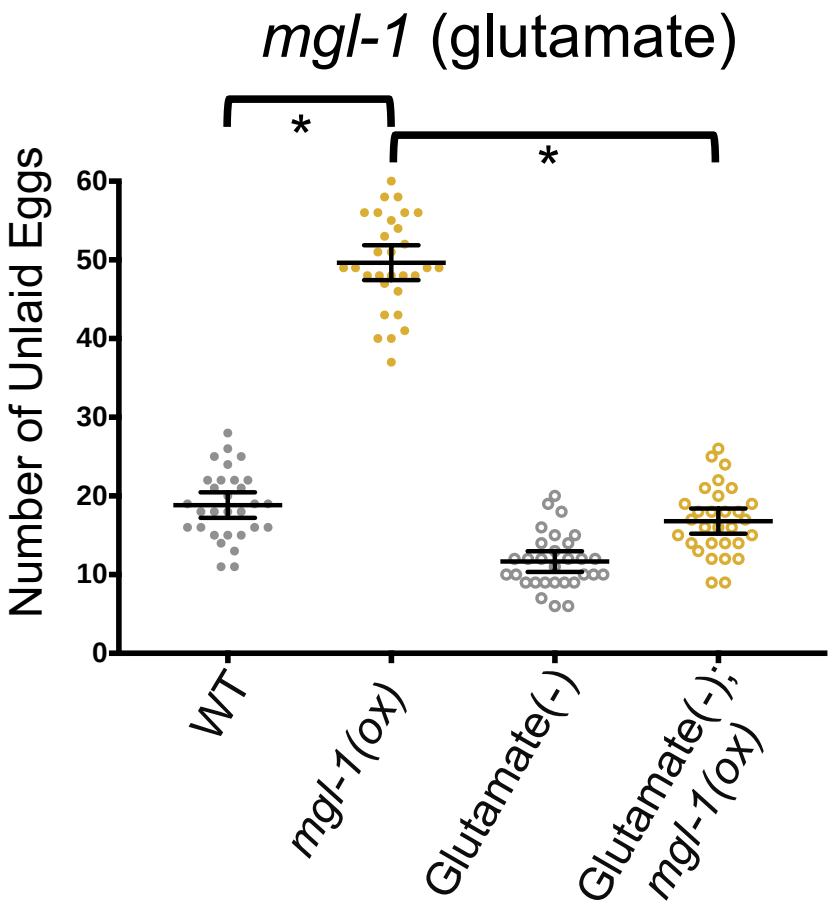

Figure 4.19 Overexpression of the glutamate GPCR MGL-1 leads to an abundance in the number of eggs retained in the uterus of the worm, which is completely rescued upon knock out of the vesicular glutamate transporter EAT-4. WT: Wild-type; Open circle: knockout of the vesicular glutamate transporter EAT-4 [*eat-4(ky5)) III*]; ox: overexpression of GPCR::GFP transgenic strain. *mgl-1(ox)* is an integrated glutamate GPCR::GFP transgenic strain that is 2x outcrossed. Light gray: control; Yellow: Glutamate GPCR. n ≥ 30 for each strain. Statistical significance was tested using one-way ANOVA with a Tukey's test to determine statistical significance for multiple comparisons for the Unlaid Egg Assay. p ≥0.05 was considered not significant (ns) and p <0.05 (*) was considered significant.

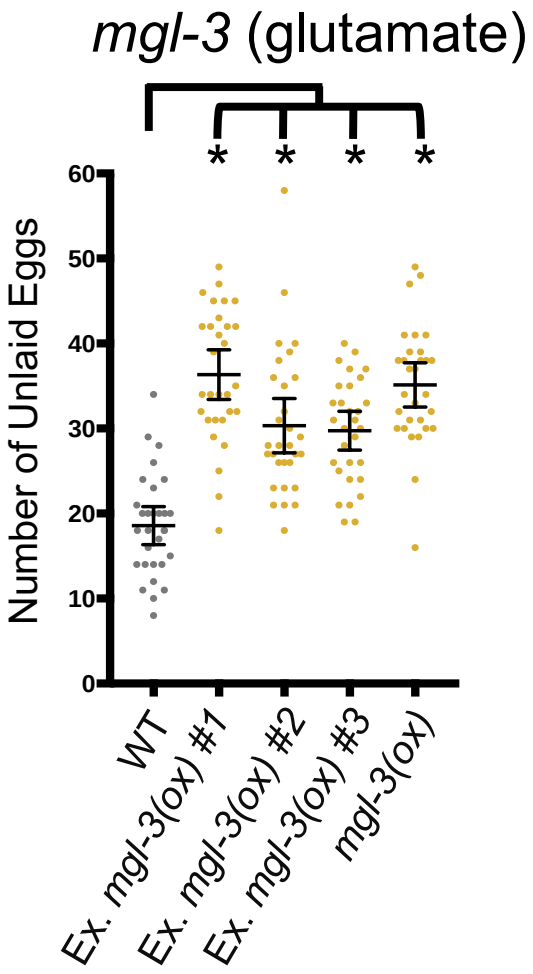

Figure 4.20 Overexpression of the glutamate GPCR MGL-3 reveals strong egg-laying defects that is validated by several extrachromosomal strains for MGL-3. WT: Wild-type; Ex: extrachromosomal transgenic GPCR::GFP strain; ox: overexpression of GPCR::GFP transgenic strain. *mgl-3(ox)* is an integrated glutamate GPCR::GFP transgenic strain that is 2x outcrossed derived from Ex. *mgl-3(ox)* #1. Light gray: controls; Yellow: Glutamate GPCR. n ≥ 30 for each strain. Statistical significance was tested using one-way ANOVA with a Tukey's test to determine statistical significance for multiple comparisons for the Unlaid Egg Assay. $p \geq 0.05$ was considered not significant (ns) and $p < 0.05$ (*) was considered significant.

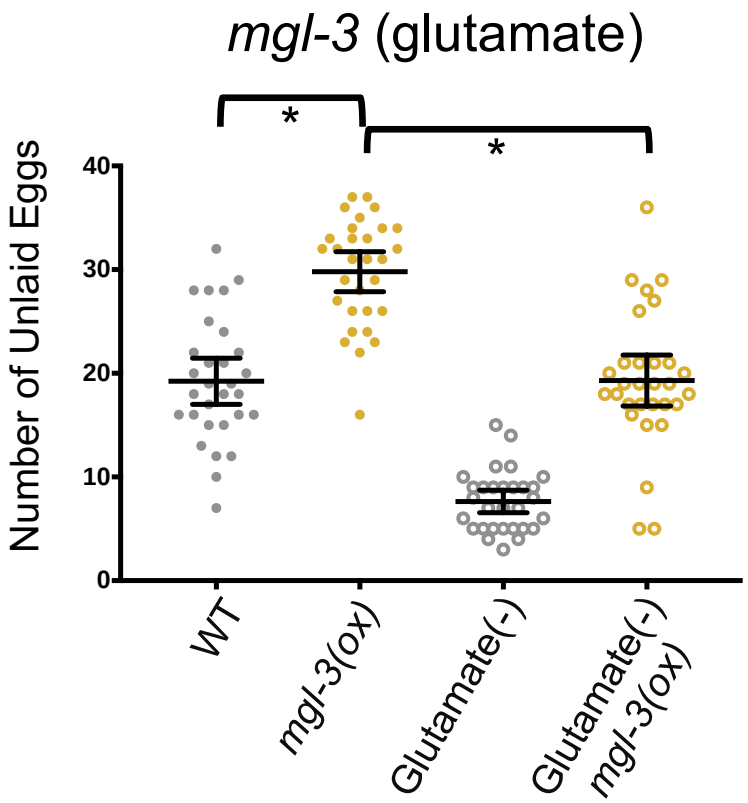

Figure 4.21 Overexpression of the glutamate GPCR MGL-3 leads to an abundance in the number of eggs retained in the uterus of the worm, which is partially rescued upon knock out of the vesicular glutamate transporter EAT-4. WT: Wild-type; Open circle: knockout of the vesicular glutamate transporter EAT-4 [*eat-4(ky5)) III*]; ox: overexpression of GPCR::GFP transgenic strain. *mgl-3(ox)* is an integrated glutamate GPCR::GFP transgenic strain that is 2x outcrossed. Light gray: control; Yellow: Glutamate GPCR. n ≥ 30 for each strain. Statistical significance was tested using one-way ANOVA with a Tukey's test to determine statistical significance for multiple comparisons for the Unlaid Egg Assay. p ≥0.05 was considered not significant (ns) and p <0.05 (*) was considered significant.

4.10 Discussion and Conclusion

In summary, there is a lot of functional redundancy in the *C. elegans* egg-laying system as we were not able to find reproducible, strong egg-laying defects when knocking out single or several neurotransmitter GPCRs. However, when overexpressing neurotransmitter GPCRs, we were able to elucidate several egg-laying defects for different classes of neurotransmitter GPCRs. Furthermore, we developed a strategy that verified that that the egg-laying defects seen in the neurotransmitter GPCRs overexpressors were most likely due to increased receptor signaling as knocking out the ligand for the specific neurotransmitter GPCR reduced the egg-laying defect of the neurotransmitter GPCRs overexpressors. Future work will have to be done to determine how these neurotransmitter GPCRs overexpressors are cause egg-laying defects, specifically which egg-laying cells are these receptors acting in and how are they regulating activity of the egg-laying circuit. For all the neurotransmitter GPCRs that have an egg-laying defect, Table 4.2 shows the different cells of the egg-laying system these receptors are expressed in, which can be used as a starting point for future studies.

Neurotransmitter GPCRs	Cellular Expression Patterns		
	Egg-laying neurons	Egg-laying muscles	Other cells
SER-1 ($G\alpha_q$)	HSN	vm2, um1, um2	ut2, ut3, sp
DOP-4 ($G\alpha_s$)	vm1		sp, bwm
SER-3 ($G\alpha_q$)	uv1		ut1, ut2, ut3, ut4, uv3, sp
SER-6 ($G\alpha_s$)	uv1		ut1, ut2, ut3, ut4, uv3, vt, sp
SER-2 ($G\alpha_o$)	HSN, uv1	um2	vt, utse, sp
GAR-1 ($G\alpha_o$)	HSN, uv1	vm1, vm2	sp
MGL-1	HSN, uv1		u4, uv3, utse, sp
MGL-3	uv1, VC4, VC5		

Table 4.2 Neurotransmitter GPCRs with known egg-laying defects and their cellular expression patterns in the *C. elegans* egg-laying system. Underline denotes weak GPCR::GFP expression in the particular egg-laying cell. Cell types are denoted by the following abbreviations: bwm: body wall muscles; HSN: hermaphrodite-specific neuron; sp: spermatheca; sp-ut: spermathecal-uterine valve; um: uterine muscle; ut: uterine toroid cell; utse: uterine seam; uv: uterine ventral cell; VC: ventral cord type C neuron; vm: vulval muscle; vt: vulval toroid cells.

Chapter 5: Materials and Methods

5.1 General methods

5.1.1 *C. elegans* strains

C. elegans strains used in this study were maintained at 20°C on standard nematode growth media (NGM) seeded with the OP50 strain of *Escherichia coli* (*E.coli*) as their food source. Null alleles for neurotransmitter receptors, biosynthetic enzyme or the vesicular glutamate transporter were obtained through Caenorhabditis Genetics Center (CGC), National BioResource Project (NBRP), or previously made in our lab for other studies. Null alleles were backcrossed 2-10 times to N2 (wild-type), as indicated. New strains were constructed using standard procedures and all genotypes were confirmed by PCR or sequencing. Extrachromosomal array transgenic strains for neurotransmitter GPCRs were generated through microinjection and at least one independent line was kept. Extrachromosomal strains for neurotransmitter GPCRs were chromosomally integrated through UV/TMP mutagenesis and at least one chromosomally integrated GPCR::GFP transgenic strain was kept per neurotransmitter GPCR. Integrated strains for neurotransmitter GPCRs were backcrossed 2-4 times to N2 (wild-type) as indicated. A complete list of all of the *C. elegans* strains and alleles used in this thesis are provided in Appendix Chapter 5.

5.2 Methods for Chapter 2

5.2.1 Isolating and sequencing recombineered GPCR::GFP transgenes

Recombineered GPCR::GFP transgenes were received by TransgeneOme (Sarov et al., 2012) in EPI300 *E.coli* non-clonal cells. Due to the recombination method used in Sarov et al., 2012, the EPI300 non-clonal cells for a specific GPCR::GFP construct contained 83% of the correct recombineered GPCR::GFP construct, 7% of the recombineered GPCR::GFP construct had mismatches, 4% were intermediate products of the recombineering process to generate the GPCR::GFP construct, and 5% were cross-contaminants. The non-clonal cells were streaked onto a triple antibiotic plate (15µg/mL Chloramphenicol, 100µg/mL Streptomycin, and 50µg/mL ClonNat) to select for the recombineered GPCR::GFP construct. From the triple antibiotic plates, an individual colony was inoculated for 14-16hrs in LB broth with 1X Fosmid Autoinduction solution and triple antibiotics. The recombineered GPCR::GFP transgene was isolated from the bacterial culture at a high concentration using a modified protocol from the Qiagen Plasmid Mini Kit. The purified product was run on a 0.4% Agarose Gel to determine the recombineered GPCR::GFP transgene was at the correct size and not sheared. We sequenced for the presence of GFP for the recombineered GPCR::GFP transgene that was isolated from the bacterial culture using primers for GFP (provided by TransgeneOme and listed in Appendix Chapter 2) to determine GFP was tagged at the correct position and we did not select for an intermediate product in the recombineering process.

5.2.2 Microinjections of GPCR::GFP transgenes

Initially, recombineered GPCR::GFP transgenes that we received from TransgeneOme had the *unc-119* gene in its backbone, therefore this construct was microinjected at 20-100ng/uL into *unc-119* mutant animals. As *unc-119* mutant animals have uncoordinated locomotion, a successful transformation is indicated by the presence of coordinated locomotion and bright GFP+ animals in independent lines. Most of the recombineered GPCR::GFP transgenes that were later recombineered no longer had the *unc-119* gene in its backbone, therefore these constructs were microinjected at 20-100ng/uL with a co-injection marker PL15EK at 50ng/uL + DH5α at 25ng/uL in *lin-15(765ts)* animals. As *lin-15(765ts)* animals have a multi-vulva phenotype at 20C, a successful transformation is indicated by the absence of the multi-vulva phenotype and bright GFP+ animals in independent lines. As our GPCR::GFP constructs contain repetitive sequences and may be prone to GFP silencing, we co-injected our GPCR::GFP construct with DH5α, as it is a complex array with no repetitive sequences. A complete list of the concentrations used for microinjection of the GPCR::GFP construct and rescue marker are in listed Appendix 6.9.

5.2.3 Chromosomal integrations

Extrachromosomal GPCR::GFP transgenic strains were chromosomally integrated following a modified protocol for UV/TMP mutagenesis. Several NGM plates containing late-L4 animals for our extrachromosomal GPCR::GFP transgenic strain of interest were combined in M9 buffer containing 30ug/mL TMP. These extrachromosomal GPCR::GFP transgenic strains were UV

irradiated in a Stratalinker with 365nm bulbs at an energy setting of 300uJ for 15 seconds. 60-100 late L4 or young adult extrachromosomal GPCR::GFP transgenic animals that were UV irradiated were picked to singe plates. The following includes modifications to the standard integration protocol: we selected 300-400 F1 bright GFP+ young adult animals to single plates. From the 300-400 F1 plates, we separated F1 plates that had >75% GFP+ or non-Muv (depending on our selection marker) animals. This resulted in 30 – 60 F1 plates that matched our criteria. From these plates, we picked 6 F2 animals to single plates for each set of the 30 – 60 F1 plates. We screened our F2 plates to ensure that 100% of the F2 progeny were all GFP+ indicating it is a candidate GPCR::GFP integrant. To confirm a successful integration event for each of the plates that contained 100% GFP+ F2 progeny, we picked 6 GFP+ F3 animals to single plates and ensure all of the resulting F3 progeny were all GFP+. This integration method resulted in 1-7 independent GPCR::GFP integrants.

5.2.4 mCherry marker strains

All mCherry marker strains used in our study were chromosomally integrated. The pBR1 plasmid for *ida-1::mCherry* (a gift from Kevin Collins) was microinjected to generate extrachromosomal lines and chromosomally integrated lines. The *ida-1::mCherry* transgenic strain was used for cell identifications of the HSN, uv1s, VC4, and VC5 of the *C. elegans* egg-laying circuit. Independent integrants for *unc-103e::mCherry* were previously generated in our lab. *unc-103e::mCherry* is an mCherry marker for cell identifications of the vulval muscles (vm1 and vm2) and a landmark to identify the uterine muscles (um1 and um2).

The *ajm-1::mCherry* integrated strain was received from the Gottschalk lab. The *ajm-1::mCherry* labels the apical borders of epithelial cells that was used for cell identifications of the uterine toroid (ut1, ut2, ut3, and ut4) cells, uterine ventral cells (uv2 and uv3), vulval toroid (vt) cells, spermatheca-uterine (sp-ut) valve, spermatheca (sp), dorsal uterine cell (du). The *ajm-1::mCherry* marker was also used as a landmark to identify the uterine seam (utse), and body wall muscles (bwm).

5.2.5 GPCR::GFP transgenic strains

The following is a summary of how the recombineered GFP constructs were made for all of the 26 neurotransmitter GPCRs.

C-terminal GFP constructs*:* The majority of the neurotransmitter receptors were recombineered to have GFP tagged at the last coding exon with the exception of *gbb-2* which was recombineered to have GFP inserted in the middle of exon 14 (Appendix Chapter 2). Further information on the C-terminal tagged GFP transgenes is available from TransgeneOme (Sarov et al., 2012).

SL2::NLS::GFP constructs*:* Microinjection of four C-terminal GFP transgenes (*dop-1::gfp*, *dop-4::gfp*, *gar-2::gfp*, and *F35H10.10::GFP*) resulted in weak GFP expression as the neurotransmitter GPCR was subcellularly localized and did not fill out cell bodies. Using available fosmids for the four neurotransmitter GPCRs described in Appendix Chapter 2, these receptors were recombineered to include a SL2::NLS::GFP following the protocol provided by Tursun et al., 2009 allowing us to visualize GFP in the cell bodies. A list of all the primers used for the recombineering process are in Appendix Chapter 2.

Other constructs: *ser-4::gfp* construct (Tsalik et al., 2003) is an integrated strain derived from a PCR fusion that covers 4.1kb of the 5' upstream of the start codon and 3.7kb out of 9.7kb coding region of the *ser-4* gene. The *mgl-2::gfp* plasmid was a gift from Oliver Hobert (Yemini et al., 2019) and covers 7.9kb of the 5' upstream of the start codon, which was injected to generate extrachromosomal lines and then chromosomally integrated to produce several independent lines.

Restriction digest*:* Microinjection of five recombineered transgenes (*dop-3::gfp*; *tyra-2::gfp*; *tyra-3::gfp*; *mgl-3::gfp*; *dop-5::gfp*) resulted in lethality or an absence of strong GFP expression in the extrachromosomal transgenic lines. To overcome these issues, 1-3µg of the five recombineered transgene were digested with restriction enzymes to cut out unwanted genes on the fosmid backbone as described in Appendix Chapter 2. The 45.4kb *dop-3::gfp* recombineered fosmid was digested with 10U NotI-HF and 10U AfeI incubated at 37°C for 2 hours resulting in a 28.6kb *dop-3::gfp* recombineered fosmid. The 53.8kb *tyra-2::gfp* recombineered fosmid was digested with 10U SacII and 10U StuI incubated at 37°C for 2 hours resulting in a 39.7kb *tyra-2::gfp* recombineered fosmid. The 49.1kb *tyra-3::gfp* recombineered fosmid was digested with 5U SbfI and 5U AfeI incubated at 37°C for 3 hours resulting in a 31.5kb *tyra-3::gfp* recombineered fosmid. The 44.8kb *mgl-3::gfp* recombineered fosmid was digested with 10U PluTI and 10U BmtI-HF incubated at 37°C for 2 hours resulting in a 25.2kb *-3::gfp* recombineered fosmid. The 44.6kb *dop-5::gfp* recombineered fosmid was digested with 10U AhdI and 10U AvrII incubated at 37°C for 2 hours resulting in a 25.4kb *dop-5::gfp* recombineered fosmid. After

restriction digest, the recombineered fosmids were run on 0.4% agarose gel for >10 hours to ensure expected products were properly separated and gel extracted using the QIAEX II Gel Extraction Kit (Qiagen). The resulting product yielded a purified sample of 30ng/uL, which ran on a 0.4% agarose gel to determine the product was at the expected size. For two of our constructs (MGL-3 and DOP-5), the restriction digest of the entire GPCR::GFP construct yielded other products that were a few kilobases in size below our product of interest (GPCR::GFP construct with parts of the vector backbone digested). Therefore, we wanted to further confirm the correct product (GPCR::GFP transgene with parts of the vector backbone digested) was purified after restriction digest. We designed primers (Appendix Chapter 2) to amplify the 5' and 3' flanking ends of the transgene (MGL-3 and DOP-5) and the products were run on a 0.4% agarose gel. All the purified transgenes used for microinjections resulted in no lethality or absent GFP expression. Further information on the construct size and fosmid used for recombineering are in a table in Appendix Chapter 2. There is also a visual representation for the GFP constructs for all 26 neurotransmitter GPCRs in Appendix Chapter 2.

5.2.6 Confocal imaging of GPCR::GFP transgenic strains

Young adult animals were mounted on 2% agarose pads [containing 120mM Optiprep (Sigma-Aldrich) to reduce refractive index mismatch (Boothe et al., 2017)] on premium microscope slides superfrost (Fisher Scientific). A 22x22-1 microscope cover glass (Fisher Scientific) was placed on top of the 2% agarose pad. Young adult animals were anesthetized using 150mM sodium azide

(Sigma-Aldrich) with 120mM Optiprep. Confocal images were taken on a Zeiss LSM 710 at 40X magnification, specifically z-stacks of ~100-130 slices (each ~0.60μm thick) of the midbody of young adult animals. For each double-labeled transgenic animal, at least 10 individual animals were imaged. Image reconstruction was performed using the Vaa3D imaging software.

5.2.7 Cell identification process

Each double-labeled transgenic strain was analyzed on the Vaa3D imaging software and cell identifications were annotated, which included the following: double-labeled GPCR::GFP egg-laying::mCherry transgenic strain number, allele corresponding to GFP and mCherry transgenic strain, # of animals imaged, confocal imaging acquisition date, cells labeled by the mCherry transgenic strain, intensity and frequency of for each GFP transgenic strain. GFP Intensity is defined as +++ (among the strongest cells labeled), ++ (easily detectable), and + (slightly above background), and – (no detectable GFP expression). For annotating the final intensity of GPCR::GFP expression in an egg-laying cell, we took the average GFP intensity for all animals imaged in the specific egg-laying cell of interest. For example, if we imaged a total of 10 GPCR::GFP animals in the *ida-1::mCherry* background, and saw GFP intensity in the HSN for 6 animals that are +++ and 4 animals that are ++, the average GFP intensity in the HSN for that specific neurotransmitter GPCR is reported as +++. We also annotated the frequency of GFP expression in a particular egg-laying cell, specifically the presence or absence of GFP expression in each egg-laying cell. Variable GFP expression is annotated by a “v” for GPCR::GFP expression that was seen for

less than 50% of all animals imaged. For example, if we saw GPCR::GFP expression in the HSN for 4 out of 10 animals, then we noted this as variable. All of this information is annotated in Figure 3.9.

5.3 Methods for Chapter 3

5.3.1 Strong and weak GPCR::GFP expression

Figure 3.9 contains the raw data where the average GFP intensity is reported for all 26 neurotransmitter GPCRs expressed in different cells of the *C. elegans* egg-laying system. Using the information in Figure 3.9, we generated Figure 3.10 where dark green indicates the cells that express GFP the strongest (+++) or at easily detectable (++) levels, bright green indicates cells in which GFP is just above background (+) in at least two different animals, and white indicates cells in which GFP was not reproducibly observed. "v" further denotes cells in which GFP expressed, but was present in less than 50% of the animals observed.

5.3.2 Annotating cases where receptors are positioned to receive synaptic vs. extrasynaptic signals in the *C. elegans* egg-laying system

The *C. elegans* connectome tells us the neurons that make synapses onto the egg-laying neurons and egg-laying muscles. This connectivity information was derived from The Structure of the Nervous System of the Nematode *Caenorhabditis elegans* (The Mind of the Worm) on WormAtlas, WormWiring, and the Database of Synaptic Connectivity of *C. elegans* for Computation (Albertson & Thomas, 1976; White et al., 1986; Oshio et al., 2003; Xu et al., 2013). The neurotransmitter map tells us the identity of every neurotransmitter expressed in every *C. elegans* neuron (Serrano-Saiz et al., 2013; Pereira et al.,

2016; Gendrel et al., 2016). Our neurotransmitter GPCR Atlas tells us all of the 26 neurotransmitter GPCRs that are expressed in different cells of the *C. elegans* egg-laying system. Combining the *C. elegans* connectome, neurotransmitter maps, and Neurotransmitter GPCR Atlas of the *C. elegans* egg-laying system, we can annotate cases where receptors in egg-laying cells are positioned to receive synaptic or extrasynaptic signaling. Cases of synaptic signaling were noted as neurotransmitter-releasing neurons that make synapse(s) onto a neuron or muscle that expresses the neurotransmitter receptor for that cognate neurotransmitter-releasing neuron. For example, serotonin-releasing neurons make synapses onto the HSN, which expresses a serotonin GPCR; the serotonin GPCR on the HSN is positioned to receive synaptic signals from the serotonin-releasing neuron. Cases of extrasynaptic signaling were noted as neurotransmitter-releasing neurons make no synapses onto a neuron or muscle that expresses the neurotransmitter receptor for that cognate neurotransmitter-releasing neuron. For example, octopamine-releasing neurons make no synapses onto the HSN, yet the HSN expresses an octopamine GPCR; the octopamine GPCR on the HSN is positioned to receive extrasynaptic signals from the octopamine-releasing neuron. A summary of all possible cases of synaptic or extrasynaptic signaling in the *C. elegans* egg-laying system is shown in Table 3.6.

5.4 Methods for Chapter 4

5.4.1 Egg-laying assays

For all egg-laying assays, unlaid eggs and early-staged eggs laid were quantified at 40 hours past the late L4 stage (Waggoner et al., 1998; Chase and Koelle, 2004; Collins and Koelle, 2013; Brewer et al., 2019). In the unlaid egg assay, 30 staged adults were individually dissolved in 5% sodium hypochlorite and the resulting eggs were counted for each animal. For the early-staged egg-laying assay, 50 staged adults were placed on an NGM plate seeded with a thin lawn of OP50 bacteria where the 50 staged adults laid egg for 30 minutes. Under a Lecia 420 dissecting microscope, we counted 100 eggs and categorized them as early-staged (eight cells or fewer) or late-staged (greater than eight cells).

5.4.2 Statistical Analysis

Data graphs were made using Prism 7.0 software (GraphPad, La Jolla, CA). Scatter plots show individual data points (dots), mean (horizontal line), and error bars indicate 95% confidence intervals (C.I.) for the mean. N values are indicated in the figure legends and sample size for behavioral assays followed previous studies (Waggoner et al., 1998; Chase and Koelle, 2004; Collins and Koelle, 2013; Brewer et al., 2019). Statistical significance was tested using one-way ANOVA with Bonferroni correction for multiple comparisons for the Unlaid Egg Assay and Fisher's exact test for the Early-Staged Egg-Laying Assay. For the Unlaid Egg Assay for the *dop-4* rescue experiment, validation of the neurotransmitter GPCR overexpressors, and the Biosynthetic Enzyme knockouts, the Tukey's test was used to determine statistical significance. For

the Early-staged Egg-laying Assay, the Wilson-Brown Method was used to determine the 95% C.I. for binomial data. $p \geq 0.05$ was considered not significant (ns) and $p < 0.05$ (*) was considered significant.

References

Agnati, L.F., Leo, G., Zanardi, A., Genedani, S., Rivera, A., Fuxe, K., and Guidolin, D. (2006). Volume transmission and wiring transmission from cellular to molecular networks: history and perspectives. *Acta Physiol (Oxf)*, *187*(1-2), 329-344. doi: 10.1111/j.1748-1716.2006.01579.x

Albertson, D.G., and Thomson, J.N. (1976). The pharynx of *Caenorhabditis elegans*. *Philos Trans R Soc Lond B Biol Sci*, *275*(938), 299-325. doi: 10.1098/rstb.1976.0085

Bamber, B.A., Beg, A.A., Twyman, R.E., and Jorgensen, E.M. (1999). The *Caenorhabditis elegans* unc-49 locus encodes multiple subunits of a heteromultimeric GABA receptor. *J Neurosci*, *19*(13), 5348-5359.

Banerjee, N., Bhattacharya, R., Gorczyca, M., Collins, K.M., and Francis, M.M. (2017). Local neuropeptide signaling modulates serotonergic transmission to shape the temporal organization of *C. elegans* egg-laying behavior. *PLoS Genet*, *13*(4), e1006697. doi: 10.1371/journal.pgen.1006697

Bany, I.A., Dong, M.Q., and Koelle, M.R. (2003). Genetic and cellular basis for acetylcholine inhibition of *Caenorhabditis elegans* egg-laying behavior. *J Neurosci*, *23*(22), 8060-8069.

Bargmann, C.I., and Marder, E. (2013). From the connectome to brain function. *Nat Methods*, *10*(6), 483-490. doi: 10.1038/nmeth.2451

Boothe, T., Hilbert, L., Heide, M., Berninger, L., Huttner, W.B., Zaburdaev, V., Vastenhouw, N.L., Myers, E.W., Drechsel, D.N., and Rink, J.C. (2017). A

tunable refractive index matching medium for live imaging cells, tissues and model organisms. *eLife*, *6*. doi: 10.7554/eLife.27240

Brewer, J.C., Olson, A.C., Collins, K.M., and Koelle, M.R. (2019). Serotonin and neuropeptides are both released by the HSN command neuron to initiate *Caenorhabditis elegans* egg laying. *PLoS Genet*, *15*(1), e1007896. doi: 10.1371/journal.pgen.1007896

Carnell, L., Illi, J., Hong, S.W., and McIntire, S.L. (2005). The G-protein-coupled serotonin receptor SER-1 regulates egg laying and male mating behaviors in *Caenorhabditis elegans*. *J Neurosci*, *25*(46), 10671-10681. doi: 10.1523/JNEUROSCI.3399-05.2005

Carre-Pierrat, M., Baillie, D., Johnsen, R., Hyde, R., Hart, A., Granger, L., and Ségalat, L. (2006). Characterization of the *Caenorhabditis elegans* G protein-coupled serotonin receptors. *Invert Neurosci*, *6*(4), 189-205. doi: 10.1007/s10158-006-0033-z

Chase, D.L., Pepper, J.S., and Koelle, M.R. (2004). Mechanism of extrasynaptic dopamine signaling in *Caenorhabditis elegans*. *Nat Neurosci*, *7*(10), 1096-1103. doi: 10.1038/nn1316

Cho, J.H., Bandyopadhyay, J., Lee, J., Park, C.S., and Ahnn, J. (2000). Two isoforms of sarco/endoplasmic reticulum calcium ATPase (SERCA) are essential in *Caenorhabditis elegans*. *Gene*, *261*(2), 211-219. doi: 10.1016/s0378-1119(00)00536-9

Collins, K.M., and Koelle, M.R. (2013). Postsynaptic ERG potassium channels limit muscle excitability to allow distinct egg-laying behavior states in

Caenorhabditis elegans. *J Neurosci*, *33*(2), 761-775. doi: 10.1523/JNEUROSCI.3896-12.2013

Collins, K.M., Bode, A., Fernandez, R.W., Tanis, J.E., Brewer, J.C., Creamer, M.S., and Koelle, M.R. (2016). Activity of the *C. elegans* egg-laying behavior circuit is controlled by competing activation and feedback inhibition. *eLife*, *5*. doi: 10.7554/eLife.21126

Dempsey, C.M., Mackenzie, S.M., Gargus, A., Blanco, G., and Sze, J.Y. (2005). Serotonin (5HT), fluoxetine, imipramine and dopamine target distinct 5HT receptor signaling to modulate *Caenorhabditis elegans* egg-laying behavior. *Genetics*, *169*(3), 1425-1436. doi: 10.1534/genetics.104.032540

Desai, C., Garriga, G., McIntire, S.L., and Horvitz, H.R. (1988). A genetic pathway for the development of the *Caenorhabditis elegans* HSN motor neurons. *Nature*, *336*(6200), 638-646. doi: 10.1038/336638a0

Dittman, J.S., and Kaplan, J.M. (2008). Behavioral impact of neurotransmitter-activated G-protein-coupled receptors: muscarinic and GABAB receptors regulate *Caenorhabditis elegans* locomotion. *J Neurosci*, *28*(28), 7104-7112. doi:10.1523/JNEUROSCI.0378-08.2008

Ecsedi, M., Rausch, M., and Großhans, H. (2015). The let-7 microRNA directs vulval development through a single target. *Dev Cell*, *32*(3), 335-344. doi: 10.1016/j.devcel.2014.12.018

Emtage, L., Aziz-Zaman, S., Padovan-Merhar, O., Horvitz, H.R., Fang-Yen, C., and Ringstad, N. (2012). IRK-1 potassium channels mediate peptidergic inhibition of *Caenorhabditis elegans* serotonin neurons via a G(o)

signaling pathway. *J Neurosci*, *32*(46), 16285-16295. doi: 10.1523/JNEUROSCI.2667-12.2012

Fuxe, K., Rivera, A., Jacobsen, K.X., Höistad, M., Leo, G., Horvath, T.L., Staines, W., De la Calle, A., and Agnati, L.F. (2005). Dynamics of volume transmission in the brain. Focus on catecholamine and opioid peptide communication and the role of uncoupling protein 2. *J Neural Transm (Vienna)*, *112*(1), 65-76. doi: 10.1007/s00702-004-0158-3

Fuxe, K., Borroto-Escuela, D.O., Romero-Fernandez, W., Diaz-Cabiale, Z., Rivera, A., Ferraro, L., Tanganelli, S., Tarakanov, A.O., Garriga, P., Narváez, J.A., Ciruela, F., Guescini, M., and Agnati, L.F. (2012). Extrasynaptic neurotransmission in the modulation of brain function. Focus on the striatal neuronal-glial networks. *Front Physiol*, *3*, 136. doi: 10.3389/fphys.2012.00136

Gendrel, M., Atlas, E.G., and Hobert, O. (2016). A cellular and regulatory map of the GABAergic nervous system of *C. elegans*. *eLife*, *5*. doi: 10.7554/eLife.17686

Ghosh, S., and Sternberg, P.W. (2014). Spatial and molecular cues for cell outgrowth during *C. elegans* uterine development. *Dev Biol*, *396*(1), 121-135. doi: 10.1016/j.ydbio.2014.09.028

Gürel, G., Gustafson, M.A., Pepper, J.S., Horvitz, H.R., and Koelle, M.R. (2012). Receptors and other signaling proteins required for serotonin control of locomotion in *Caenorhabditis elegans*. *Genetics*, *192*(4), 1359-1371. doi: 10.1534/genetics.112.142125

Hapiak, V.M., Hobson, R.J., Hughes, L., Smith, K., Harris, G., Condon, C., Komuniecki, P., and Komuniecki, R.W. (2009). Dual excitatory and inhibitory serotonergic inputs modulate egg laying in *Caenorhabditis elegans*. *Genetics*, *181*(1),153-163. doi: 10.1534/genetics.108.096891

Hobert, O. (2013). The neuronal genome of *Caenorhabditis elegans*. *Wormbook*. *13*, 1-106. doi: 10.1895/wormbook.1.161.1

Hobson, R.J., Hapiak, V.M., Xiao, H., Buehrer, K.L., Komuniecki, P.R., and Komuniecki, R.W. (2005). SER-7, a *Caenorhabditis elegans* 5-HT7-like receptor, is essential for the 5-HT stimulation of pharyngeal pumping and egg laying. *Genetics*, *172*(1), 159-169. doi: 10.1534/genetics.105.044495

Horvitz, H.R., Chalfie, M., Trent, C., Sulston, J.E., and Evans P.D. (1982). Serotonin and octopamine in the nematode *Caenorhabditis elegans*. *Science*, *216*(4549), 1012-1014. doi: 10.1126/science.6805073

Jose, A.M., Bany, I.A., Chase, D.L., and Koelle, M.R. (2007). A specific subset of transient receptor potential vanilloid-type channel subunits in Caenorhabditis elegans endocrine cells function as mixed heteromers to promote neurotransmitter release. *Genetics*, *175*(1), 93-105. Doi: 10.1534/genetics.106.065516

Kim, J., Poole, D.S., Waggoner, L.E., Kempf, A., Ramirez, D.S., Treschow, P.A., and Schafer, W.R. (2001). Genes affecting the activity of nicotinic receptors involved in *Caenorhabditis elegans* egg-laying behavior. *Genetics*, *157*(4), 1599-1610.

Koelle, M.R. (2018). Neurotransmitter signaling through heterotrimeric G proteins: insights from studies in *C. elegans*. *WormBook 2018*, 1-52. doi: 10.1895/wormbook.1.75.2

Lee, Y.S., Park, Y.S., Nam, S., Suh, S.J., Lee, J., Kaang, B.K., and Cho, N.J. (2000). Characterization of GAR-2, a novel G protein-linked acetylcholine receptor from *Caenorhabditis elegans*. *J Neurochem*, *75*(5), 1800-1809. doi: 10.1046/j.1471-4159.2000.0751800.x

Marder, E. (2012). Neuromodulation of neuronal circuits: back to the future. *Neuron*, *76*(1), 1-11. doi: 10.1016/j.neuron.2012.09.010

McCorvy, J.D., and Roth, B.L. (2015). Structure and function of serotonin G protein-coupled receptors. *Pharmacol Ther*, *150*, 129-142. doi: 10.1016/j.pharmthera.2015.01.009

Mendel, J.E., Korswagen, H.C., Liu, K.S., Hajdu-Cronin, Y.M., Simon, M.I., Plasterk, R.H., and Sternberg, P.W. (1995). Participation of the protein Go in multiple aspects of behavior in *C. elegans*. *Science, 267*(5204), 1652-1655. doil: 10.1126/science.7886455

Nagashima, T., Oami, E., Kutsuna, N., Ishiura, S., and Suo, S. (2016). Dopamine regulates body size in *Caenorhabditis elegans*. *Dev Bio*, *412*(1), 128-138. doi: 10.1016/j.ydbio.2016.02.021

Oshio, E., Iwasaki, Y., Morita, S., Osana, Y., Gomi, S., Akiyama, E., Omata, K., Oka, K., and Kawamura, K. (2003). Database of Synaptic Connectivity of *C. elegans* for computation. *Technical Report of CCeP, Keio Future*, *No. 3*. http://ims.dse.ibaraki.ac.jp/ccep/

Pereira, L., Kratsios, P., Serrano-Saiz, E., Sheftel, H., Mayo, A.E., Hall, D.H., White, J.G., LeBoeuf, B., Garcia, L.R., Alon, U., and Hobert, O. (2015). A cellular and regulatory map of the cholinergic nervous system of *C. elegans*. *eLife*, *4*. doi: 10.7554/eLife.12432

Plummer, I. (2011). Asymmetry in distribution systems: causes, harmful effects and remedies. PhD thesis, Louisiana State University. https://digitalcommons.lsu.edu/gradschool_theses/1490

Rand, J.B. (1989). Genetic Analysis of the Cha-1 Unc-17 Gene Complex in *Caenorhabditis*. *Genetics*, *122*(1), 73-80.

Rex, E., Molitor, S.C., Hapiak, V., Xiao, H., Henderson, M., and Komuniecki, R. (2004). Tyramine receptor (SER-2) isoforms are involved in the regulation of pharyngeal pumping and foraging behavior in *Caenorhabditis elegans*. *J Neurochem*, *91*(5):1104-1115. doi: 10.1111/j.1471-4159.2004.02787.x

Ringstad, N., and Horvitz, H.R. (2008). FMRFamide neuropeptides and acetylcholine synergistically inhibit egg-laying by *C. elegans*. *Nat Neurosci*, *11*(10), 1168-1176. doi: 10.1038/nn.2186

Sarov, M., Murray, J.I., Schanze, K., Pozniakovski, A., Niu, W., Angermann, K., Hasse, S., Rupprecht, M., Vinis, E., Tinney, M., Preston, E., Zinke, A., Enst, S., Teichgraber, T., Janette, J., Reis, K., Janosch, S., Schloissnig, S., Ejsmont, R.K., Slightam, C., Xu, X., Kim, S.K., Reinke, V., Stewart, A.F., Snyder, M., Waterston, R.H., and Hyman, A.A. (2012). A genome-scale resource for in vivo tag-based protein function exploration in *C. elegans*. *Cell*, *150*(4), 855-866. doi: 10.1016/j.cell.2012.08.001

Schafer, W.R., and Kenyon, C.J. (1995). A calcium-channel homologue required for adaptation to dopamine and serotonin in *Caenorhabditis elegans*. *Nature*, *375*(6526): 73-78. doi: 10.1038/375073a0

Schindler, A.J., and Sherwood, D.R. (2013). Morphogenesis of the *caenorhabditis elegans* vulva. *Wiley Interdiscip Rev Dev Biol*, *2*(1),75-95. doi: 10.1002/wdev.87

Ségalat, L., Elkes, D.A., and Kaplan, J.M. (1995). Modulation of serotonin-controlled behaviors by Go in *Caenorhabditis elegans*. *Science*, *267*(5204), 1648-1651. doi: 10.1126/science.7886454

Serrano-Saiz, E., Poole, R.J., Felton, T., Zhang, F., De La Cruz, E.D., and Hobert, O. (2013). Modular control of glutamatergic neuronal identity in C. elegans by distinct homeodomain proteins. *Cell*, *155*(3), 659-673. doi:10.1016/j.cell.2013.09.052

Shyn, S.I., Kerr, R., and Schafer, W.R. (2003). Serotonin and Go modulate functional states of neurons and muscles controlling *C. elegans* egg-laying behavior. *Curr Biol*, *13*(21), 1910-5. doi: 10.1016/j.cub.2003.10.025

Suo, S., Sasagawa, N., and Ishiura, S. (2003). Cloning and characterization of a *Caenorhabditis elegans* D2-like dopamine receptor. *J Neurochem*, *86*(4): 869-878. doi: 10.1046/j.1471-4159.2003.01896.x

Suo, S., Kimura, Y., and Van Tol, H.H. (2006). Starvation induces cAMP response element-binding protein-dependent gene expression through octopamine-Gq signaling in *Caenorhabditis elegans*. *J Neurosci*, *26*(40):10082-10090. doi: 10.1523/JNEUROSCI.0819-06.2006

Tanis, J.E., Moresco, J.J., Lindquist, R.A., and Koelle, M.R. (2008). Regulation of serotonin biosynthesis by the G proteins Galphao and Galphaq controls serotonin signaling in *Caenorhabditis elegans*. *Genetics*, *178*(1), 157-169. doi: 10.1534/genetics.107.079780

Tsalik, E.L., Niacaris, T., Wenick, A.S., Pau, K., Avery, L., and Hobert, O. (2003). LIM homeobox gene-dependent expression of biogenic amine receptors in restricted regions of the *C. elegans* nervous system. *Dev Biol*, *263*(1), 81-102. doi: 10.1016/s0012-1606(03)00447-0

Tursun, B., Cochella, L., Carrera, I., and Hobert, O. (2009). A toolkit and robust pipeline for the generation of fosmid-based reporter genes in *C. elegans*. *PLoS One*, *4*(3), e4625. doi: 10.1371/journal.pone.0004625

Vidal-Gadea, A.G., Davis, S., Becker, L., and Pierce-Shimomura, J.T. (2012). Coordination of behavioral hierarchies during environmental transitions in *Caenorhabditis elegans*. *Worm*, *1*(1): 5-11. doi: 10.4161/worm.19148

Waggoner, L.E., Zhou, G.T., Schafer, R.W., and Schafer W.R. (1998). Control of alternative behavioral states by serotonin in *Caenorhabditis elegans*. *Neuron*, *21*(1), 203-214. doi: 10.1016/s0896-6273(00)80527-9

White, J.G., Southgate, E., Thomson, J.N., and Brenner, S. (1986). The structure of the nervous system of the nematode *Caenorhabditis elegans*. *Philos Trans R Soc Lond B Biol Sci*, *314*(1165), 1-340. doi: 10.1098/rstb.1986.0056

Wragg, R.T., Hapiak, V., Miller, S.B., Harris, G.P., Gray, J., Komuniecki, P.R., and Komuniecki, R.W. (2007). Tyramine and octopamine independently

inhibit serotonin-stimulated aversive behaviors in *Caenorhabditis elegans* through two novel amine receptors. *J Neurosci*, *27*(49), 13402-13412. doi: 10.1523/JNEUROSCI.3495-07.2007

Xiao, H., Hapiak, V.M., Smith, K.A., Lin, L., Hobson, R.J., Plenefisch, J., and Komuniecki R. (2006). SER-1, a *Caenorhabditis elegans* 5-HT2-like receptor, and a multi-PDZ domain containing protein (MPZ-1) interact in vulval muscle to facilitate serotonin-stimulated egg-laying. *Dev Biol*, *298*(2), 379-391. doi: 10.1016/j.ydbio.2006.06.044

Xu, M., Jarrell, T.A., Wang, Y., Cook, S.J., Hall, D.H., and Emmons, S.W. (2013). Computer assisted assembly of connectomes from electron micrographs: application to *Caenorhabditis elegans*. *PLoS One 8*(1), e54050. doi: 10.1371/journal.pone.0054050

Yemini, E., Lin, A., Nejatbakjsj, A., Varol, E., Sun, R., Mena, G.E., Samuel, A.D.T., Paninski, L., Venkatachalam, L., and Hobert, O. (2019). NeuroPal: A Neuronal Polychromatic Atlas of Landmarks for Whole-Brain Imaging in *C.elegans*. *bioRxiv*. doi: https://doi.org/10.1101/676312

Appendix

Chapter 2 Figure

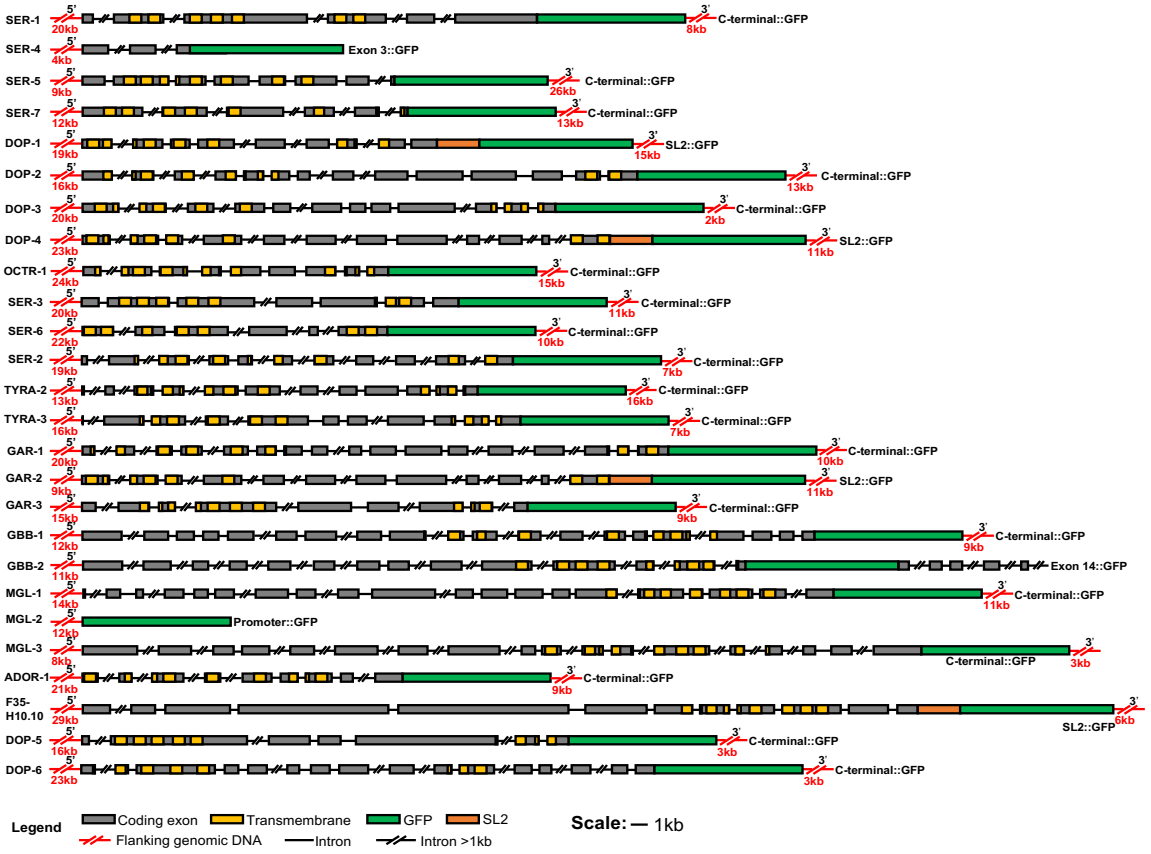

Figure A1. GFP reporter transgenes for Neurotransmitter GPCRs. Schematic of GFP reporters used in this study. C-terminal::GFP constructs are illustrated for 19 neurotransmitter receptors, which express a receptor with GFP fused to its C-terminus. SL2::GFP constructs are illustrated for four neurotransmitter receptors: an SL2 trans-splicing signal followed by GFP coding sequences were inserted immediately downstream of the neurotransmitter GPCR stop codon so that such reporters co-expresses a neurotransmitter GPCR and GFP as separate proteins. Three transgenes were constructed in other manners. The *ser-4::gfp* transgene (Tsalik et al., 2003; Gürel et al., 2012) has GFP coding sequences fused to the third coding exon of *ser-4.* Repetitive sequences in the *ser-4* genomic DNA 3' of this position prevented us from including the downstream regions of *ser-4* in the transgenes. The *gbb-2*::gfp reporter had GFP coding sequences inserted between two arginine codons in exon 14 of the *gbb-2* gene. The details of splicing downstream of exon 14 remain uncertain, preventing us from inserting GFP coding sequences more 3' to this exon. The *mgl-2::gfp* reporter is a transcriptional fusion with a promoter fragment extending 7.9 kb 5' to the *mgl-2* start codon inserted upstream of GFP coding sequences in the plasmid pPD955_75 (Addgene). The lengths of the 5' promoter and 3' downstream regions are indicated in kilobases (kb). Coding exons are indicated by gray boxes, predicted transmembrane domain coding regions by yellow boxes, GFP coding regions by green boxes, and the SL2 trans-splicing signal region by an orange box. Flanking genomic DNA is indicated in red. Introns 1kb or less are drawn to scale with a black line. Introns greater than 1 kb are not drawn to scale and indicated with slashed black lines.

Chapter 2 Table
A2.1 Neurotransmitter GPCR::GFP Transgenes

Neurotrans-mitter GPCR	Size (kb)[a]	5' upstream of start codon (kb)[b]	Coding region size (kb)[c]	3' downstream of stop codon (kb)[d]	Type of Reporter[e]	Fosmid Recombi-neered[f]
SER-1	41.4	20.4 – 22.7	5.5 - 7.7	4.1	C-terminal::GFP	WRM0640 b_B09[g]
SER-4	12.3	4.1	3.7[m]	N/A	GFP fusion at exon 3	N/A[j]
SER-5	37.2	8.5	1.8	25.9	C-terminal::GFP	WRM0619 a_G10[i]
SER-7	42.8	11.8	7.3 - 8.4	13.4 – 14.6	C-terminal::GFP	WRM0618 b_D08[h]
DOP-1	39.6	18.6	4.5	15.3	SL2::GFP	WRM069c _F02[i]
DOP-2	47.1	15.8	6.2	13.2	C-terminal::GFP	WRM061g _E12[g]
DOP-3	28.6[n]	20.0	3.3 – 5.2	2.1 - 3.9	C-terminal::GFP	WRM0628 c_G08[g]
DOP-4	38.5	23.3	3.4	10.6	SL2::GFP	WRM0638 a_D09[i]
OCTR-1	52.2	23.8	1.9	14.5	C-terminal::GFP	WRM065d _C11[g]
SER-3	45.7	20.3	2.2	11.3	C-terminal::GFP	WRM0610 c_C02[g]
SER-6	47.8	22.3	4.0	9.6	C-terminal::GFP	WRM0640 c_E05[g]
SER-2	45.5	11.0 - 19.1	5.1 – 13.0	6.5 - 9.6	C-terminal::GFP	WRM0628 c_A02[g]
TYRA-2	39.6[o]	13.0 - 17.1	4.2 – 8.3	15.7	C-terminal::GFP	WRM0633 a_G12[g]
TYRA-3	31.4[p]	16.1 - 23.1	3.0 – 7.0	7.3	C-terminal::GFP	WRM0610 d_C10[g]
GAR-1	47.1	19.8	5.2	10.2	C-terminal::GFP	WRM0613 a_A04[g]
GAR-2	35.7	9.1 - 17.5	2.8 – 11.2	14.3-19.4	SL2::GFP	WRM0634 d_D01[i]
GAR-3	38.4	15.3	4.9	9.08	C-terminal::GFP	WRM0615 a_E07[h]
GBB-1	43.0	12.0 - 20.7	1.2 – 9.8	9.3 - 15.3	C-terminal::GFP	WRM0618 b_F01[g]
GBB-2	28.2	10.5	16.3	1.0	GFP fusion at exon 14[l]	WRM0640 d_H01[i]
MGL-1	44.0	13.8 – 16.6	4.4 – 7.7	11.2	C-terminal::GFP	WRM0618 a_C08[g]
MGL-2	12.3	7.9	N/A	N/A	Promoter::GFP	N/A[k]

MGL-3	25.1[q]	7.5 – 14.6	4.5 – 11.6	2.9	C-terminal::GFP	WRM0620a_H12[g]
ADOR-1	47.2	21.1	5.5	8.8	C-terminal::GFP	WRM0641b_G10[g]
F35H10.10	41.4	28.8	5.3	6.14	SL2::GFP	WRM0628b_G02[i]
DOP-5	23.9[r]	16.1	3.6	3.3	C-terminal::GFP	WRM0639a_H11[h]
DOP-6	41.1	23.0	6.5	2.6	C-terminal::GFP	WRM0621c_G04[h]

a. Size of the entire transgene. For plasmids this includes the fosmid vector backbone and the *C. elegans* genomic DNA insert tagged with GFP. Other transgenes, as indicated by footnotes, are linear DNA fragments generated by restriction digests of larger fosmid constructs or by PCR, some of which do not contain vector sequences.

b. Length of *C. elegans* promoter region genomic DNA 5' of the start codon of the neurotransmitter GPCR gene. If the gene produces alternative transcripts with different 5' coding exons and start codons, the range of lengths 5' of the various start codons is given.

c. Length of the coding region (exons plus introns) of the neurotransmitter GPCR gene. If the gene produces alternative transcripts, range of length of various transcripts are given.

d. This number shows the length of *C. elegans* genomic DNA present 3' of the stop codon of the GPCR gene. If the gene produces alternative transcripts with different 3' coding exons and stop codons, the range of lengths 3' of the various stop codons is given.

e. C-terminal::GFP reporters express a receptor::GFP fusion protein with GFP fused immediately after the C-terminal amino acid of the receptor. SL2::GFP reporters express a primary RNA transcript that is trans-spliced to produced two separate mRNAs so that the full-length receptor and GFP are expressed as separate proteins. "GFP fusion at exon..." indicates that GFP coding sequences were fused in-frame to the receptor coding sequences prior to the last receptor codon, within the receptor coding exon indicated. For SER-4 (Tsalik et al. 2003), this strategy was used because repetitive genomic sequences in the 3' end of the *ser-4* gene made it impossible to PCR amplify or clone that region of genomic DNA. For GBB-2 this strategy was used because the coding exons 3' of exon 14 remain unmapped. The transcriptional construct used for MGL-2 (Yemini et al. 2019) was generated by PCR amplifying a 7.9 kb fragment 5' to the MGL-2 start codon and inserting it upstream of GFP coding sequences in the plasmid pPD955_75 (Addgene).

f. Fosmid clones engineered to generate GFP reporters each contained ~20-50 kb of *C. elegans* genomic DNA with a receptor gene located near the center. Detailed information on each fosmid is available at www.wormbase.org.

g. These thirteen fosmid clones were engineered into GFP reporters by Sarov et al. (2012).

h. These four fosmid clones were newly engineered for this work into GFP reporters using the method of Sarov et al. (2012).

i. These six fosmid clones were newly engineered for this work into GFP reporters using the method of Tursun et al. (2009).

j. The SER-4::GFP transgene was made by Tsalik et al. (2003) and chromosomally integrated by Gürel et al. (2012).

k. **The MGL-2::GFP transgene** was made by Yemini et al. (2019).

l. The GBB-2::GFP reporter had GFP-coding sequences inserted between two arginine codons in exon 14 of the *gbb-2* gene. This fuses GFP to the predicted C-terminal cytoplasmic tail of the receptor, but prior to the most C-terminal amino acid of GBB-2. This design was used because

the splicing of the 3'-most coding exon(s) of *gbb-2* remained uncertain, so GFP was fused after the most C-terminal amino acid we could be sure was part of the GBB-2 protein.

m. The *ser-4::gfp* construct contains 3.7kb of out of the full 9.7kb coding region for *ser-4*. GFP coding sequences were fused to the third coding exon of *ser-4* because the more 3' regions of *ser-4* genomic DNA contained repetitive sequences never recovered in any *C. elegans* cosmid or fosmid library and that we also could not amplify by PCR from *C. elegans* genomic DNA.

n. The *dop-3::gfp* construct was initially made by inserting GFP into a fosmid generating a 45.4kb plasmid. We were unable to transform this full construct into *C. elegans* because regions flanking the *dop-3* gene were toxic at high copy. Therefore, we used a NotI-HF and AfeI restriction digest to isolate a 28.6kb fragment containing the *dop-3::gfp* gene and used this to generate a transgenic strain.

o. The *tyra-2::gfp* construct was initially made by inserting GFP into a fosmid generating a 53.8kb plasmid. We were unable to transform this full construct into *C. elegans* because regions flanking the *tyra-2* gene were toxic at high copy. Therefore, we used a SacII and StuI restriction digest to isolate a 39.7kb fragment containing the *tyra-2::gfp* gene and used this to generate a transgenic strain.

p. The *tyra-3::gfp* construct was initially made by inserting GFP into a fosmid generating a 49.1kb plasmid. We were unable to transform this full construct into *C. elegans* because regions flanking the *tyra-3* gene were toxic at high copy. Therefore, we used a SbfI and AfeI restriction digest to isolate a 31.5kb fragment containing the *tyra-3::gfp* gene and used this to generate a transgenic strain.

q. The *mgl-3::gfp* construct was initially made by inserting GFP into a fosmid generating a 44.8kb plasmid. We were unable to transform this full construct into *C. elegans* because regions flanking the *mgl-3* gene were toxic at high copy. Therefore, we used a PluTI and BmtI restriction digest to isolate a 25.2kb fragment containing the *mgl-3::gfp* gene and used this to generate a transgenic strain.

r. The *dop-5::gfp* construct was initially made by inserting GFP into a fosmid generating a 44.6kb plasmid. We were unable to transform this full construct into *C. elegans* because regions flanking the *dop-5* gene were toxic at high copy. Therefore, we used a AhdI and AvrII restriction digest to isolate a 25.4kb fragment containing the *dop-5::gfp* gene and used this to generate a transgenic strain.

Chapter 2 Primers

Primer	DNA sequence
GFP Forward Primer	GAGTTTGTAACAGCTGCTGGG
GFP Forward Internal Primer	ACGGGAACTACAAGACAC
GFP Reverse Primer	CCATCTAATTCAACAAGAATTGGG
GFP Reverse Internal Primer	GTTTGTCCGCCATGATGT
pBALU9 GFP Forward Primer for recombineering fosmid WRM0640d_H01 for *gbb-2::gfp*	TAATCGAATTGGCTCGAAATCCGGTTGGCAAGAGC CAAGAGCTATCGAATGAGTAAAGGAGAAGAACTTTT C
pBALU9 GFP Reverse Primer for recombineering fosmid WRM0640d_H01 for *gbb-2::gfp*	GGTGACATTGGCTGTGAAGTCTTCGCGACAACACT CTTCATAAGACCCCCCGTTTGTATAGTTCATCCATG CCATG
pBALU9 GFP Forward Primer for recombineering fosmid WRM069c_F02 for *dop-1::SL2::NLS::gfp*	CTCCGCCTGAATCTTCTTTCGAATAATAACGAGGAA ACCATTCCGGAATAGGCTGTCTCCATCCTACTTTCA CCTAGTTAAC
pBALU9 GFP Reverse Primer for recombineering fosmid WRM069c_F02 for *dop-1::SL2::NLS::gfp*	AGGGTAATTGAATAAAGAAAGCATGCAATAAAACTG GAAAATTTTGAAAGTCTATTTGTATAGTTCATCCATG CCATG
pBALU9 GFP Forward Primer for recombineering fosmid WRM0638a_D09 for *dop-4::SL2::NLS::gfp*	TCTCGGTCACCCAAATGTGGGAGCAACCGCCGAAT ACTTTCAATTGAATAGGCTGTCTCATCCTACTTTCAC CTAGTTAAC
pBALU9 GFP Reverse Primer for recombineering fosmid WRM0638a_D09 for *dop-4::SL2::NLS::gfp*	TCATATTAAAATTGAAAAAAAATCAAAAATAAAAAATA CAAAATAAAAACTATTTGTATAGTTCATCCATGCCAT G
pBALU9 GFP Forward Primer for recombineering fosmid WRM0634d_D01 for *gar-2::SL2::NLS::gfp*:	AGTTCAAGAAAACGCTCACTAGGATTTTCAAAGGAG ATTTTCGAAGAGTTTGAGCTGTCTCATCCTACTTTCA CCTAGTTAAC
pBALU9 GFP Reverse Primer for recombineering fosmid WRM0634d_D01 for *gar-2::SL2::NLS::gfp*:	TGACATATTTAACAAAGAAGTTGAGCGGTGAACTAA TTGAAAAATGCGACTATTTGTATAGTTCATCATGCCA TG
pBALU9 GFP Forward Primer for recombineering fosmid WRM0628b_G02 for *F35H10.10::SL2::NLS::gfp*	GAGTGGCCATATCGCCACCAATTCGAGACTATAATT CGATCAATCATTGAGCTGTCTCATCCTACTTTCACCT AGTTAAC
pBALU9 GFP Reverse Primer for recombineering fosmid WRM0628b_G02 for *F35H10.10::SL2::NLS::gfp*	TATGTGGGGGTTCGGCGAGGAGGTTTTGGGATGGG GAGGGGGTATGTACACTATTTGTATAGTTCATCCAT GCCATG
PlutI Restriction Digest Confirmation of *mgl-3::gfp* end Forward Primer	CATCGCCCTTTTCAACTCTTCTT
PlutI Restriction Digest Confirmation of *mgl-3::gfp* end Reverse Primer	ACTCTTAACCGAGCAGCACAC
BmtI Restriction Digest Confirmation of *mgl-3::gfp* end Forward Primer	CCGCGGTTATCGATCTGGACA

BmtI Restriction Digest Confirmation of *mgl-3::gfp* end Reverse Primer	CCACTCTTATTGGCTCCACCG
AvrII Restriction Digest Confirmation of *dop-5::gfp* end Forward Primer	TTCCCCGATGTGTCACGATTG
AvrII Restriction Digest Confirmation of *dop-5::gfp* end Reverse Primer	GGAATGGTAGAGAGAAACAGATCGA
AhdII Restriction Digest Confirmation of *dop-5::gfp* end Forward Primer	GAGCGAAATTGTGGAGGGCA
AhdII Restriction Digest Confirmation of *dop-5::gfp* end Forward Primer	GAGCTGTCATTTCAAACATACCG

Chapter 4 Primers

Primer	DNA sequence
ok371 Forward Primer	GGATAAAGGAGGGCGCGACC
ok371 Forward Internal Primer	CATGACCAGCAGTCCGACTAGC
ok371 Reverse Primer	GTGTCAGTTTCTTGGTCGGCTAAG
ok520 Forward Primer	ACACTTTTTACCCCCATCCAGGAACTT
ok520 Forward Internal Primer	GACCAACACTTACAGGTGGGTTCAAG
ok520 Reverse Primer	GGTGTTGCTCTAGCAGTCCCT
ok755 Forward Primer	GATTCTGAGTCAGCGGCTGG
ok755 Forward Internal Primer	GTGAAACAGGCCGAGGGAAC
ok755 Reverse Primer	ATGCTAGTTGTGTGGAACAGAGTTAATTTTC
vs105 Forward Primer	GAACTACGCTGGACTTTCTCTTATTGTT
vs105 Forward Internal Primer	TACTCCGGTACCGAGCACTGC
vs105 Reverse Primer	CAACAAATTACTGTCTTGGTCGCC
tm1165 Forward Primer	ATATAGTTCGGCTCATTCAGCTGG
tm1165 Forward Internal Primer	TGTGTGCTGGTCACATGGGC
tm1165 Reverse Primer	ACCATTAGGACTCCTTTGACTGC
tm1406 Forward Primer	AGTTGAGATGGCACTGAAAGATGTC
tm1406 Forward Internal Primer	TTCCACCCCCAGAAGAGCATT
tm1406 Reverse Primer	CAATGCGAGCGCCCTGAAATATC
tm1392 Forward Primer	CCACAGTCTGGGCGACAGAG
tm1392 Reverse Internal Primer	CGCGTCGCAATTATGTAGACC
tm1392 Reverse Primer	GGTCTCGGCACAGCAAATTTC
ok2007 Forward Primer	GAGTATAAATAATAGGTCTTCCCTTCTCCGC
ok2007 Forward Internal Primer	TAAATCGTGGAGCGGTTGGAGC
ok2007 Reverse Primer	TTTCATATGCACCGGCTGTCCT
tm355 Forward Primer	TGGTGGCATCTGAAGTTGATATCTCTTG
tm355 Forward Internal Primer	TAGCCTACAAAACCCTAACCCTGAAAG
tm355 Reverse Primer	TGTTCCATTTCCTAGAGAGCATTTCTGTGC
tm1766 Forward Primer	CGAATAATCATACGCAGGGGTCTT
tm1766 Forward Internal Primer	TGCTGATACGGGATCCTATGGTGA
tm1766 Reverse Primer	ATGCATTCGGATTAGGAGATCTCTGG
mg280 Forward Primer	CATATGGATTCGTTGTTTCAGATG
mg280 Reverse Internal Primer	CCATGTAAAGAAAAAATAATGAGAGTCTATG
mg280 Reverse Primer	GAAATTGTTTCAATAACACGCCC
n3419 Forward Primer	GAAACCTAGGACTGATCCCATTCTTC
n3419 Forward Internal Primer	CTGGGCGATCGTTTTGTGATCC
n3419 Reverse Primer	GGGGAGCAAGGTGAAAGTTCC
n3247 Forward Primer	GAGTAGCTTGCTGTGTGCAAAAC
n3247 Forward Internal Primer	CGACGCAGGAATTATGGAACTTGGTTTA
n3247 Reverse Primer	TTTGTGTACTCCCTAAACAGAATGTATCTCAAT
ky5 Forward Primer	GAGAACCTAACACAACAGGTGT
ky5 Forward Internal Primer	CCCACAGAAATGTAAGTGTATAAAGAGC
ky5 Reverse Primer	CTCCAGACACCATGCATAGCAG

Chapter 5 Strains and Alleles

A5.1 mCherry marker strains

Strain	Feature	Genotype
LX2478 (**Other integrants**: LX2479, LX2480)	egg-laying neurons expressing mCherry [0x outcrossed]	*lin-15(n765ts)* X; *vsIs269* [*ida-1::mCherry*]
LX2096 (**Other integrant**: LX2097)	vulval and uterine muscles expressing mCherry [0x outcrossed]	*lin-15(n765ts)* X; *vsIs191* [*unc-103e::mCherry*]
LX2562	apical borders of epithelial cells labelled with mCherry [2x outcrossed]	*mjIs15* [*ajm-1::mCherry*]

A5.2 Neurotransmitter GPCR single knockout strains

Strain	Feature	Genotype
DA1814	*ser-1* null mutant [10X outcrossed]	*ser-1(ok345)* X
AQ866	*ser-4* null mutant [5X outcrossed]	*ser-4(ok512)* III
LX2467	*ser-5* null mutant [6X outcrossed]	*ser-5(ok3087)* I
LX1984	*ser-7* null mutant [6X outcrossed]	*ser-7(gk414345)* X
FX00535	*dop-1* null mutant [0x outcrossed]	*dop-1(tm535)* X
LX702	*dop-2* null mutant [4x outcrossed]	*dop-2(vs105)* V
LX703	*dop-3* null mutant [4x outcrossed]	*dop-3(vs106)* X
LX2725	*dop-4* null mutant [2x outcrossed]	*dop-4(tm1392)* X
CX13079	*octr-1* null mutant [4x outcrossed]	*octr-1(ok371)* X
LX2552	*ser-3* null mutant [2x outcrossed]	*ser-3(ok2007)* I
FX17797	*ser-6* null mutant [2x outcrossed]	*ser-6(tm2146)* IV
OH313	*ser-2* null mutant [4x outcrossed]	*ser-2(pk1357)* X
RWK210	*tyra-2* null mutant [4x outcrossed]	*tyra-2(tm1846)* X
VC125	*tyra-3* null mutant [4x outcrossed]	*tyra-3(ok325)* X
LX740	*gar-1* null mutant [4x outcrossed]	*gar-1(ok755)* X
LX2549	*gar-2* null mutant [2x outcrossed]	*gar-2(ok520)* III
VC670	*gar-3* null mutant [0x outcrossed]	*gar-3(gk337)* V
LX2703	*gbb-1* null mutant [2x outcrossed]	*gbb-1(tm1406)* X
LX2550	*gbb-2* null mutant [2x outcrossed]	*gbb-2(tm1165)* IV
FX31004	*mgl-1* null mutant [0x] Outcrossed]	*mgl-1(tm7090)* X
LX2705	*mgl-2* null mutant [2x outcrossed]	*mgl-2(tm355)* I
LX2706	*mgl-3* null mutant [2x outcrossed]	*mgl-3(tm1766)* IV
FX17843	*ador-1* null mutant [0x outcrossed]	*ador-1(tm3971)* II
FX03179	*F35H10.10* null mutant [0x outcrossed]	*F35H10.10(tm3179)* IV
RB785	*dop-5* null mutant [0x outcrossed]	*dop-5(ok568)* V
RB1680	*dop-6* null mutant [0x outcrossed]	*dop-6(ok2090)* X

A5.3 Neurotransmitter GPCR combination knockout strains

Strain	Feature	Genotype
LX2567	*gar-2*; *gbb-2* double mutant	*gar-2(ok520)* III; *gbb-2(tm1165)* IV
LX2548	*gar-2*; *dop-2* double mutant	*gar-2(ok520)* III; *dop-2(vs105)* V
LX2547	*gar-2*; *octr-1* double mutant	*gar-2(ok520)* III; *octr-1(ok371)* X
LX739	*gar-2*; *gar-1* double mutant	*gar-2(ok520)* III; *gar-1(ok755)* X
LX2588	*octr-1 gar-1* double mutant	*octr-1(ok371)* X *gar-1(ok755)* X
LX2599	*gar-2*; *gbb-2*; *gar-1* triple mutant	*gar-2(ok520)* III; *gbb-2(tm1165)* IV; *gar-1(ok755)* X
LX2602	*gar-2*; *octr-1 gar-1* triple mutant	*gar-2(ok520)* III; *octr-1(ok371)* X *gar-1(ok755)* X
LX2566	*gar-2*; *dop-2*; *gar-1* triple mutant	*gar-2(ok520)* III; *dop-2(vs105)* V; *gar-1(ok755)* X
LX2603	*dop-2*; *octr-1 gar-1* triple mutant	*dop-2(vs105)* V; *octr-1(ok371)* X *gar-1(ok755)* X
LX2604	*gbb-2*; *octr-1 gar-1* triple mutant	*gbb-2(tm1165)* IV; *octr-1(ok371)* X *gar-1(ok755)* X
LX2605	*gar-2*; *dop-2*; *octr-1 gar-1* quadruple mutant	*gar-2(ok520)* III; *dop-2(vs105)* V; *octr-1(ok371)* X *gar-1(ok755)* X
LX2601	*gar-2*; *gbb-2*; *dop-2*; *gar-1* quadruple mutant	*gar-2(ok520)* III; *gbb-2(tm1165)* IV; *dop-2(vs105)* V; *gar-1(ok755)* X
LX2606	*gar-2*; *gbb-2*; *octr-1* and *gar-1* quadruple mutant	*gar-2(ok520)* III; *gbb-2(tm1165)* IV; *octr-1(ok371)* X *gar-1(ok755)* X
LX2607	*gbb-2*; *dop-2*; *octr-1 gar-1* quadruple mutant	*gbb-2(tm1165)* IV; *dop-2(vs105)* V; *octr-1(ok371)* X *gar-1(ok755)* X
LX2608	*gar-2; gbb-2*; *dop-2*; *octr-1 gar-1* quintuple mutant	*gar-2(ok520)* III; *gbb-2(tm1165)* IV; *dop-2(vs105)* V; *octr-1(ok371)* X *gar-1(ok755)* X

A5.4 Neurotransmitter GPCR::GFP transgenic strains

Strain	Feature	Genotype
LX2679 (**Other integrants**: LX2378, LX2379)	*ser-1(ox)* translational, GFP reporter [2x outcrossed]	*vsIs244* [*ser-1(fosmid)::gfp*]
AQ570	*ser-4* transcriptional (PCR), GFP reporter	*ljIs570* [*ser-4(7.8kb)::gfp*]
LX2641	*ser-5(ox)* translational, GFP reporter [0x outcrossed]	*lin-15(n765ts)* X; *vsIs282* [*ser-5(fosmid)::gfp*]
LX2357 (**Other integrants**: LX2356, LX2358, LX2359)	*ser-7(ox)* translational, GFP reporter [0x outcrossed]	*lin-15(n765ts)* X; *vsIs238* [*ser-7(fosmid)::gfp*]
LX2690 (**Other integrants:** LX2683, LX2684)	*dop-1(ox)* transcriptional (SL2), GFP reporter [0x outcrossed]	*lin-15(n765ts)* X; *vsIs284* [*dop-1(fosmid)::SL2::NLS::GFP*]
LX2301 (**Other integrants**: LX2300, LX2302)	*dop-2(ox)* translational, GFP reporter [0x outcrossed]	*lin-15(n765ts)* X; *vsIs233* [*dop-2(fosmid)*::gfp]
LX2440 (**Other integrants**: LX2439, LX2441)	*dop-3(ox)* translational, GFP reporter [0x outcrossed]	*lin-15(n765ts)* X; *vsIs258* [*dop-3(fosmid)::gfp*]
LX2707 (**Other integrants**: LX2686, LX2687, LX2688, LX2689, LX2691)	*dop-4(ox)* transcriptional (SL2), GFP reporter [2x outcrossed]	*vsIs287* [*dop-4(fosmid)::SL2::NLS::GFP*]
LX2227	*octr-1(ox)* translational, GFP reporter [2x outcrossed]	*vsIs208* [*octr-1(fosmid)*::gfp]
LX2730 (**Other integrant**: LX2228)	*ser-3(ox)* translational, GFP reporter [4x outcrossed]	*vsIs298* [*ser-3(fosmid)::gfp*]
LX2677 (**Other integrants**: LX2263, LX2264, LX2265)	*ser-6(ox)* translational, GFP reporter [2x outcrossed]	*vsIs220* [*ser-6(fosmid)::gfp*]
LX2701	*ser-2(ox)* translational, GFP reporter [2x outcrossed]	*vsIs213* [*ser-2(fosmid)::gfp*]
LX2444 (**Other integrants**: LX2442, LX2443, LX2445)	*tyra-2(ox)* translational, GFP reporter [0x outcrossed]	*lin-15(n765ts)* X; *vsIs262* [*tyra-2(fosmid)::gfp*]
LX2738	*tyra-3(ox)* translational, GFP reporter [4x outcrossed]	*vsIs251* [*tyra-3(fosmid)::gfp*]
LX2205	*gar-1(ox)* translational, GFP reporter [2x outcrossed]	*vsIs205* [*gar-1(fosmid)::gfp*]
LX2436	*gar-2(ox)* transcriptional (SL2), GFP reporter [0x outcrossed]	*lin-15(n765ts)* X; *vsIs255* [*gar-2(fosmid)::SL2::NLS::GFP*]
LX2382 (**Other integrants:** LX2381, LX2383, LX2384)	*gar-3(ox)* translational, GFP reporter [0x outcrossed]	*lin-15(n765ts)* X; *vsIs248* [*gar-3(fosmid)::gfp*]
LX2202 (**Other integrant:** LX2304**)**	*gbb-1(ox)* translational, GFP reporter [4x outcrossed]	*vsIs206* [*gbb-1(fosmid)*::gfp]

LX2465 (**Other integrant**: LX2464)	*gbb-2(ox)* translational, GFP reporter [0x outcrossed]	*lin-15(n765ts)* X; *vsIs267* [*gbb-2(fosmid)::gfp*]
LX2678 (**Other integrants**: LX2252, LX2253, LX2254)	*mgl-1(ox)* translational, GFP reporter [2x outcrossed]	*vsIs214* [*mgl-1(fosmid)::gfp*]
LX2633	*mgl-2* transcriptional, GFP reporter [0x outcrossed]	*lin-15(n765ts)* X; *vsIs281* [*mgl-2(7.9kb)::gfp*]
LX2680	*mgl-3(ox)* translational, GFP reporter [2x outcrossed]	*vsIs256* [*mgl-3(fosmid)::gfp*]
LX2208 (**Other integrants**: LX2203, LX2206, LX2207)	*ador-1(ox)* translational, GFP reporter [0x outcrossed]	*vsIs229* [*ador-1(fosmid)::gfp*]
LX2699 (**Other integrants**: LX2640, LX2696, LX2697, LX2698, LX2700)	*F35H10.10(ox)* transcriptional (SL2), GFP reporter [0x outcrossed]	*lin-15(n765ts)* X; *vsIs296* [*F35H10.10(fosmid)::SL2::NLS::GFP*]
LX2426 (**Other integrants**: LX2424, LX2425)	*dop-5(ox)* translational, GFP reporter [0x outcrossed]	*lin-15(n765ts)* X; *vsIs254* [*dop-5(fosmid)::gfp*]
LX2360 (**Other integrant:** LX2361)	*dop-6(ox)* translational, GFP reporter [0x outcrossed]	*lin-15(n765ts)* X; *vsIs241* [*dop-6(fosmid)::gfp*]

A5.5 Neurotransmitter GPCR::GFP double-labeled strains

Strain	Feature	Genotype
LX2614	*ser-1* transgene expressing GFP egg-laying neurons expressing mCherry	*lin-15(n765ts) X; vsIs244* [*ser-1(fosmid)::gfp*]; *vsIs269* [*ida-1::mCherry*]
LX2412	*ser-1* transgene expressing GFP vulval and uterine muscles expressing mCherry	*lin-15(n765ts)* X; *vsIs246* [*ser-1(fosmid)::gfp*]; *vsIs191* [*unc-103e::mCherry*]
LX2579	*ser-1* transgene expressing GFP apical borders of epithelial cells expressing mCherry	*vsIs244 [ser-1(fosmid)::gfp]; mjIs15* [*ajm-1::mCherry*]
LX2623	*ser-4* PCR fusion GFP construct egg-laying neurons expressing mCherry	*ljIs570* [*ser-4(7.8kb)::gfp*]; *vsIs270* [*ida-1::mCherry*]
LX2121	*ser-4* PCR fusion GFP construct vulval and uterine muscles expressing mCherry	*ljIs570* [*ser-4(7.8kb)::gfp*]; *vsIs191* [*unc-103e::mCherry*]
LX2672	*ser-5* transgene expressing GFP egg-laying neurons expressing mCherry	*vsIs282* [*ser-5(fosmid)::gfp*]; *vsIs271* [*ida-1::mCherry*]
LX2673	*ser-5* transgene expressing GFP vulval and uterine muscles expressing mCherry	*vsIs282* [*ser-5(fosmid)::gfp*]; *vsIs192* [*unc-103e::mCherry*]
LX2671	*ser-5* transgene expressing GFP apical borders of epithelial cells expressing mCherry	*vsIs282* [*ser-5(fosmid)::gfp*]; *mjIs15* [*ajm-1::mCherry*]
LX2538	*ser-7* transgene expressing GFP egg-laying neurons expressing mCherry	*lin-15(n765ts)* X; *vsIs237* [*ser-7(fosmid)::gfp*]; *vsIs269* [*ida-1::mCherry*]
LX2418	*ser-7* transgene expressing GFP vulval and uterine muscles expressing mCherry	*lin-15(n765ts)* X; *vsIs238* [*ser-7(fosmid)::gfp*]; *vsIs191* [*unc-103e::mCherry*]
LX2613	*ser-7* transgene expressing GFP apical borders of epithelial cells expressing mCherry	*vsIs238* [*ser-7(fosmid)::gfp*]; *mjIs15* [*ajm-1::mCherry*]
LX2713	*dop-1* transgene expressing GFP egg-laying neurons expressing mCherry	*lin-15(n765ts)* X; *vsIs284* [*dop-1(fosmid)::SL2::NLS::GFP*]; *vsIs271* [*ida-1::mCherry*]
LX2714	*dop-1* transgene expressing GFP apical borders of epithelial cells expressing mCherry	*vsIs284* [*dop-1(fosmid)::SL2::NLS::GFP*]; *mjIs15* [*ajm-1::mCherry*]
LX2625	*dop-2* transgene expressing GFP egg-laying neurons expressing mCherry	*lin-15(n765ts)* X; *vsIs233* [*dop-2(fosmid)::gfp*]; *vsIs270* [*ida-1::mCherry*]
LX2661	*dop-2* transgene expressing GFP apical borders of epithelial cells expressing mCherry	*vsIs233* [*dop-2(fosmid)::gfp*]; *mjIs15* [*ajm-1::mCherry*]
LX2531	*dop-3* transgene expressing GFP egg-laying neurons expressing mCherry	*lin-15(n765ts)* X; *vsIs258* [*dop-3(fosmid)::gfp*]; *vsIs269* [*ida-1::mCherry*]
LX2737	*dop-3* transgene expressing GFP apical borders of epithelial cells expressing mCherry	*vsIs258* [*dop-3(fosmid)::gfp*]; *mjIs15* [*ajm-1::mCherry*]
LX2716	*dop-4* transgene expressing GFP egg-laying neurons expressing mCherry	*lin-15(n765ts)* X; *vsIs287* [*dop-4(fosmid)::SL2::NLS::GFP*]; *vsIs270* [*ida-1::mCherry*]

LX2717	*dop-4* transgene expressing GFP vulval and uterine muscles expressing mCherry	*lin-15(n765ts)* X; *vsIs287* [*dop-4(fosmid)::SL2::NLS::GFP*]; *vsIs192* [*unc-103e::mCherry*]
LX2715	*dop-4* transgene expressing GFP apical borders of epithelial cells expressing mCherry	*vsIs287* [*dop-4(fosmid)::SL2::NLS::GFP*]; *mjIs15* [*ajm-1::mCherry*]
LX2535	*octr-1* transgene expressing GFP egg-laying neurons expressing mCherry	*vsIs208* [*octr-1(fosmid)::gfp*]; *vsIs269* [*ida-1::mCherry*]
LX2542	*octr-1* transgene expressing GFP vulval and uterine muscles expressing mCherry	*vsIs208* [*octr-1(fosmid)::gfp*]; *vsIs191* [*unc-103e::mCherry*]
LX2580	*octr-1* transgene expressing GFP apical borders of epithelial cells expressing mCherry	*vsIs208* [*octr-1(fosmid)::gfp*]; *mjIs15* [*ajm-1::mCherry*]
LX2618	*ser-3* transgene expressing GFP egg-laying neurons expressing mCherry	*vsIs209* [*ser-3(fosmid)::gfp*]; *vsIs269* [*ida-1::mCherry*]
LX2638	*ser-3* transgene expressing GFP egg-laying neurons expressing mCherry	*vsIs209* [*ser-3(fosmid)::gfp*]; *mjIs15* [*ajm-1::mCherry*]
LX2537	*ser-6* transgene expressing GFP egg-laying neurons expressing mCherry	*vsIs220* [*ser-6(fosmid)::gfp*]; *vsIs269* [*ida-1::mCherry*]
LX2578	*ser-6* transgene expressing GFP apical borders of epithelial cells expressing mCherry	*vsIs220* [*ser-6(fosmid)::gfp*]; *mjIs15* [*ajm-1::mCherry*]
LX2541	*ser-2* transgene expressing GFP egg-laying neurons expressing mCherry	*vsIs213* [*ser-2(fosmid)::gfp*]; *vsIs269* [*ida-1::mCherry*]
LX2544	*ser-2* transgene expressing GFP vulval and uterine muscles expressing mCherry	*vsIs213* [*ser-2(fosmid)::gfp*]; *vsIs191* [*unc-103e::mCherry*]
LX2581	*ser-2* transgene expressing GFP apical borders of epithelial cells expressing mCherry	*vsIs213* [*ser-2(fosmid)::gfp*]; *mjIs15* [*ajm-1::mCherry*]
LX2627	*tyra-2* transgene expressing GFP egg-laying neurons expressing mCherry	*lin-15(n765ts)* X; *vsIs262* [*tyra-2(fosmid)::gfp*]; *vsIs270* [*ida-1::mCherry*]
LX2724	*tyra-2* transgene expressing GFP apical borders of epithelial cells expressing mCherry	*vsIs262* [*tyra-2(fosmid)::gfp*]; *mjIs15* [*ajm-1::mCherry*]
LX2533	*tyra-3* transgene expressing GFP egg-laying neurons expressing mCherry	*lin-15(n765ts)* X; *vsIs251* [*tyra-3(fosmid)::gfp*]; *vsIs269* [*ida-1::mCherry*]
LX2564	*tyra-3* transgene expressing GFP vulval and uterine muscles expressing mCherry	*lin-15(n765ts)* X; *vsIs251* [*tyra-3(fosmid)::gfp*]; *vsIs192* [*unc-103e::mCherry*]
LX2582	*tyra-3* transgene expressing GFP apical borders of epithelial cells expressing mCherry	*vsIs251* [*tyra-3(fosmid)::gfp*]; *mjIs15* [*ajm-1::mCherry*]
LX2536	*gar-1* transgene expressing GFP egg-laying neurons expressing mCherry	*vsIs205* [*gar-1(fosmid)::gfp*]; *vsIs269* [*ida-1::mCherry*]
LX2214	*gar-1* transgene expressing GFP vulval and uterine muscles expressing mCherry	*vsIs205* [*gar-1(fosmid)::gfp*];*::mCherry*] *vsIs191* [*unc-103e::mCherry*]
LX2663	*gar-1* transgene expressing GFP apical borders of epithelial cells expressing mCherry	*vsIs205* [*gar-1(fosmid)::gfp*]; *mjIs15* [*ajm-1::mCherry*]

LX2534	*gar-2* transgene expressing GFP egg-laying neurons expressing mCherry	*lin-15(n765ts)* X; *vsIs255* [*gar-2(fosmid)::SL2::NLS::GFP*]; *vsIs269* [*ida-1::mCherry*]
LX2543	*gar-2* transgene expressing GFP vulval and uterine muscles expressing mCherry	*lin-15(n765ts)* X; *vsIs255* [*gar-2(fosmid)::SL2::NLS::GFP*]; *vsIs191 [unc-103e::mCherry*]
LX2616	*gar-3* transgene expressing GFP egg-laying neurons expressing mCherry	*lin-15(n765ts)* X; *vsIs248* [*gar-3(fosmid)::gfp*]; *vsIs269* [*ida-1::mCherry*]
LX2628	*gar-3* transgene expressing GFP vulval and uterine muscles expressing mCherry	*lin-15(n765ts)* X; *vsIs248* [*gar-3(fosmid)::gfp*]; *vsIs192* [*unc-103e::mCherry*]
LX2723	*gar-3* transgene expressing GFP apical borders of epithelial cells expressing mCherry	*vsIs248* [*gar-3(fosmid)::gfp*]; *mjIs15* [*ajm-1::mCherry*]
LX2767	*gbb-1* transgene expressing GFP egg-laying neurons expressing mCherry	*vsIs206* [*gbb-1(fosmid)::gfp*]; *vsIs269* [*ida-1::mCherry*]
LX2563	*gbb-1* transgene expressing GFP vulval and uterine muscles expressing mCherry	*vsIs206* [*gbb-1(fosmid)::gfp*]; *vsIs191* [*unc-103e::mCherry*]
LX2630	*gbb-1* transgene expressing GFP apical borders of epithelial cells expressing mCherry	*vsIs206* [*gbb-1(fosmid)::gfp*]; *mjIs15* [*ajm-1::mCherry*]
LX2539	*gbb-2* transgene expressing GFP egg-laying neurons expressing mCherry	*lin-15(n765ts)* X; *vsIs267* [*gbb-2(fosmid)::gfp*]; *vsIs269* [*ida-1::mCherry*]
LX2736	*gbb-2* transgene expressing GFP apical borders of epithelial cells expressing mCherry	*vsIs267* [*gbb-2(fosmid)::gfp*]; *mjIs15* [*ajm-1::mCherry*]
LX2615	*mgl-1* transgene expressing GFP egg-laying neurons expressing mCherry	*vsIs214* [*mgl-1(fosmid)::gfp*] *vsIs269* [*ida-1::mCherry*]
LX2639	*mgl-1* transgene expressing GFP vulval and uterine muscles expressing mCherry	*vsIs214* [*mgl-1(fosmid)::gfp*]; *vsIs192* [*unc-103e::mCherry*]
LX2631	*mgl-1* transgene expressing GFP apical borders of epithelial cells expressing mCherry	*vsIs214* [*mgl-1(fosmid)::gfp*]; *mjIs15* [*ajm-1::mCherry*]
LX2675	*mgl-2* transgene expressing GFP egg-laying neurons expressing mCherry	*lin-15(n765ts)* X; *vsIs281* [*mgl-2(7.9kb)::gfp*] *vsIs271* [*ida-1::mCherry*]
LX2617	*mgl-3* transgene expressing GFP egg-laying neurons expressing mCherry	*lin-15(n765ts)* X; *vsIs256* [*mgl-3(fosmid)::gfp*] *vsIs269* [*ida-1::mCherry*]
LX2540	*ador-1* transgene expressing GFP egg-laying neurons expressing mCherry	*vsIs229* [*ador-1(fosmid)::gfp*] *vsIs269* [*ida-1::mCherry*]
LX2565	*ador-1* transgene expressing GFP vulval and uterine muscles expressing mCherry	*vsIs229* [*ador-1(fosmid)::gfp*]; *vsIs192 [unc-103e::mCherry*]
LX2710	*F35H10.10* transgene expressing GFP egg-laying neurons expressing mCherry	*lin-15(n765ts)* X; *vsIs296* [*F35H10.10(fosmid)::SL2::NLS::GFP*]*; vsIs271* [*ida-1::mCherry*]
LX2711	*F35H10.10* transgene expressing GFP vulval and uterine muscles expressing mCherry	*lin-15(n765ts)* X; *vsIs296* [*F35H10.10(fosmid)::SL2::NLS::GFP*]*; vsIs192* [*unc-103e::mCherry*]]

LX2712	*F35H10.10* transgene expressing GFP apical borders of epithelial cells expressing mCherry	*vsIs296* [*F35H10.10(fosmid)::SL2::NLS::GFP*]; *mjIs15* [*ajm-1::mCherry*]
LX2624	*dop-5* transgene expressing GFP egg-laying neurons expressing mCherry	*vsIs254* [*dop-5(fosmid)::gfp*]; *vsIs271* [*ida-1::mCherry*]
LX2664	*dop-5* transgene expressing GFP apical borders of epithelial cells expressing mCherry	*vsIs254* [*dop-5(fosmid)::gfp*]; *mjIs15* [*ajm-1::mCherry*]
LX2626	*dop-6* transgene expressing GFP egg-laying neurons expressing mCherry	*lin-15(n765ts)* X; *vsIs241* [*dop-6(fosmid)::gfp*]; *vsIs269* [*ida-1::mCherry*]
LX2375	*dop-6* transgene expressing GFP vulval and uterine muscles expressing mCherry	*lin-15(n765ts)* X; *vsIs241* [*dop-6(fosmid)::gfp*]; *vsIs191* [*unc-103e::mCherry*]

A5.6 Other strains used in this study

Strain	Feature	Genotype
MT15434	null deletion for serotonin biosynthetic enzyme	*tph-1(mg280)* II
MT13113	null mutant for an enzyme required for both octopamine and tyramine biosynthesis	*tdc-1(n3419)* II
MT9455	null mutant for the octopamine biosynthetic enzyme	*tbh-1(n3247)* X
MT6308	null deletion for vesicular glutamate transporter	*eat-4(ky5)* III
LX2740	*dop-4* null mutant in the *dop-4* transgene background	*dop-4(tm1392) X*; *vsIs287* [*dop-4(fosmid)::SL2::NLS::GFP*]
LX2709	null deletion for serotonin biosynthetic enzyme *ser-1* transgene expressing GFP	*tph-1(mg280)* II; *vsIs244* [*ser-1(fosmid)::gfp*]
LX2727	null mutant for both the octopamine and tyramine biosynthetic enzyme *ser-2* transgene expressing GFP	*tdc-1(n3419)* II; *vsIs213* [*ser-2(fosmid)::gfp*]
LX2708	null deletion for the octopamine biosynthetic enzyme *ser-6* transgene expressing GFP	*tbh-1(n3247)* X; *vsIs220* [*ser-6(fosmid)::gfp*]
LX2729	null deletion for vesicular glutamate transporter *mgl-3* transgene expressing GFP	*eat-4(ky5)* III; *vsIs214* [*mgl-1(fosmid)::gfp*]
LX2728	null deletion for vesicular glutamate transporter *mgl-3* transgene expressing GFP	*eat-4(ky5)* III; *vsIs256* [*mgl-3(fosmid)::gfp*]
MT2426	null deletion for the heterotrimeric G protein alpha subunit Go	*goa-1(n1134)* I
MT8504	null deletion for the RGS protein	*egl-10(md176)* V

Chapter 5 Alleles

A5.7 Allele information for mCherry markers

Gene	Genotype	Reference
ida-1	*vsIs269* [*ida-1::mCherry*]	This thesis
ida-1	*vsIs270* [*ida-1::mCherry*]	This thesis
ida-1	*vsIs271* [*ida-1::mCherry*]	This thesis
ida-1	*vsIs272* [*ida-1::mCherry*]	Koelle Lab
ida-1	*vsIs273* [*ida-1::mCherry*]	Koelle Lab
unc-103e	*vsIs191* [*unc-103e::mCherry*]	This thesis
unc-103e	*vsIs192* [*unc-103e::mCherry*]	This thesis
unc-103e	*vsIs193* [*unc-103e::mCherry*]	Koelle Lab
unc-103e	*vsIs194* [*unc-103e::mCherry*]	Koelle Lab
unc-103e	*vsIs195* [*unc-103e::mCherry*]	Koelle Lab
ajm-1	*mjIs15* [*ajm-1::mCherry*]	Ecsedi et al. (2015)

A5.8 Allele information for Neurotransmitter GPCR mutants

Gene	Genotype	Reference
ser-1	*ser-1(ok345) I*	The *C. elegans* Deletion Mutant Consortium et al. (2012)
ser-4	*ser-4(ok512) III*	The *C. elegans* Deletion Mutant Consortium et al. (2012)
ser-5	*ser-5(ok3087) I*	The *C. elegans* Deletion Mutant Consortium et al. (2012)
ser-7	*ser-7(gk414345) X*	Thompson O et al. (2013)
dop-1	*dop-1(tm535) X*	The *C. elegans* Deletion Mutant Consortium et al. (2012)
dop-2	*dop-2(vs105) V*	Chase DL et al. (2004)
dop-3	*dop-3(vs106) X*	Chase DL et al. (2004)
dop-4	*dop-4(tm1392) X*	The *C. elegans* Deletion Mutant Consortium et al. (2012)
octr-1	*octr-1(ok371) X*	The *C. elegans* Deletion Mutant Consortium et al. (2012)
ser-3	*ser-3(ok2007) I*	The *C. elegans* Deletion Mutant Consortium et al. (2012)
ser-6	*ser-6(tm2146) IV*	The *C. elegans* Deletion Mutant Consortium et al. (2012)
ser-2	*ser-2(pk1357) X*	Tsalik et al. (2003)
tyra-2	*tyra-2(tm1846) X*	The *C. elegans* Deletion Mutant Consortium et al. (2012)
tyra-3	*tyra-3(ok325) X*	The *C. elegans* Deletion Mutant Consortium et al. (2012)
gar-1	*gar-1(ok755) X*	The *C. elegans* Deletion Mutant Consortium et al. (2012)
gar-2	*gar-2(ok520) III*	The *C. elegans* Deletion Mutant Consortium et al. (2012)
gar-3	*gar-3(gk337) V*	The *C. elegans* Deletion Mutant Consortium et al. (2012)
gbb-1	*gbb-1(tm1406) X*	The *C. elegans* Deletion Mutant Consortium et al. (2012)
gbb-2	*gbb-2(tm1165) IV*	The *C. elegans* Deletion Mutant Consortium et al. (2012)
mgl-1	*mgl-1(tm7090) X*	The *C. elegans* Deletion Mutant Consortium et al. (2012)
mgl-2	*mgl-2(tm355) I*	The *C. elegans* Deletion Mutant Consortium et al. (2012)
mgl-3	*mgl-3(tm1766) IV*	The *C. elegans* Deletion Mutant Consortium et al. (2012)
ador-1	*ador-1(tm3971) II*	The *C. elegans* Deletion Mutant Consortium et al. (2012)
F35H10.10	*F35H10.10 (tm3179) IV*	The *C. elegans* Deletion Mutant Consortium et al. (2012)
dop-5	*dop-5(ok568) V*	The *C. elegans* Deletion Mutant Consortium et al. (2012)
dop-6	*dop-6(ok2090) X*	The *C. elegans* Deletion Mutant Consortium et al. (2012)

A5.9 Allele information for Neurotransmitter GPCR::GFP transgenes

Gene	Genotype	Reference
ser-1	*vsEx880* [*ser-1(fosmid)::GFP 60ng/uL + pLI15EK 50ng/uL + DH5α 25ng/uL*]	This thesis
ser-1	*vsIs244* [*ser-1(fosmid)::gfp*]	This thesis
ser-1	*vsIs245* [*ser-1(fosmid)::gfp*]	This thesis
ser-1	*vsIs246* [*ser-1(fosmid)::gfp*]	This thesis
ser-4	*ljIs570* [*ser-4(7.8kb)::gfp*]	Tsalik et al. (2003)
ser-5	*vsEx961* [*ser-5(fosmid)::gfp 50ng/uL + pLI15EK 50ng/uL + DH5α 25ng/uL*]	This thesis
ser-5	*vsEx962* [*ser-5(fosmid)::gfp 50ng/uL + pLI15EK 50ng/uL + DH5α 25ng/uL*]	This thesis
ser-5	*vsEx963* [*ser-5(fosmid)::gfp 50ng/uL + pLI15EK 50ng/uL + DH5α 25ng/uL*]	This thesis
ser-5	*vsEx964* [*ser-5(fosmid)::gfp 50ng/uL + pLI15EK 50ng/uL + DH5α 25ng/uL*]	This thesis
ser-5	*vsEx965* [*ser-5(fosmid)::gfp 50ng/uL + pLI15EK 50ng/uL + DH5α 25ng/uL*]	This thesis
ser-5	*vsIs282* [*ser-5(fosmid)::gfp*]	This thesis
ser-7	*vsEx870* [*ser-7(fosmid)::gfp 60ng/uL + pLI15EK 50ng/uL + DH5α 25ng/uL*]	This thesis
ser-7	*vsEx871* [*ser-7(fosmid)::gfp 60ng/uL + pLI15EK 50ng/uL + DH5α 25ng/uL*]	This thesis
ser-7	*vsIs237* [*ser-7(fosmid)::gfp*]	This thesis
ser-7	*vsIs238* [*ser-7(fosmid)::gfp*]	This thesis
ser-7	*vsIs239* [*ser-7(fosmid)::gfp*]	This thesis
ser-7	*vsIs240* [*ser-7(fosmid)::gfp*]	This thesis
dop-1	*vsEx952* [*dop-1(fosmid)::SL2::NLS::gfp 60ng/uL + pLI15EK 50ng/uL + DH5α 25ng/uL*]	This thesis
dop-1	*vsIs284* [*dop-1(fosmid)::SL2::NLS::gfp*]	This thesis
dop-1	*vsIs285* [*dop-1(fosmid)::SL2::NLS::gfp*]	This thesis
dop-1	*vsIs286* [*dop-1(fosmid)::SL2::NLS::gfp*]	This thesis
dop-2	*vsEx850* [*dop-2(fosmid)::gfp + unc-119 (+) 50ng/uL + pLI15EK 50ng/uL*]	This thesis; Sarov et al. (2012)
dop-2	*vsEx851* [*dop-2(fosmid)::gfp + unc-119 (+)* 50ng/uL + *pLI15EK* 50ng/uL]	This thesis; Sarov et al. (2012)
dop-2	*vsIs232* [*dop-2(fosmid)::gfp*]	This thesis
dop-2	*vsIs233* [*dop-2(fosmid)::gfp*]	This thesis
dop-2	*vsIs234* [*dop-2(fosmid)::gfp*]	This thesis
dop-3	*vsEx906* [*dop-3(fosmid)::gfp 20ng/uL + pLI15EK 50ng/uL + DH5α 25ng/uL*]	This paper; Sarov et al. (2012)
dop-3	*vsIs257* [dop-*3(fosmid)::gfp*]	This thesis
dop-3	*vsIs258* [*dop-3(fosmid)::gfp*]	This thesis
dop-3	*vsIs259* [*dop-3(fosmid)::gfp*]	This thesis
dop-4	*vsEx953* [*dop-4(fosmid)::SL2::NLS::gfp 60ng/uL + pLI15EK 50ng/uL + DH5α 25ng/uL*]	This thesis
dop-4	*vsEx954* [*dop-4(fosmid)::SL2::NLS::gfp 60ng/uL + pLI15EK 50ng/uL + DH5α 25ng/uL*]	This thesis
dop-4	*vsIs287* [*dop-4(fosmid)::SL2::NLS::gfp*]	This thesis
dop-4	*vsIs288* [*dop-4(fosmid)::SL2::NLS::gfp*]	This thesis

dop-4	*vsIs289* [*dop-4(fosmid)::SL2::NLS::gfp*]	This thesis
dop-4	*vsIs290* [*dop-4(fosmid)::SL2::NLS::gfp*]	This thesis
dop-4	*vsIs291* [*dop-4(fosmid)::SL2::NLS::gfp*]	This thesis
dop-4	*vsIs292* [*dop-4(fosmid)::SL2::NLS::gfp*]	This thesis
octr-1	*vsEx818* [*octr-1(fosmid)::gfp + unc-119 (+) 100ng/uL*]	This thesis; Sarov et al. (2012)
octr-1	*vsIs208* [*octr-1(fosmid)::gfp*]	This thesis
ser-3	*vsEx819* [*ser-3(fosmid)::gfp + unc-119 (+) 100ng/uL*]	This thesis; Sarov et al. (2012)
ser-3	*vsIs209* [*ser-3(fosmid)::gfp*]	This thesis
ser-3	*vsIs298* [*ser-3(fosmid)::gfp*]	This thesis
ser-6	*vsEx846* [*ser-6(fosmid)::gfp + unc-119 (+) 100ng/uL*]	This thesis; Sarov et al. (2012)
ser-6	*vsIs220* [*ser-6(fosmid)::gfp*]	This thesis
ser-2	*vsEx817* [*ser-2(fosmid)::gfp + unc-119 (+) 100ng/uL*]	This thesis; Sarov et al. (2012)
ser-2	*vsIs213* [*ser-2(fosmid)::gfp*]	This thesis
tyra-2	*vsEx910* [*tyra-2(fosmid)::gfp 20ng/uL + pLI15EK 50ng/uL + DH5α 25ng/uL*]	This thesis; Sarov et al. (2012)
tyra-2	*vsEx911* [*tyra-2(fosmid)::gfp 20ng/uL + pLI15EK 50ng/uL + DH5α 25ng/uL*]	This thesis; Sarov et al. (2012)
tyra-2	*vsIs260* [*tyra-2(fosmid)::gfp*]	This thesis
tyra-2	*vsIs261* [*tyra-2(fosmid)::gfp*]	This thesis
tyra-2	*vsIs262* [*tyra-2(fosmid)::gfp*]	This thesis
tyra-2	*vsIs263* [*tyra-2(fosmid)::gfp*]	This thesis
tyra-3	*vsEx901* [*tyra-3(fosmid)::gfp 20ng/uL + pLI15EK 50ng/uL + DH5α 25ng/uL*]	This thesis; Sarov et al. (2012)
tyra-3	*vsEx902* [*tyra-3(fosmid)::gfp 20ng/uL + pLI15EK 50ng/uL + DH5α 25ng/uL*]	This thesis; Sarov et al. (2012)
tyra-3	*vsEx903* [*tyra-3(fosmid)::gfp 20ng/uL + pLI15EK 50ng/uL + DH5α 25ng/uL*]	This thesis; Sarov et al. (2012)
tyra-3	*vsIs251* [*tyra-3(fosmid)::gfp*]	This thesis
gar-1	*vsEx809* [*gar-1(fosmid)::gfp + unc-119 (+) 100ng/uL*]	This thesis; Sarov et al. (2012)
gar-1	*vsIs205* [*gar-1(fosmid)::gfp*]	This thesis
gar-2	*vsEx912* [*gar-2(fosmid)::SL2::NLS::gfp 60ng/uL + pLI15EK 50ng/uL + DH5α 25ng/uL*]	This thesis
gar-2	*vsEx913* [*gar-2(fosmid)::SL2::NLS::gfp 60ng/uL + pLI15EK 50ng/uL + DH5α 25ng/uL*]	This thesis
gar-2	*vsIs255* [*gar-2(fosmid)::SL2::NLS::gfp*]	This thesis
gar-3	*vsEx878* [*gar-3(fosmid)::gfp 60ng/uL + pLI15EK 50ng/uL + DH5α 25ng/uL*]	This thesis
gar-3	*vsEx879* [*gar-3(fosmid)::gfp 60ng/uL + pLI15EK 50ng/uL + DH5α 25ng/uL*]	This thesis

gar-3	*vsIs247* [*gar-3(fosmid)::gfp*]	This thesis
gar-3	*vsIs248* [*gar-3(fosmid)::gfp*]	This thesis
gar-3	*vsIs249* [*gar-3(fosmid)::gfp*]	This thesis
gar-3	*vsIs250* [*gar-3(fosmid)::gfp*]	This thesis
gbb-1	*vsEx793* [*gbb-1(fosmid)::gfp + unc-119 (+) 100ng/uL*]	This thesis; Sarov et al. (2012)
gbb-1	*vsIs206* [*gbb-1(fosmid)::gfp*]	This thesis
gbb-1	*vsIs236* [*gbb-1(fosmid)::gfp*]	This thesis
gbb-2	*vsEx925* [*gbb-2(fosmid)::gfp 60ng/uL + pLI15EK 50ng/uL + DH5α 25ng/uL*]	This thesis
gbb-2	*vsEx926* [*gbb-2(fosmid)::gfp 60ng/uL + pLI15EK 50ng/uL + DH5α 25ng/uL*]	This thesis
gbb-2	*vsIs266* [*gbb-2(fosmid)::gfp*]	This thesis
gbb-2	*vsIs267* [*gbb-2(fosmid)::gfp*]	This thesis
mgl-1	*vsEx813* [*mgl-1(fosmid)::gfp + unc-119 (+) 100ng/uL*]	This thesis; Sarov et al. (2012)
mgl-1	*vsIs214* [*mgl-1(fosmid)::gfp*]	This thesis
mgl-1	*vsIs215* [*mgl-1(fosmid)::gfp*]	This thesis
mgl-1	*vsIs216* [*mgl-1(fosmid)::gfp*]	This thesis
mgl-1	*vsIs217* [*mgl-1(fosmid)::gfp*]	This thesis
mgl-2	*vsEx957* [*mgl-2(7.9kb)::gfp 30ng/uL + pLI15EK 50ng/uL + DH5α 25ng/uL*]	This thesis; Yemini et al. (2019)
mgl-2	*vsEx958* [*mgl-2(7.9kb)::gfp 30ng/uL + pLI15EK 50ng/uL + DH5α 25ng/uL*]	This thesis; Yemini et al. (2019)
mgl-2	*vsIs281* [*mgl-2(7.9kb)::gfp*]	This thesis
mgl-3	*vsEx907* [*mgl-3(fosmid)::gfp 20ng/uL + pLI15EK 50ng/uL + DH5α 25ng/uL*]	This thesis; Sarov et al. (2012)
mgl-3	*vsEx908* [*mgl-3(fosmid)::gfp 20ng/uL + pLI15EK 50ng/uL + DH5α 25ng/uL*]	This thesis
mgl-3	*vsEx909* [*mgl-3(fosmid)::gfp 20ng/uL + pLI15EK 50ng/uL + DH5α 25ng/uL*]	This thesis
mgl-3	*vsIs255* [*mgl-3(fosmid)::gfp*]	This thesis
ador-1	*vsEx792* [*ador-1(fosmid)::gfp + unc-119 (+) 100ng/uL*]	This thesis; Sarov et al. (2012)
ador-1	*vsIs207* [*ador-1(fosmid)::gfp*]	This thesis
ador-1	*vsIs229* [*ador-1(fosmid)::gfp*]	This thesis
ador-1	*vsIs230* [*ador-1(fosmid)::gfp*]	This thesis
ador-1	*vsIs231* [*ador-1(fosmid)::gfp*]	This thesis
F35H10.10	*vsEx955* [*F35H10.10(fosmid)::SL2::NLS::gfp 60ng/uL + pLI15EK 50ng/uL + DH5α 25ng/uL*]	This thesis
F35H10.10	*vsEx956* [*F35H10.10(fosmid)::SL2::NLS::gfp 60ng/uL + pLI15EK 50ng/uL + DH5α 25ng/uL*]	This thesis
F35H10.10	*vsIs283* [*F35H10.10(fosmid)::SL2::NLS::gfp*]	This thesis
F35H10.10	*vsIs293* [*F35H10.10(fosmid)::SL2::NLS::gfp*]	This thesis
F35H10.10	*vsIs294* [*F35H10.10(fosmid)::SL2::NLS::gfp*]	This thesis
F35H10.10	*vsIs295* [*F35H10.10(fosmid)::SL2::NLS::gfp*]	This thesis
F35H10.10	*vsIs296* [*F35H10.10(fosmid)::SL2::NLS::gfp*]	This thesis
F35H10.10	*vsIs297* [*F35H10.10(fosmid)::SL2::NLS::gfp*]	This thesis

dop-5	*vsEx904* [*dop-5(fosmid)::gfp 20ng/uL + pLI15EK 50ng/uL + DH5α 25ng/uL*]	This thesis
dop-5	*vsIs252* [*dop-5(fosmid)::gfp*]	This thesis
dop-5	*vsIs253* [*dop-5(fosmid)::gfp*]	This thesis
dop-5	*vsIs254* [*dop-5(fosmid)::gfp*]	This thesis
dop-6	*vsEx874* [*dop-6(fosmid)::gfp 60ng/uL + pLI15EK 50ng/uL + DH5α 25ng/uL*]	This thesis
dop-6	*vsEx875* [*dop-6(fosmid)::gfp 60ng/uL + pLI15EK 50ng/uL + DH5α 25ng/uL*]	This thesis
dop-6	*vsIs241* [*dop-6(fosmid)::GFP*]	This thesis
dop-6	*vsIs242* [*dop-6(fosmid)::GFP*]	This thesis